國 立 交 通 大 學

運輸科技與管理學系

博 士 論 文

跟車現象及穩定性之微觀分析

Microscopic Analysis of Car-Following Phenomena and Stability

研 究 生：吳育婷

指導教授：卓訓榮　教授

中 華 民 國 九 十 七 年 元 月

跟車現象及穩定性之微觀分析
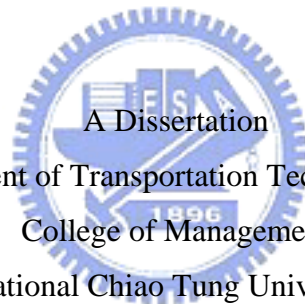# Microscopic Analysis of Car-Following Phenomena and Stability

研 究 生：吳育婷　　　　　Student：Yuh-Ting Wu

指導教授：卓訓榮　　　　　Advisor：Hsun-Jung Cho

國 立 交 通 大 學
運 輸 科 技 與 管 理 學 系
博 士 論 文

A Dissertation

Submitted to Department of Transportation Technology and Management

College of Management

National Chiao Tung University

in partial Fulfillment of the Requirements

for the Degree of

Doctor of Philosophy

in

Transportation Technology and Management

January 2008

Hsinchu, Taiwan, Republic of China

中華民國九十七年元月

跟車現象及穩定性之微觀分析

學生：吳育婷   指導教授：卓訓榮

國立交通大學 運輸科技與管理學系

摘要

隨著對運輸品質的要求增加，近年來大力發展智慧型運輸系統。而智慧型運輸系統中的先進旅行者資訊系統及先進交通管理系統，則各需車流模式提供交通資訊預估及車流分析。因此本研究發展一簡單的車流模式，以期其能描述車流現象，且不需複雜的計算以節省模擬時間，並能據以分析車流性質，最終並可延伸至巨觀車流模式。

本研究所提出的跟車模式引入外生變數－個人最大速度，以描述駕駛人的差異性，及不同外在環境所造成的影響。而模擬結果及數學分析顯示，本模式確能反應並且解釋在相同的車流狀況下，為何不同的駕駛人採取不同的行為反應。

為瞭解本模式是否確能反應車流現象，本研究探討均衡及非均衡狀態下的各種車流現象，並且探討系統收斂到均衡狀態的條件（穩定性分析）及時間。在穩定性分析方面，本模式發現若個人最大速度與車流均衡速度差異不大，則車流會收斂到均衡狀態；反之，則車流會一直處於非均衡狀態。此一分析可解釋為何在擁擠的狀況下，車流常呈現不穩定的狀態。此外，在車流由非均衡狀態收斂到均衡狀態所需的鬆弛時間方面，模擬結果顯示，個人最大速度與車流均衡速度差異越大，其鬆弛時間越長。在均衡狀態的探討方面，均衡時的車間距只取決於均衡速度與個人最大速度，與起始狀態無關。個人最大速度愈大者，其駕駛行為越激進，所保持的車間距也愈短。另外假設駕駛人為均質，將微觀均衡狀態延伸到巨觀均衡狀態，則自由流速率越高者其容量愈高。不同的參數值，其車流基礎構圖所呈現出來的形態也不同。而在非均衡狀態方面，本研究探討走走停停、closing-in、shying-away、及車流磁滯現象，並分別進行數學分析及提供數值範例。數學分析顯示，在相同的車流狀況下，激進的駕駛人可能選擇加速，而保守的駕駛人可能選擇減速。而單一駕駛人，其在加速及減速上的速度與車間距之間的關係並不相同；不同的起始條件及邊界條件，將可模擬出不同的車流磁滯現象形態。

Microscopic Analysis of Car-Following Phenomena and Stability

Student：Yuh-Ting Wu   Advisor：Hsun-Jung Cho

Department of Transportation Technology and Management
National Chiao Tung University

Abstract

The increment of vehicle number and life quality request lead to develop ITS in the recent years. ATIS needs traffic flow model to provide real time prediction. ATMS needs traffic flow models to analyze traffic flow properties so that they can provide better traffic control strategies. Thus, this dissertation aims to develop a simple car-following model which can analyze traffic properties, represent traffic flow phenomena, save execution time, and have potential for extending to macroscopic models.

The proposed model employs driver's individual maximum speed as an exogenous variable to reflect the external environment and driver's characteristics. The proposed model can explain why speeds and spacing differ among drivers even when the driving conditions are identical.

This dissertation discusses the equilibrium and disequilibrium states of the proposed model, local stability between two moving cars, and relaxation time of different equilibrium states. The stability analysis indicates that traffic is stable if driver's individual maximum speed is close to the equilibrium speed. Otherwise, if the difference between the individual maximum speed and the equilibrium speed is large, traffic may be unstable. It can explain why heavy traffic is unstable. Furthermore, numerical examples show that relaxation time increases if the difference between the individual maximum speed and the equilibrium speed increases.

This dissertation derives the equilibrium state of the proposed model, and it indicates that equilibrium state is only dependent on the individual maximum speed and the equilibrium speed, not on initial conditions. A driver with higher individual maximum speed is more aggressive and keeps shorter equilibrium spacing under identical equilibrium speed. Fundamental diagrams based on microscopic equilibrium state and homogeneous drivers are also discussed. The capacity increases with free flow speed, and different parameter values result in different fundamental diagram patterns.

Some traffic phenomena of disequilibrium states are discussed, such as closing-in, shying-away, stop-and-go, and traffic hysteresis. The mathematical analysis indicates that aggressive drivers may decide to accelerate while conservative drivers may decide to decelerate under identical driving condition. The speed-spacing relationships for acceleration and deceleration traffic are different. Different initial conditions and boundary conditions result in various traffic hysteresis patterns.

Contents

List of Tables

List of Figures

Glossary of Symbols

$V_{n,t+1}$: speed of the following vehicle at time step t+1

$v_{n,d}$: individual maximum speed of the following vehicle

$V_{n,t}$: speed of the following vehicle n at time step t

$V_{n-1,t}$: speed of the lead vehicle n-1 at time step t

$H_{n,t}$: spacing between vehicle n-1 and vehicle n at time step t

S_n : safe standstill spacing of the following vehicle n

λ : positive parameter

α : positive parameter

β : positive parameter

γ : positive parameter

L : positive parameter

T : length of a time interval, it equals reaction time of drivers

$a_{n,d}$: desired start acceleration of the following vehicle n

Z_n : minimum start spacing, $Z_n > S_n$

$\psi_{H,n}$: sensitivity to $H_{n,t}$

$\psi_{V,n-1}$: sensitivity to $V_{n-1,t}$

$\psi_{V,n}$: sensitivity to $V_{n,t}$

$V_{n,e}$: equilibrium speed of the following vehicle

$H_{n,e}$: equilibrium spacing

$V_{n-1,e}$: equilibrium speed of the lead vehicle

$V_{n,t,a}$: $V_{n,t}$ value for acceleration traffic

$V_{n,t,d}$: $V_{n,t}$ value for deceleration traffic

$V_{n-1,t,a}$: $V_{n-1,t}$ value for acceleration traffic

$V_{n-1,t,d}$: $V_{n-1,t}$ value for deceleration traffic

$H_{n,t,a}$: $H_{n,t}$ value for acceleration traffic

$H_{n,t,d}$: $H_{n,t}$ value for deceleration traffic

D_n : $V_{n,e} / v_{n,d}$

q : flow

k : density

u : space-mean speed

q_e : equilibrium flow

k_e : equilibrium density

u_e : equilibrium space-mean speed

τ : time length of observation

X : road length of observation

x_i : travel distance of vehicle i

t_i : travel time of vehicle i

Chapter 1
Introduction

1.1 Problem Statement

The increment of vehicle number and life quality request lead to develop ITS (Intelligent Transportation Systems) in the recent years. ATMS (Advanced Traffic Management System) and ATIS (Advanced Traveler Information System) are two sub-systems of ITS. Information systems need traffic flow model to provide prediction, such as travel time prediction. Traffic management systems need traffic flow models to analyze traffic flow properties so that they can provide better traffic control strategies.

Microscopic traffic flow models describe vehicles interaction at a high level of detail, and they have behavioral meanings. Since microscopic models describe traffic flow in detail, they can describe complicated vehicle interaction, and predict traffic flow more accurate. But they need more computation time. Hence, they can hardly provide real-time prediction, especially in large-scale traffic network [Zhang and Owen, 1998].

Macroscopic traffic flow models describe vehicles and their interaction at a low level of detail. Contrary to microscopic models, most macroscopic models are derived from physical models, they lack for behavioral meanings more, and take less computation time.

Some simple microscopic models which have one or few functions, such as safe-distance models and stimulus-response models, cannot represent some traffic phenomena. On the other hand, it is easier to analyze traffic flow based on these simple models, such as traffic stability can be derived from stimulus-response models. It is also easier to extend to macroscopic traffic flow models based on simple car-following models, such as stimulus-response models can extend to Greenshield, Greenberg models based on different parameters. The models which have different rules for different conditions describe traffic flow better. The computing is more complicated and it is difficult to analyze traffic flow properties or extend to macroscopic models from them.

LWR model is a simple macroscopic model, and it assumes that traffic flow conforms to equilibrium speed-density relationships at all time. However, speed-density relationships of equilibrium state and disequilibrium state are different. Besides, LWR model cannot represent some complex traffic flow phenomena such as stop-and-go waves in long queues. In order to solve the problems of LWR model, higher order models are developed. Daganzo [1994] mentioned that although the results of higher order models are a little better than first order models, it needs more computation. He also pointed out higher order models bring the wrong result; that is, in some cases, vehicle speed will be negative. Some macroscopic models are derived from physical models, and some physical variables cannot correspond to traffic flow measurement value, such as traffic field. Hence, some macroscopic traffic flow models can be hardly applied to real world nowadays.

According to the aforementioned research background, the problems concerned in this dissertation are listed below.

1. ITS need a traffic flow model that can provide real time prediction and can analyze traffic flow properties.
2. Microscopic models can describe traffic flow at a high level of detail, but it takes more time. Simple models cannot represent some traffic phenomena. As the complexity of a model increases, the more phenomena can be represented and the more computation time.
3. Under complicated vehicle interaction, such as: weaving section, and signalized intersection, microscopic simulation can provide better prediction. Thus, microscopic traffic flow models are necessary for information systems under some traffic conditions.
4. Most macroscopic traffic flow models are derived from physical models, they lack of behavioral discussion, and they have some deficiencies in describing some basic traffic phenomena, such as LWR model cannot represent disequilibrium traffic state, and higher order models may make vehicle speed be negative.

1.2 Research Motivations and Objectives

Macroscopic traffic flow models lack for behavioral discussion, and it is better to apply microscopic models under some conditions, such as complicated vehicle interaction section. This research try to develop a simple car-following model that employs one rule or fewer rules, and it can solve aforementioned problems:

1. Less execution time: It is simple for save execution time, and it has the potential for extending to macroscopic models. Thus, it can provide real time prediction of large-scale traffic network.

2. Reproducing traffic phenomena: It can describe equilibrium and disequilibrium traffic phenomena.

3. Traffic properties: It can be a tool to analyze traffic properties.

1.3 Framework of Research

In order to achieve research objectives, the framework of this research is shown as Figure 1-1.

1. Car-following model development

    A simple car-following will be developed. It can:

    ■ reflect the difference among different drivers,

    ■ avoid some deficiencies of traditional car-following models, such as drivers have to determine the deceleration capability of their lead vehicle, and

    ■ reproduce equilibrium and disequilibrium traffic phenomena.

2. Sensitivity analysis

    It will discuss how the proposed model output varies with changes in model inputs.

3. Stability analysis

    Local stability between two moving cars will be discussed. The discussion is on the stability of a following vehicle when its lead vehicle is in equilibrium state and the following vehicle has no acceleration limit. A method of discussing linearized stability of a dynamical system will be applied.

4. Equilibrium state discussion

    A system is either in equilibrium or in disequilibrium. A vehicle is in equilibrium state if its speed and spacing never change as time passes. The microscopic and macroscopic equilibrium states of the proposed car-following model will be discussed. Fundamental diagram based on the microscopic equilibrium state will be also discussed.

5. Disequilibrium state discussion

    Some traffic phenomena of disequilibrium state will be discussed, such as closing-in, shying-away, stop-and-go, and traffic hysteresis. Simulation examples will be provided.

6. Relaxation time discussion

    Relaxation time refers to the time needed for a system to relax under external stimuli. When a perturbation occurs at an equilibrium system, the system will depart from equilibrium state. This study discusses how much time the system needs to return to the equilibrium state.

7. Parameters discussion and mathematical analysis

    This study possesses analytical properties that are logical in representing physical phenomena, and prove that some traffic phenomena still hold under any parameters or some traffic phenomena have various patterns under different parameter values.
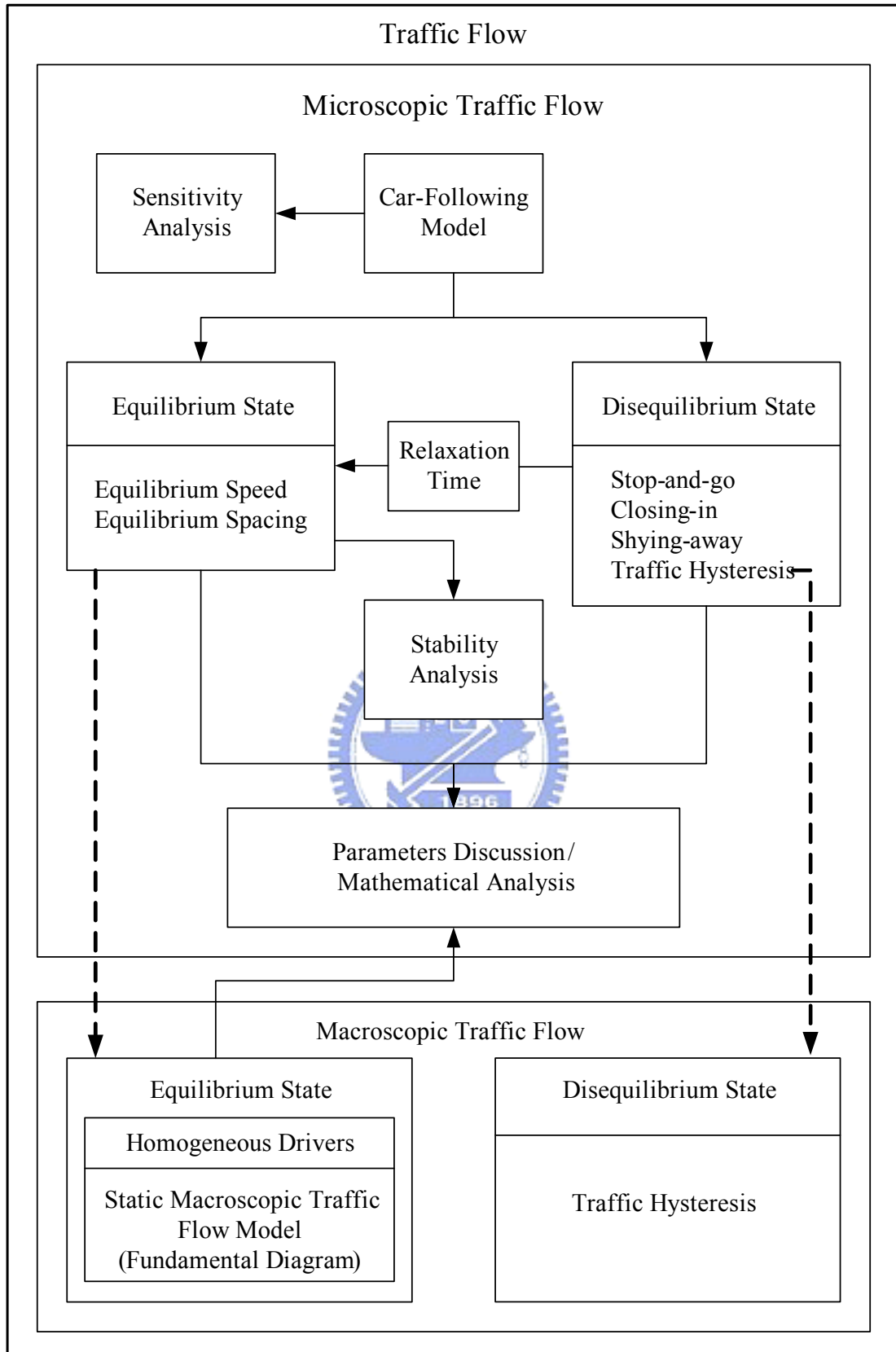
Figure 1-1 Framework of research

Chapter 2
Literature Review

The research purpose of this dissertation is to develop a simple car-following model which can analyze traffic properties, represent traffic flow phenomena, save execution time, and have potential for extending to macroscopic models. Thus, traffic flow characteristics are reviewed in section 2.1. Section 2.2 reviews some car-following models. Section 2.3 presents some static macroscopic traffic flow models. Section 2.4 review linearized stability of dynamical systems. Finally, a brief summary and discussion is given in section 2.5.

2.1 Traffic Flow Characteristics

A system is either in equilibrium state or disequilibrium state. Section 2.1.1 reviews traffic stability that discusses whether a following car will reach the equilibrium state or not. Section 2.1.2 reviews some traffic phenomena of disequilibrium states.

2.1.1 Traffic Stability

Car-following models describe both the space-time behavior of vehicles and their interactions individually on a single lane. After car-following for a long time, the speed or spacing of the vehicle might be kept at a particular value (i.e., stable traffic) or changed again and again over time (i.e., unstable traffic). The fundamental diagram (as shown in Fig. 2-1.) of traffic flow indicates that traffic flow is unstable at low speed (i.e., under heavy traffic), and stable at high speed.
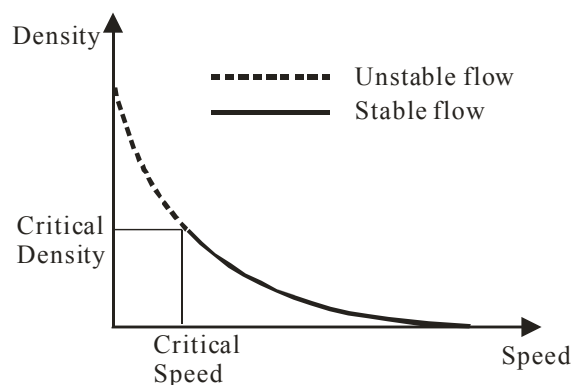
Figure 2-1 Relationship among speed and density [Mschane & Roess, 1990].

Traffic stability can be analyzed from the viewpoint of macroscopic traffic flow. Zhang [1999b] found that various instability criteria can be reduced to a single criterion derived from first order waves traveling faster than slow second order waves in the higher order theories. Nagatani [2000] pointed out when the density is larger than a critical value, the traffic becomes unstable. Yi et al [2003] derived a nonlinear traffic flow stability criterion using a wavefront expansion technique. Jiang and Wu [2003] found that stability depends on the equilibrium speed density relationship, and it is also affected by the sensitivity parameters in the corresponding car-following model.

Some researchers analyzed traffic stability from the viewpoint of microscopic traffic. It is found that unstable traffic is likely to occur under higher reaction time and higher sensitivity response based on stimulus-response models [Herman et al, 1959; May, 1990; Zhang & Jarret, 1997; Holland, 1998]. This cannot explain why heavy traffic is unstable, unless drivers have different reaction time or different sensitivity response under different spacings.

2.1.2 Disequilibrium Traffic Flow

A following car is in equilibrium state if it keeps its velocity and spacing at some particular value. If a following car is in disequilibrium state, it implies the car is accelerating or decelerating. This section reviews some traffic phenomena of acceleration and deceleration traffic.

A. Closing-in and Shying-away

Sometimes the following vehicle accelerates despite the lead vehicle traveling slower than it is (i.e. closing-in), and sometimes the follower decelerates even its speed is slower than its lead vehicle's speed (i.e. shying-away) [Chakroborty & Kikuchi, 1999]. Figure 2-2 shows that in about 20% of the points in the second and fourth quadrants of the car-following process, they are closing-in or shying-away. Since closing-in and shying-away often occur in a car-following process, a car-following model should be able to describe closing-in and shying-away.
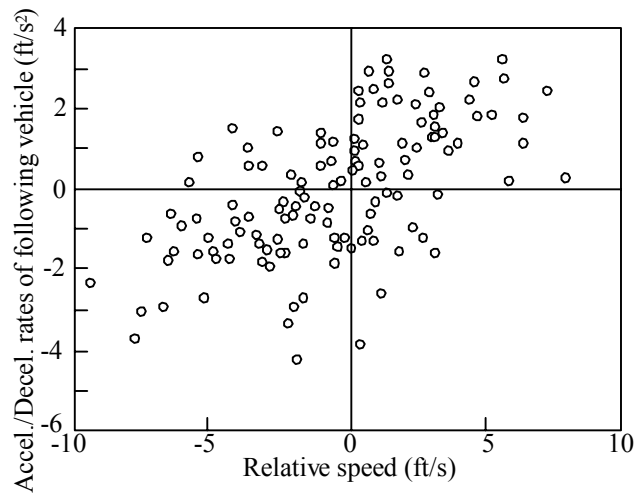
Figure 2-2 Acceleration/Deceleration rate of the following vehicle at time t versus the relative speed of the lead and following vehicles at time t-1 [Chakroborty & Kikuchi, 1999] (reproduced)

B. Hysteresis

Static macroscopic traffic flow models describe the relationship between speed and density. These relationship models frequently serve as a state equation in dynamic macroscopic traffic flow models. However, speed-density relationships of equilibrium state and disequilibrium state are different. In fact, when traffic flow is not in an equilibrium state (i.e. acceleration or deceleration), the speed-density relationship is not one-to-one. The acceleration curve differs from the deceleration curve, known as the traffic hysteresis phenomenon. Igarashi [Igarashi et al, 2001] said that hysteresis phenomena associated with discontinuous phase transitions. Figure 2-4 is the speed-density relationship obtained by Treiterer and Meyers [Zhang, 1999a]. It indicates that speed-density curve for transient traffic is not unique [Zhang, 1999a]. Such curves contain two branches for acceleration and deceleration traffic, respectively. The curves form two hysteresis loops. The acceleration curve lies above the deceleration curve under low density whereas the deceleration curve lies above the acceleration curve under high density. Maes' observation is shown as Figure 2-3, and he observed that the deceleration curve lies above the acceleration curve under light and heavy density.

Zhang [1999a, 2001] proposed a mathematical theory of traffic hysteresis, and the model presented that acceleration and deceleration curves lies on both sides of the equilibrium curve. These two branches meet with the equilibrium curve.

Other researchers also proposed models to reproduce hysteresis. Heidemann [2001] proposed a queueing theory, Daganzo [2002] proposed a macroscopic behavioral theory, and Zhao and Gao [2005] presented a full velocity and acceleration difference model. Wong and Wong [2002] indicated that multi-class LWR model can reproduce hysteresis.
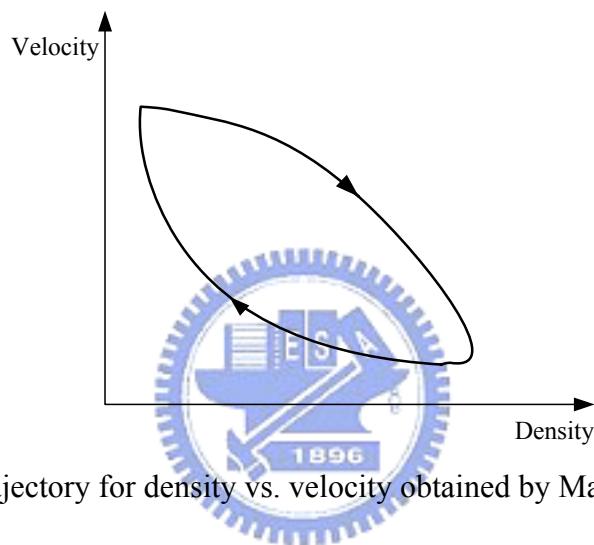
Figure 2-3 Trajectory for density vs. velocity obtained by Maes (reproduced)
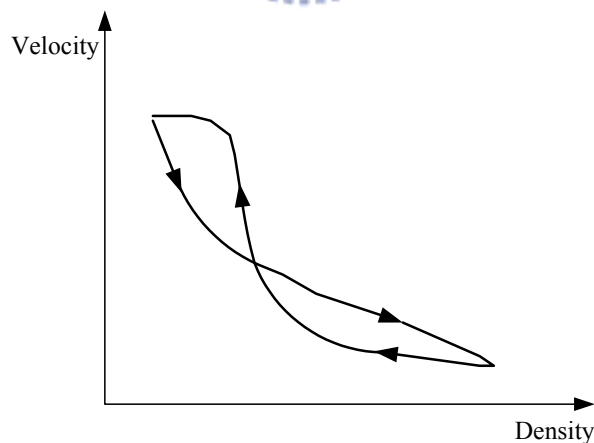
Figure 2-4 Trajectory for density vs. velocity obtained by Treiterer and Meyers
(reproduced)

2.2 Microscopic Traffic Flow Models

According to the level of detail, traffic flow models can be divided into microscopic, mesoscopic, and macroscopic models [Hoogendoorn & Bovey, 2001]. Microscopic traffic flow includes car-following and lane-changing. This study focuses on car-following. Various car-following models are reviewed and discussed below.

Pipes [1953] proposed a safe-distance model, and applied a very simple rule. The PITT [Wicks & Andrews, 1980] model is also a type of safe-distance model. This model assumes that the vehicle follows its leader by maintaining some spacing. It employed a sensitivity factor to describe different driver behaviors. The stimulus-response model [Chandler, 1958; Gazis, 1959; Herman, 1959; Edie, 1961] expresses the concept that a driver of a vehicle responds to a given stimulus based on the stimulus and its sensitivity. The psycho-physical spacing model [Widemann, 1974; Leutzbach, 1986, 1988] divides the car-following process into several behavior zones, each with its own behavioral rules. Benekohal proposed the CARSIM model [Benekohal & Treiterer, 1988], which computes various acceleration rates for different situations and chooses the most suitable one. Fuzzy models [Kikuchi & Chakroborty, 1992; McDonald et al, 1997] comprise a set of fuzzy inference rules related to specific driving environments. The intelligent driver model [Treiber et al, 2000] possesses only a few intuitive parameters with realistic values; the model reproduces a realistic collective dynamics, and leads to the plausible microscopic acceleration and deceleration behavior of single drivers. Newell [2002] designed a very simple car-following rule for a homogeneous highway in which a vehicle follows the same trajectory as its lead vehicle except for a translation in space and time. However, it did not deal with the question of what determines speed. Zhang & Kim [2005] developed a theory for explaining car-following behaviors in multiphase traffic flow. It specifies different functional forms of gap-time for different spacings, and it can reproduce both the so-called capacity drop and traffic hysteresis.

Some microscopic traffic flow models are reviewed in detail as following.

(1). Stimulus-Response Car-Following Model

Stimulus-response models were first derived from Reuschel [1950] and Pipes [1953]. Chandler et al [1958] derived the stimulus-response function:

$$x''_{n+1}(t+T) = \lambda(x'_{n+1}(t) - x'_n(t)) \qquad (2.1)$$

where λ is a constant, T denotes the reaction time, $x_n(t)$ denotes the position of the lead vehicle at time t, and $x_{n+1}(t)$ denotes the position of the following vehicle at time t.

A series of stimulus-response models were developed later, these models can be summarized as Table 2.1

Table 2.1 Governing equations of car-following models

Model	Governing equation
Chandler et al. [1958]	$x''_n(t+T) = \lambda(x'_{n+1}(t) - x'_n(t))$
California Chandler et al. [1958]	$x''_n(t+T) = \lambda[x_{n+1}(t) - x_n(t) + c - T_1 x'_n(t)]$
Gazis et al. [1959]	$x''_n(t+T) = \dfrac{\lambda(x'_{n+1}(t) - x'_n(t))}{(x_{n+1}(t) - x_n(t))}$
Herman et al. [1959]	$x''_n(t+T) = \lambda_1[x'_{n+1} - x'_n]_{t-T_1} + \lambda_2[x'_{n+2} - x'_n]_{t-T_2}$
Edie [1961]	$x''_n(t+T) = \dfrac{\lambda x'_n(x'_{n+1}(t) - x'_n(t))}{(x_{n+1}(t) - x_n(t))^2}$
Newell [1961]	$x''_n(t+T) = V(x_{n+1}(t) - x_n(t))$
Gazis et al. [1961] (General Form)	$x''_n(t+T) = \dfrac{\lambda(x'_n(t))^l (x'_{n+1}(t) - x'_n(t))}{(x_{n+1}(t) - x_n(t))^m}$
Bando et al. [1995]	$x''_n(t+T) = a[V(x_{n+1}(t) - x_n(t)) - x'_n(t)]$

Some macroscopic traffic flow models can be derived from stimulus-response models. Gazis's model [1961] is a general form of stimulus-response models. The case $m = 0$, $l = 2$ can be identified with a model developed by Greenshield [1934]. The case for $m = 0$ and $l = 1$ generates a steady-state relation that was developed by Greenberg [1959]. When $m = 1$ and $l = 2$, the stimulus-response model can be lead to Edie's model. While $m = 1$ and $l = 3$, the model can be lead to Edie's model.

The deficiencies of stimulus-response are described as following [Chakroborty, 1999].

1. Response to stimuli in car-following is asymmetric, but stimulus-response model is symmetric.

2. It cannot represent closing-in and shying-away phenomena.

3. Stable distance headway of stimulus-response model is dependent on number of factors, such as initial conditions, but the stable distance is actually only dependent

on the final speed.

4. It ignores the acceleration capability of a vehicle.

(2). PITT Model

PITT is a FRESIM model in CORSIM which was developed by FHWA. Its theory is keeping specific space headway [Wicks & Andrews, 1980]:

$$H = L_L + k \times V_F + 10 + b \times k \times (V_L - V_F) \qquad (2.2)$$

In Eq. (2.2):

H : space headway(ft)

V_F : the velocity of the following car at end of time step

V_L : the velocity of the lead car at the end of time step

L_L : the length of the lead car

k : the sensitivity of a driver

b : constant, when $V_L = V_F \leq 10$, $b=0.1$, otherwise, $b=0$

For keeping above-mentioned space headway, the acceleration of the follower is:

$$A_F = \frac{2\left[X_L - X_F^i - L - 10 - V_F^i \times (k \times T) - b \times k \times (V_L - V_F^i)^2\right]}{(T^2 + 2 \times k \times T)} \qquad (2.3)$$

In Eq. (2.3):

A_F : the acceleration of the following car

X_L : the position of the lead car

X_F^i : the position of the follower at the beginning of time step

V_F^i : velocity of the follower at the beginning of time step

T : time step

Considering the reaction time of following car c, the velocity of follower should be $V_F = V_F^i + A_F \times (T - c)$. To avoid traffic accident, PITT designs three constraint functions for different traffic conditions.

The deficiencies of PITT are described as following [Benekohal, 1988] [Aycin, 1999].

1. It dose not take into account the star-up delay of stopped vehicles.

2. The dual behavior of traffic in congested and non-congested conditions has not been taken into consideration.

3. It is difficult to reflect all traffic condition since only one type of spacing equation is applied for different conditions such as stop-and-go and noncongested traffic.

4. It performs car-following by considering emergency braking of the lead vehicle, but a follower cannot have the information about the deceleration capability of its leader.

5. It considers driver's reaction time, and it results in a driver with higher reaction time keeps longer spacing.

(3). Psycho-Physical Spacing Models

Stimulus-response models presume that the following driver reacts to very small changes in relative velocity even when the spacing is very large. On the other hand, if the relative velocity is zero, the follower's response is zero even the spacing is very small or large. Researchers developed psycho-physical spacing models to remedy these unreasonable assumptions. The basis of psycho-physical spacing models is:

1. at large spacings, the follower is not influenced by the relative velocity, and

2. at small spacings, there are some combinations of relative speeds and spacings do not yield a response of the follower, because the relative motion is too small.

This implies that there is a perceptual threshold. Only when thresholds are reached, the following driver can perceive the changes in the relative speed or spacing. Such perceptual thresholds are shown as Figure 2-5.

Widemann [1974] introduces the Psycho-Physical Spacing Model into microscopic simulator and design the INTAC Model to be Behavioral Threshold Model. Traffic flow is classified into several reaction zones (as shown in Figure 2-6).

The meaning of each threshold is [Fellendorf, 1997]:

A. Standstill spacing (AX): the desired distance between two cars in a standing queue.

B. Minimum safe spacing (BX): the minimum safe spacing when the velocity of follower is close to its lead vehicle.

C. Perceptual velocity difference threshold (SDV): action point where a driver consciously observes that he approaches a slower lead vehicle. SDV increases with speed difference.

D. Maximum car-following spacing (SDX): concerning the difference among different drivers, the range of SDX is about 1.5-2.5 times BX.

E. OPDV: action point where a driver notices that he is slower than the lead vehicle and starts to accelerate again.
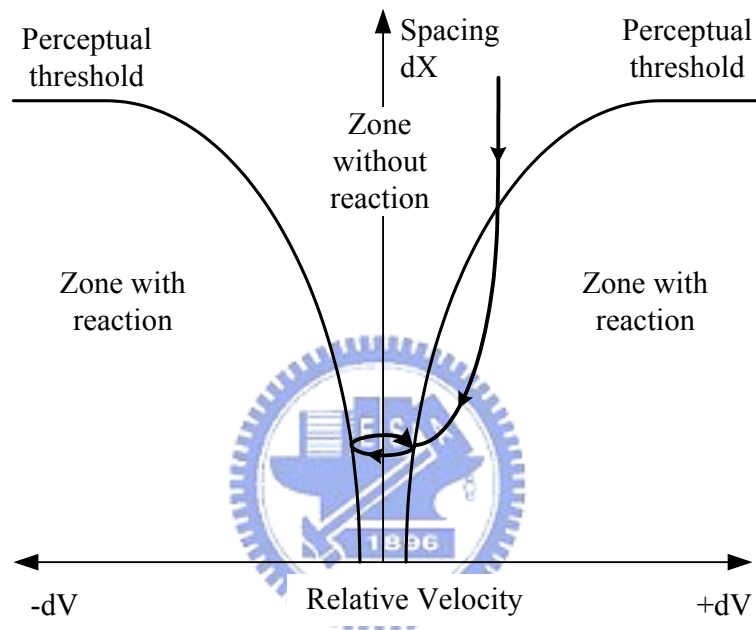
Figure 2-5 Perceptual thresholds of car-following process
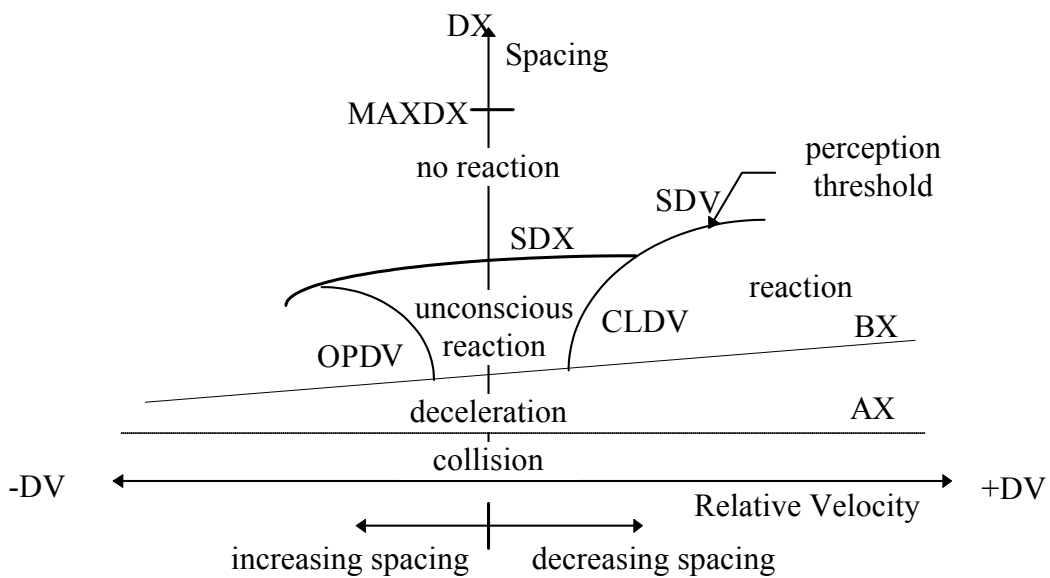
Figure 2-6 Behavioral zones of behavioral threshold model

(4). CARSIM

CARSIM (CAR-Following Simulation Model) is developed by Benekohal [1988]. Several acceleration or deceleration rates are computed for different conditions, and the most suitable one is selected for each vehicle in each time interval. Each condition is described as following.

A1: The following vehicle is moving but has not reached its speed limit or desired speed.

A2: The following vehicle has reached its speed limit or desired speed.

A3: The follower was stopped and has to start from a standing still position

A4: The follower's performance is governed by the car-following algorithm while space headway constraint is satisfied. The acceleration is computed from the following equation

$$X_L - \left(X_F + V_F(DT) + 0.5(A4)(DT)^2\right) \geq L_L + K, \tag{2.4}$$

where

X_L : the position of the lead vehicle

X_F : the position of the following vehicle

L_L : the length of the lead vehicle

K : the buffer space between vehicles

DT : the simulation scanning time interval (1 second)

$A4$: the acceleration or deceleration in the condition

A5: The following vehicle is advanced according to the car-following algorithm with non-collision constraint. The following equation is used to assure that enough spacing is provided.

$$X_L - \left(X_F + V_F(DT) + 0.5(A5)(DT)^2\right) - L_L - K \geq$$
$$\text{maximum of} \begin{vmatrix} [V_F + (A5)(DT)](BRT), \\ \left[[V_F + (A5)(DT)](BRT) + \frac{[V_F + (A5)(DT)]^2}{2(MX.F)} - \frac{X_L^2}{2(MX.L)} \right] \end{vmatrix} \tag{2.5}$$

where:

BRT : brake-reaction time of a driver

V_L : velocity of the lead car at the end of time interval

MX.F : maximum deceleration rate of the following car

MX.L : maximum deceleration rate of the lead car

A5 : the acceleration and deceleration in the condition

The strengths of CARSIM are described as following [Benekohal, 1988].

1. The vehicles' acceleration and deceleration rates were kept with the reasonable values observed in actual traffic conditions, and marginally safe spacings were provided for all vehicles.

2. The delay in response of the follower to the lead vehicle's deceleration was taken into account. The delay is equal to the reaction time of the driver.

3. The start-up delay of a stopped vehicle was taken into consideration.

4. The dual behavior of traffic in congested and non-congested conditions is taken into account.

5. CARSIM uses varying reaction times for an individual driver and different reaction times for different drivers. The reaction time of a driver in congested traffic is less than the reaction time of light traffic.

6. CARSIM can simulate stop-and-go condition.

The deficiencies of CARSIM are described as following [Aycin, 1999].

1. CARSIM performs car-following by considering emergency braking of the lead vehicle, but a follower cannot have the information about the deceleration capability of its leader.

2. CARSIM considers driver's reaction time, and it results in a driver with higher reaction time keeps longer spacing.

(5). Fuzzy Models

Kakuchi [Kakuchi, 1992, Chakroborty, 1999] proposed a fuzzy inference car-following model. It consists of 396 rules which are based on the relative speed, the spacing, and the acceleration of the lead vehicle. After defuzzifying, the model outputs the acceleration of the following vehicle.

McDonald [1997] proposed another fuzzy model, and it includes car-following and lane-changing. The model takes into account desired car-following spacing, and the inference rules are based on distance divergence and relative velocity.

Most of traditional car-following models are deterministic, but drivers do not completely follow any deterministic behavior. Fuzzy models represent an approximate nature behavior. They represent the natural language based "rules-of-thumb" of driving which is believed to be reasonable and uses the compromise of more than one rule of behavior.

The strengths of fuzzy models are described as following.

1. Car-following is an approximate nature behavior, and fuzzy models represent the property.

2. Fuzzy models can describe closing-in and shying-away phenomena.

3. The response of fuzzy models is asymmetric.

4. In fact, stable distance headway is only dependent on final speed, and fuzzy models represent it.

2.3 Static Macroscopic Traffic Flow Models

Macroscopic traffic flow models discuss flow, density, and speed. The relationship between these variables is $q = ku$, where q denotes flow, k denotes density, and u denotes velocity.

Some researchers discussed the relationship between density and velocity based on filed data or some theory. Greenshield [1934], as one of the early investigators of traffic characteristics, proposed a linear relationship. Greenberg [1959], using a theoretical background, has postulated a logarithmic speed-density model. Greenberg's model is useful under high density but not under low density. Underwood [1961] proposed a speed-density model for low density traffic. Later, Pipes [1967] and Munjal [1971] developed a general family of speed-density models of which the linear model is a special case. Drew [1968] proposed a family of models of which Greenberg's logarithmic model is a special case.

As some aforementioned models are only useful under some traffic condition, some researchers proposed multi-regime models. Edie [1961] described a model that

is a composite of Greenberg and Underwood models, where Greenberg is useful at high density and Underwood is useful at low density. Other research results of the static macroscopic model are summarized in Table 2.2 and Table 2.3 May [1990].

Table 2.2 Table of single-regime models

Single-regime models	Equations
Greenshields model (1934)	$u = u_f \left(1 - \dfrac{k}{k_j}\right)$
Greenberg model (1959)	$u = u_0 \ln\left(\dfrac{k_j}{k}\right)$
Underwood model (1961)	$u = u_f e^{-k/k_0}$
Northwestern's model (1967)	$u = u_f e^{-1/2\left(k/k_o\right)^2}$
Drew model (1968)	$u = u_f \left[1 - \left(\dfrac{k}{k_j}\right)^{(n+1)/2}\right]$
Pipes-Munjal model (1967)	$u = u_f \left[1 - \left(\dfrac{k}{k_j}\right)^n\right]$
	u_f ：free flow speed $\quad k_j$ ：congested density $\quad u_o$ ：critical speed $\quad k_o$ ：critical density

Table 2.3 Table of multi-regime models

Multiregime models	Free-flow regime	Transitional-flow regime	Congested-flow regime
Edie model (1961)	$u = u_f e^{-k/k_0}$ $\left(k \le k_o\right)$	—	$u = u_0 \ln\left(\dfrac{k_j}{k}\right)$ $\left(k \ge k_o\right)$
Two-regime linear model (1967)	$u = u_f \left(1 - \dfrac{k}{k_j}\right)$ $\left(k \le k_1\right)$	—	$u = u_f \left(1 - \dfrac{k}{k_j}\right)$ $\left(k \ge k_1\right)$
Modified Greenberg model (1967)	constant speed $\left(k \le k_2\right)$	—	$u = u_0 \ln\left(\dfrac{k_j}{k}\right)$ $\left(k \ge k_2\right)$
Three-regime linear model (1967)	$u = u_f \left(1 - \dfrac{k}{k_j}\right)$ $\left(k \le k_3\right)$	$u = u_f \left(1 - \dfrac{k}{k_j}\right)$ $\left(k_4 \le k \le k_3\right)$	$u = u_f \left(1 - \dfrac{k}{k_j}\right)$ $\left(k \ge k_4\right)$
	k_i ：specified traffic density ，i=1.2.3.4		

Different free-flow speeds result in different speed-flow relationships. Figure 2-7 indicates that average speed under the same flow rate increases with free-flow speed. The speed is insensitive to flow in the low to moderate range.
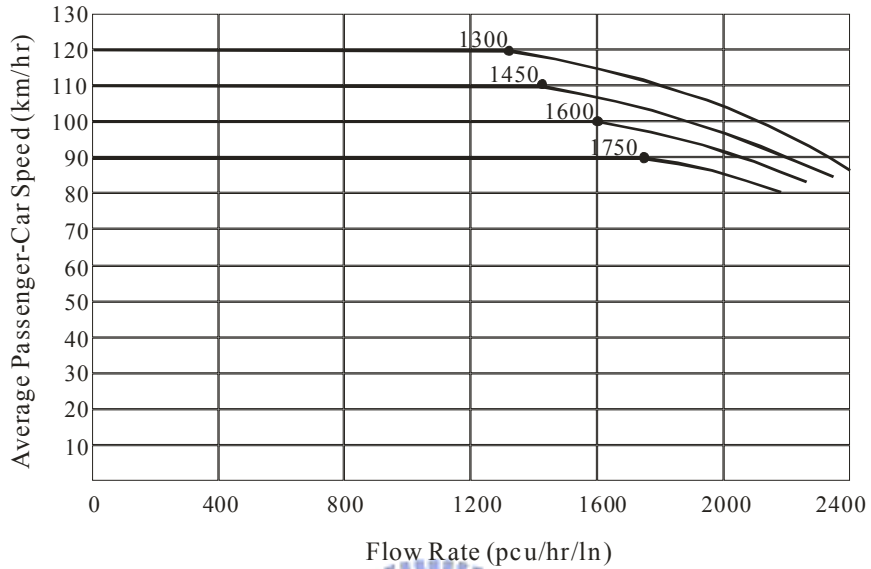
Figure 2-7 Speed-flow relationships (reproduced) [TRB, 2000]
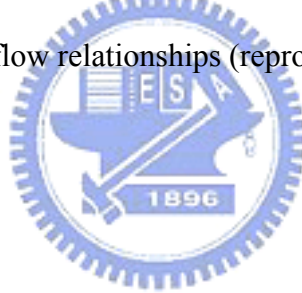
2.4 Linearized Stability of Dynamical Systems

The general forms for dynamical system are shown as Eqs. (2.6) and (2.7) .

$$\mathbf{x}' = f(\mathbf{x}) \qquad \text{for continuous time,} \qquad (2.6)$$

$$\mathbf{x}_{k+1} = f(\mathbf{x}_k) \qquad \text{for discrete time,} \qquad (2.7)$$

where $\mathbf{x} \in R^n$.

$\mathbf{x}$ is the state of the continuous dynamical system, and $\mathbf{x}_k$ is the state of the discrete dynamical system at time k. f is the state-transition function. For any initial state $\mathbf{x}_0$, Eq (2.7) uniquely determines the state trajectory, $\mathbf{x}_k$, $k \geq 0$.

Any state of a dynamical system is either an equilibrium state or a disequilibrium state. An equilibrium state of a dynamical system is a state $\bar{\mathbf{x}}$ with the property that if the system is ever in the state $\bar{\mathbf{x}}$, it will remain in that state for all time until perturbation occurs.

The equilibrium solution of a continuous dynamical system is $f(\bar{\mathbf{x}}) = 0$. The equilibrium solution of a discrete dynamical system is $\bar{\mathbf{x}} = f(\bar{\mathbf{x}})$

An equilibrium state $\bar{\mathbf{x}}$ is called stable or marginally stable if for arbitrary $\varepsilon > 0$, there is a $\delta > 0$ such that $\|\mathbf{x}_0 - \bar{\mathbf{x}}\| < \delta$ implies that for all $k \geq 0$, $\|\mathbf{x}_k - \bar{\mathbf{x}}\| < \varepsilon$. An equilibrium state is asymptotically stable if it is marginally stable and there exists a $\Delta > 0$ such that $\|\mathbf{x}_0 - \bar{\mathbf{x}}\| < \Delta$ implies that $\mathbf{x}_k \to \bar{\mathbf{x}}$ as $k \to \infty$. An equilibrium is globally asymptotically stable if it is marginally stable and $\mathbf{x}_k \to \bar{\mathbf{x}}$ as $k \to \infty$ with any arbitrary initial state $\mathbf{x}_0$ [Li & Szidarovszky, 1999].

$\bar{\mathbf{x}}$ is asymptotically stable if all eigenvalues of $Df(\bar{\mathbf{x}})$ have negative real parts for a continuous dynamical system [Wiggins, 1990]. For a discrete dynamical system, $\bar{\mathbf{x}}$ is asymptotically stable if all eigenvalues of $Df(\bar{\mathbf{x}})$ are less than 1.

2.5 Summary and Discussion

According to the above-mentioned review, some traffic phenomena are summarized as following.

(1) Equilibrium spacing: If a following vehicle reaches and keeps at a particular spacing, the particular spacing is only dependent on final speed. Hence, a driver with higher reaction time has longer equilibrium spacing is not very reasonable, since the equilibrium spacing is not dependent on driver's reaction time.

(2) Traffic stability: From the viewpoint of microscopic traffic flow, higher reaction time makes unstable traffic likely to occur.

(3) Closing-in and shying-away: Relative speed cannot ensure the acceleration is positive or negative.

(4) Traffic hysteresis: Speed-density relationships for acceleration and deceleration traffic are different.

(5) Driver characteristics: Different drivers have different behaviors. Some drivers are aggressive, some are not. Drivers may keep different velocities or different spacings under the same conditions.

(6) Stable traffic versus unstable traffic: unstable traffic occurs at high density.

Some strengths or deficiencies of car-following models are summarized as following.

(1) Relative speed form: If driver's acceleration is only dependent on relative speed, the model cannot represent closing-in and shying-away phenomena, and cannot describe asymmetric response.

(2) Considering enough spacing: If a driver takes enough spacing into account, he must consider emergency braking of the lead vehicle, but he cannot have the information about the deceleration capability of his leader. Furthermore, he should consider his reaction time, and it results in a driver with higher reaction time keeps longer spacing.

(3) Driver characteristics: Some traditional car-following models cannot reflect the difference between drivers. Some models employ sensitivity or aggressiveness factor to describe the diver difference. However, these factors cannot be measured directly.

(4) Simple models versus complex models: simple models that have one or few functions, such as safe-distance models and stimulus-response model, cannot describe some traffic phenomena. On the other hand, simple models can extend to macroscopic traffic flow more easily. For example, stimulus-response model can extend to macroscopic models, such as Greenshield's model, Greenberg's model, and Edie's model [May, 1990]. The models that have different rules for different conditions describe the traffic flow better, but their computations are more complicated. It is difficult to develop a macroscopic traffic flow model based on these models. It is also difficult to derive traffic properties from complex models.

Static macroscopic traffic flow models frequently serve as a state equation in dynamic macroscopic traffic flow models, and they are regarded as the equilibrium state of traffic flow. According to aforementioned, static traffic flow models may be developed based on disequilibrium field data, i.e., include acceleration and deceleration traffic. For example, Greenberg proposed his model for high density traffic, but heavy traffic could hardly reach its equilibrium state.

Chapter 3
Car-Following Model

A simple car-following model is developed in this section, and the model should achieve the following objectives. First, the model should describe microscopic car-following phenomena, such as closing-in, shying-away, and traffic hysteresis. Second, the model should reflect differences among individual drivers. Third, it should avoid certain deficiencies mentioned in Chapter 2, such as drivers having to determine the deceleration capability of their lead vehicle. Finally, the model should minimize the number of rules employed to facilitate its extension to macroscopic traffic flow models.

3.1 Model Assumption

The car-following process is influenced by driver characteristics, external environment, and lead vehicle. If there is no lead vehicle, a vehicle will run at a specific speed (its individual maximum speed) influenced only by driver characteristics and external environment. Hence, an individual maximum speed of a vehicle is influenced by driver characteristics and external environment. In other words, the influence of driver characteristics and external environment on a vehicle is presented in the individual maximum speed of the vehicle. Driving alone, different drivers may run at different speeds on the same road, implying that different drivers (i.e. different driver characteristics) have different individual maximum speeds. Driver individual maximum speed may vary with external environment, such as freeway, urban street, and sunny versus rainy days. As driver characteristics and external environment are difficult to measure, the proposed model considers individual maximum speed to help reflecting the influence of driver characteristics and external environment. The individual maximum speed of a vehicle can be measured under certain situations. Where no lead vehicle is present, the vehicle speed is the individual maximum speed. Otherwise, if the speed of the following vehicle does not change with lead vehicle speed or spacing, its speed is considered to be its individual maximum speed.

If there is a lead vehicle, and as the spacing decreases, the following vehicle may slow down so that it cannot run at its individual maximum speed. According to the literature, following vehicle speed depends on the speed of the lead vehicle, the speed

23

of itself, and the spacing between vehicles. Hence, the variables of the proposed model are individual maximum speed, the speed of the lead vehicle, the speed of itself, and the spacing between vehicles.

To model the aforementioned phenomena, the proposed model assumes that repulsion and thrust act on the following vehicle, which then sets an appropriate speed accordingly. Figure 3-1 presents the proposed model. The model assumptions are listed below:

Figure 3-1 Illustration of the car-following concept

(1) Aggressiveness

The proposed model assumes that driver aggression increases with individual maximum speed. Drivers with high individual maximum speed maintain a higher speed or shorter spacing than do drivers with low individual maximum speed under identical conditions, and also have faster acceleration or deceleration.

(2) Velocity Decision

The following vehicle decides its appropriate velocity based on existing thrust and repulsion, with the appropriate velocity equaling thrust minus repulsion.

(3) Thrust

Each vehicle has its own individual maximum speed, which is regarded as the thrust. The individual maximum speed thus becomes the force driving the following vehicle forward. If there is no lead vehicle, the vehicle will run at its individual maximum speed $v_{n,d}$. Individual maximum speed depends on external environment and driver characteristics, which are not determined by car-following process. Individual maximum speed thus is an exogenous variable.

(4) Repulsion

Because the lead vehicle can prevent the following vehicle from running at its individual maximum speed $v_{n,d}$, the lead vehicle is considered to be repelling the follower. Since the following vehicle speed is influenced by the lead vehicle speed $V_{n-1,t}$, the follower speed $V_{n,t}$, and the spacing $H_{n,t}$, the repulsion is related to these factors.

(a) *Spacing* $H_{n,t}$

(i) Given longer spacing $H_{n,t}$, the repulsion should be reduced because a driver will maintain higher velocity $V_{n,t+1}$ under no changes in the lead vehicle speed $V_{n-1,t}$ and the following vehicle speed $V_{n,t}$.

(ii) The following vehicle speed $V_{n,t+1}$ varies with changes in the spacing $H_{n,t}$. The variation of $H_{n,t}$ in $V_{n,t+1}$ is regarded as the sensitivity to $H_{n,t}$, and $\psi_{H,n}$ denotes the sensitivity. At a large spacing $H_{n,t}$, the following vehicle is not influenced by the lead vehicle, and thus $V_{n,t+1}$ is not sensitive to the changes in $H_{n,t}$, i.e. the sensitivity $\psi_{H,n}$ is zero. On the other hand, when the spacing $H_{n,t}$ is shorter, a driver is more sensitive to the changes in spacing. Hence, the sensitivity $\psi_{H,n}$ increases with reducing spacing.

(iii) Continued from the preceding assumption (ii), when spacing is very short, a following driver may be very sensitive to or not sensitive to the changes in spacing. Because a driver may perceive that the spacing is too short, running at a very low velocity $V_{n,t+1}$ is his unique choice even though the spacing becomes slightly longer. Hence, the sensitivity $\psi_{H,n}$ may be very large or very small at short $H_{n,t}$.

(iv) If the spacing is in some specific car-following distance, the following vehicle is influenced by its leader. Otherwise, if the spacing is out of some specific car-following distance, the following vehicle is not influenced by its leader. The specific car-following distance is defined as critical car-following distance. At identical following vehicle speed $V_{n,t}$, the critical car-following distance increases with reducing lead vehicle speed $V_{n-1,t}$.

(v) At identical lead vehicle speed $V_{n-1,t}$, the critical car-following distance increases with the following vehicle speed.

(vi) At identical following vehicle speed, lower lead vehicle speed $V_{n-1,t}$ makes drivers be more sensitive to the movement of the lead vehicle. Thus,

drivers are more sensitive to the changes in spacing, i.e. the sensitivity $\psi_{H,n}$ increases as the lead vehicle speed $V_{n-1,t}$ decreases.

(vii) Continued from the preceding assumption (vi), if the spacing is very short, running at a very low velocity $V_{n,t+1}$ is the only choice for the driver whose lead vehicle speed $V_{n-1,t}$ is low. Otherwise, if the lead vehicle speed is faster, a driver has more flexibility in choosing his vehicle speed $V_{n,t+1}$ after a reaction time. Faster lead vehicle speed $V_{n-1,t}$ makes drivers have more flexibility in choosing their speed $V_{n,t+1}$ at short spacing, so drivers are more sensitive to the movement of their lead vehicles. Hence, the sensitivity $\psi_{H,n}$ increases with the lead vehicle speed $V_{n-1,t}$ at short spacing.

(viii) At identical lead vehicle speed $V_{n-1,t}$, a driver with higher vehicle speed $V_{n,t}$ is more sensitive to the movement of the lead vehicle, and thus he is more sensitive to the changes in spacing, i.e. the sensitivity $\psi_{H,n}$ increases with the following vehicle speed.

(ix) Continued from the preceding assumption (viii), if the spacing is very short, running at a very low velocity $V_{n,t+1}$ is the only choice for the driver whose previous vehicle speed $V_{n,t}$ is fast. Otherwise, if his previous vehicle speed $V_{n,t}$ is slower, a driver has more flexibility in choosing his vehicle speed $V_{n,t+1}$. Higher vehicle speed $V_{n,t}$ makes drivers have less flexibility in choosing their speed $V_{n,t+1}$ at short spacing. Hence, the sensitivity $\psi_{H,n}$ increases with reducing $V_{n,t}$ at short spacing.

(b) *Lead vehicle speed* $V_{n-1,t}$

(i) Under identical traffic conditions, drivers maintain higher velocity $V_{n,t+1}$ at higher lead vehicle speed $V_{n-1,t}$, and the repulsion should be reduced.

(ii) The following vehicle speed $V_{n,t+1}$ varies with changes in the lead vehicle speed $V_{n-1,t}$. The variation of $V_{n-1,t}$ in $V_{n,t+1}$ is regarded as the sensitivity

26

to $V_{n-1,t}$ and $\psi_{V,n-1}$ denotes the sensitivity. If $V_{n-1,t}$ approaches infinity, a driver may not perceive the obstacle created by the lead vehicle. Hence, $V_{n,t+1}$ is not sensitive to the changes in $V_{n-1,t}$, i.e. the sensitivity $\psi_{V,n-1}$ is zero. On the other hand, when $V_{n-1,t}$ is small, a driver is very sensitive to the changes in $V_{n-1,t}$. Hence, the sensitivity $\psi_{V,n-1}$ decreases as $V_{n-1,t}$ increases.

(iii) Continued from the preceding assumption (ii), when $V_{n-1,t}$ is very small, following driver may be very sensitive to the changes in $V_{n-1,t}$ or not sensitive. Because a driver may perceive that the lead vehicle is too slow, running at a very low velocity is his unique choice even though the lead vehicle runs slightly faster. Hence, the sensitivity $\psi_{V,n-1}$ may be very large or very small at low $V_{n-1,t}$.

(iv) At identical following vehicle speed $V_{n,t}$, lower spacing makes drivers pay more attention to the movement of their lead vehicles, and thus be more sensitive to the changes in lead vehicle speeds $V_{n-1,t}$, i.e. the sensitivity $\psi_{V,n-1}$ increases with reducing spacing.

(v) Continued from the preceding assumption (iv), if the lead vehicle speed $V_{n-1,t}$ is very low, running at a very low velocity $V_{n,t+1}$ is the only choice for the driver whose spacing is short. Otherwise, if the spacing is longer, a driver has more flexibility in choosing his vehicle speed $V_{n,t+1}$ after a reaction time. Longer spacing makes drivers have more flexibility in choosing their speed $V_{n,t+1}$ at low lead vehicle speed $V_{n-1,t}$, so drivers are more sensitive to the movement of their lead vehicles. Hence, the sensitivity $\psi_{V,n-1}$ increases with spacing at low lead vehicle speed $V_{n-1,t}$.

(vi) At identical spacing, a driver with higher velocity $V_{n,t}$ pay more attention to the movement of his lead vehicle, and thus he is more sensitive to the changes in the lead vehicle speed $V_{n-1,t}$, i.e. the sensitivity $\psi_{V,n-1}$ increases with the following vehicle speed $V_{n,t}$.

(vii) Continued from the preceding assumption (vi), if the lead vehicle runs too slow, running at a very low velocity $V_{n,t+1}$ is the only choice for the driver whose previous vehicle speed $V_{n,t}$ is high. Otherwise, if his previous vehicle speed $V_{n,t}$ is slower, a driver has more flexibility in choosing his vehicle speed $V_{n,t+1}$. Higher vehicle speed $V_{n,t}$ makes drivers have less flexibility in choosing their speed $V_{n,t+1}$ at short spacing. Hence, the sensitivity $\psi_{V,n-1}$ increases with reducing $V_{n,t}$ at low lead vehicle speed $V_{n-1,t}$.

(c) *Following vehicle speed $V_{n,t}$*

(i) A driver may slow down if his speed $V_{n,t}$ is too fast, and may speed up if his speed $V_{n,t}$ is too slow. Hence, the repulsion increases with the follower speed $V_{n,t}$.

(ii) The following vehicle speed $V_{n,t+1}$ varies with changes in the lead vehicle speed $V_{n,t}$. The variation of $V_{n,t}$ in $V_{n,t+1}$ is regarded as the sensitivity to $V_{n,t}$, and $\psi_{V,n}$ denotes the sensitivity. When $V_{n,t}$ is very large or very small, a driver may perceive that his speed is too fast or too slow. Thus, running at a low or high speed is his unique choice, and $V_{n,t+1}$ is not very sensitive to the changes in $V_{n,t}$.

(iii) When the lead vehicle and the following vehicle speeds are identical, the critical car-following distance increases with vehicles speed $V_{n,t}$ or different speeds result in identical critical car-following distance.

(iv) When the lead vehicle and the following vehicle speeds are identical, a driver with higher vehicle speed perceives the repulsion more.

As an aggressive driver may perceive the obstacle created by the lead vehicle as being of greater significance, it is also assumed that a driver with a higher individual maximum speed will perceive higher repulsion under the same traffic conditions.

(5) <u>Safety</u>

Since some drivers exhibit unsafe behaviors, the proposed model assumes that moving vehicles do not consider safe distance. Drivers only consider the standstill spacing.

3.2 Modeling

When both the lead vehicle and the following vehicle are moving, the following vehicle decides its appropriate velocity based on existing thrust and repulsion, with the appropriate velocity equaling thrust minus repulsion. The repulsion is related to the speed of the lead vehicle, the speed of the follower, and the spacing. Hence, repulsion is a function of $V_{n-1,t}$, $V_{n,t}$, $H_{n,t}$ and the vehicle speed can be represented as

$$\tilde{V}_{n,t+1} = v_{n,d} - R\left(V_{n-1,t}, V_{n,t}, H_{n,t}\right), \tag{3.1}$$

where $R\left(V_{n-1,t}, V_{n,t}, H_{n,t}\right)$ is the repulsion. A driver with a higher individual maximum speed perceives higher repulsion under identical traffic conditions. Hence the repulsion is expressed as

$$R\left(V_{n-1,t}, V_{n,t}, H_{n,t}\right) = v_{n,d}\, r\left(V_{n-1,t}, V_{n,t}, H_{n,t}\right). \tag{3.2}$$

Therefore, the vehicle speed is

$$\tilde{V}_{n,t+1} = v_{n,d}\left(1 - r\left(V_{n-1,t}, V_{n,t}, H_{n,t}\right)\right), \tag{3.3}$$

and the range of $r\left(V_{n-1,t}, V_{n,t}, H_{n,t}\right)$ is shown as Eq. (3.4):

$$0 < r\left(V_{n-1,t}, V_{n,t}, H_{n,t}\right) < 1 \ . \tag{3.4}$$

Let

$$r\left(V_{n-1,t}, V_{n,t}, H_{n,t}\right) = I\left(P\left(V_{n-1,t}, V_{n,t}, H_{n,t}\right)\right). \tag{3.5}$$

The repulsion increases with reducing $V_{n-1,t}$ or $H_{n,t}$, and it also increases with $V_{n,t}$. To describe closing-in and shying-away phenomena, the relative speed form is not selected because it cannot decide whether the acceleration of the following vehicle is positive or negative. Therefore, $r\left(V_{n-1,t}, V_{n,t}, H_{n,t}\right)$ is represented as Eq. (3.6):

$$P\left(V_{n-1,t}, V_{n,t}, H_{n,t}\right) = \frac{\left(V_{n-1,t}\right)^{\alpha}}{\left(V_{n,t}\right)^{\beta}}\left(\frac{H_{n,t} - S_n}{L}\right)^{\gamma}, \tag{3.6}$$

where α, β, γ, L are positive parameters. Since drivers take standstill distance S_n into account, $H_{n,t} - S_n$ is the gap that a driver perceives. As speed and spacing have different units, the model employs the parameter L to standardize.

Since $0 < V_{n-1,t} \leq v_{n-1,d}$, $0 < V_{n,t} \leq v_{n-1,d}$, and $S_n \leq H_{n,t}$, the range of $P\big(V_{n-1,t}, V_{n,t}, H_{n,t}\big)$ is

$$0 \leq P\big(V_{n-1,t}, V_{n,t}, H_{n,t}\big). \tag{3.7}$$

$P\big(V_{n-1,t}, V_{n,t}, H_{n,t}\big)$ is any arbitrary nonnegative number. As Eqs. (3.4), (3.5) and (3.7), $r\big(V_{n-1,t}, V_{n,t}, H_{n,t}\big)$ is represented as

$$r\big(V_{n-1,t}, V_{n,t}, H_{n,t}\big) = \frac{1}{K^{P\big(V_{n-1,t}, V_{n,t}, H_{n,t}\big)}}, \tag{3.8}$$

where K is a constant and $K > 1$. Let

$$K = \exp(\lambda), \tag{3.9}$$

where λ is a positive model parameter, and then $r\big(V_{n-1,t}, V_{n,t}, H_{n,t}\big)$ can be expressed as

$$r\big(V_{n-1,t}, V_{n,t}, H_{n,t}\big) = \exp\big(-\lambda P\big(V_{n-1,t}, V_{n,t}, H_{n,t}\big)\big). \tag{3.10}$$

As Eqs (3.3), (3.6) and (3.10), the vehicle speed $\tilde{V}_{n,t+1}$ can be expressed as

$$\tilde{V}_{n,t+1} = E\big(V_{n-1,t}, V_{n,t}, H_{n,t}\big) = v_{n,d}\left(1 - \exp\left(-\lambda \frac{\big(V_{n-1,t}\big)^\alpha}{\big(V_{n,t}\big)^\beta}\left(\frac{H_{n,t} - S_n}{L}\right)^\gamma\right)\right) \tag{3.11}$$

More detail discussions about Eq. (3.11) and assumption (4) are discussed in section 3.3.

If both the lead and following vehicles are running, the follower will choose an appropriate speed, which equals thrust minus repulsion (as shown in Eq.(3.11)). Sometimes the same condition results in different speeds for different drivers, the difference is indicated by Eq. (3.11).

If the speed of the lead vehicle is zero, the following vehicle decelerates its speed so that it can stop before a collision occurs. The distance that the following vehicle can move before collision is $H_{n,t} - S_n$. Hence,

$$0 = \big(V_{n,t}\big)^2 + 2a_{n,t}\big(H_{n,t} - S_n\big), \tag{3.12}$$

where $a_{n,t}$ is the acceleration. Thus, the acceleration $a_{n,t}$ is

$$a_{n,t} = -\frac{(V_{n,t})^2}{H_{n,t} - S_n}.$$ (3.13)

Hence, the following vehicle speed at the next time step (i.e., after a reaction time T) is

$$\tilde{V}_{n,t+1} = V_{n,t} - \frac{(V_{n,t})^2}{2(H_{n,t} - S_n)}T.$$ (3.14)

Under identical condition, the following vehicle speed should increase with its lead vehicle speed. As Eq. (3.14) implicitly assumes $V_{n-1,t} = 0$, the vehicle speed of Eq. (3.11) should be greater than the one of Eq. (3.14), i.e.

$$v_{n,d}\left(1 - \exp\left(-\lambda \frac{(V_{n-1,t})^\alpha}{(V_{n,t})^\beta}\left(\frac{H_{n,t} - S_n}{L}\right)^\gamma\right)\right) > V_{n,t} - \frac{(V_{n,t})^2}{2(H_{n,t} - S_n)}T.$$ (3.15)

But inequality (3.15) cannot always hold. For example, if $V_{n-1,t}$ in Eq. (3.11) approaches zero, the solution of Eq. (3.11) may approach zero. But the solution of Eq. (3.14) may not approach zero. Let inequality (3.15) hold, and then

$$V_{n-1,t} > \left(-\lambda^{-1}(V_{n,t})^\beta\left(\frac{H_{n,t} - S_n}{L}\right)^{-\gamma}\ln\left(1 - \frac{1}{v_{n,d}}\left(V_{n,t} - \frac{V_{n,t}^2}{H_{n,t} - S_n}T\right)\right)\right)^{1/\alpha}.$$ (3.16)

If inequality (3.16) holds, inequality (3.15) holds. Thus, if $V_{n-1,t}$ in Eq. (3.11) is greater than the RHS of (3.16), a following vehicle with a moving leading car will choose a higher speed than it with a stopped leading car under identical spacing and identical following vehicle speed. Hence, the premise of Eq. (3.11) is $V_{n-1,t} > V_{n-1,threshold}$ and

$$V_{n-1,threshold} = \left(-\lambda^{-1}(V_{n,t})^\beta\left(\frac{H_{n,t} - S_n}{L}\right)^{-\gamma}\ln\left(1 - \frac{1}{v_{n,d}}\left(V_{n,t} - \frac{V_{n,t}^2}{H_{n,t} - S_n}T\right)\right)\right)^{1/\alpha}.$$ (3.17)

On the other hand, the premise of Eq. (3.14) is $V_{n-1,t} \leq V_{n-1,threshold}$, although Eq. (3.14) implicitly assumes $V_{n-1,t} = 0$. If the lead vehicle runs at a low speed, the following vehicle may regard its leader as a stopped vehicle. Thus the following vehicle starts to slow down and Eq. (3.14) is employed.

$V_{n-1,threshold}$ depends on the spacing $H_{n,t}$, the follower speed $V_{n,t}$, and the individual maximum speed $v_{n,d}$. Under identical spacing and follower speed, different drivers have different $V_{n-1,threshold}$, and $V_{n-1,threshold}$ varies with $v_{n,d}$, that is

$$\frac{\partial V_{n-1,threshold}}{\partial v_{n,d}} = \frac{1}{\alpha}\left(-\lambda^{-1}\left(V_{n,t}\right)^{\beta}\left(\frac{H_{n,t}-S_n}{L}\right)^{-\gamma}\ln\left(1-\frac{1}{v_{n,d}}\left(V_{n,t}-\frac{V_{n,t}^2}{H_{n,t}-S_n}T\right)\right)\right)^{\frac{1}{\alpha}-1}$$
$$\cdot\left(-\lambda^{-1}\left(V_{n,t}\right)^{\beta}\left(\frac{H_{n,t}-S_n}{L}\right)^{-\gamma}\right)\left(1-\frac{1}{v_{n,d}}\left(V_{n,t}-\frac{V_{n,t}^2}{H_{n,t}-S_n}T\right)\right)^{-1}$$
$$\cdot\left(V_{n,t}-\frac{V_{n,t}^2}{H_{n,t}-S_n}T\right)\left(\frac{1}{v_{n,d}^2}\right)<0$$

(3.18)

Eq. (3.18) indicates that a driver with higher individual maximum speed has lower $V_{n-1,threshold}$. It implies that conservative drivers regard a fast lead vehicle as a stopped vehicle under identical spacing and follower speed, and start to slow down. While an aggressive driver only regards a very slow lead vehicle as a stopped vehicle. This conforms to the model assumption (1) that aggressive drivers keep higher velocity under identical traffic condition.

If the lead vehicle is moving and the following vehicle is stopped, the follower will not start to move immediately. The follower usually remains stopped, and only moves once the spacing is greater than a specific spacing Z_n (i.e. the start spacing). The follower then moves at the next time step, with its acceleration equaling its desired start acceleration (as shown in Eq. (3.21)). Finally, if the following vehicle stops and the spacing is less than the start spacing Z_n, the follower remains stopped at the next time step (as shown in Eq. (3.22)).

$$\tilde{V}_{n,t+1}=v_{n,d}\left(1-\exp\left(-\lambda\frac{\left(V_{n-1,t}\right)^{\alpha}}{\left(V_{n,t}\right)^{\beta}}\left(\frac{H_{n,t}-S_n}{L}\right)^{\gamma}\right)\right),\ for\ V_{n-1,t}>V_{n-1,threshold}\ \&\ V_{n,t}\neq 0$$

(3.19)

$$\tilde{V}_{n,t+1}=V_{n,t}-\frac{\left(V_{n,t}\right)^2}{2\left(H_{n,t}-S_n\right)}T,\qquad for\ V_{n-1,t}\leq V_{n-1,threshold}\ \&\ V_{n,t}\neq 0 \qquad (3.20)$$

$$\tilde{V}_{n,t+1}=a_{n,d}T,\qquad for\ V_{n-1,t}\neq 0\ \&\ V_{n,t}=0\ \&\ H_{n,t}\geq Z_n \qquad (3.21)$$

$$\tilde{V}_{n,t+1}=0,\qquad for\ V_{n,t}=0\ \&\ H_{n,t}<Z_n \qquad (3.22)$$

Aside from the repulsion and thrust, the speed of the following vehicle also depends on its capability. Vehicle acceleration should be between the maximum and minimum acceleration of that vehicle. Therefore, the proposed model should be modified as shown in Eq. (3.23), where $a_{n,\max}$ denotes the maximum acceleration of the follower, $a_{n,\min}$ represents the minimum acceleration (i.e. maximum deceleration) of the follower, and T is the length of the time interval.

$$
\begin{aligned}
V_{n,t+1} &= \tilde{V}_{n,t+1}, & &for \quad a_{n,\min} \le a_{n,t+1} \le a_{n,\max} \\
V_{n,t+1} &= V_{n,t} + a_{n,\max}T, & &for \quad a_{n,t+1} > a_{n,\max} \\
V_{n,t+1} &= V_{n,t} + a_{n,\min}T, & &for \quad a_{n,t+1} < a_{n,\min}
\end{aligned} \tag{3.23}
$$

3.3 Sensitivity Analysis

This section discusses how the proposed model output varies with changes in model inputs. The total increment of $\tilde{V}_{n,t+1}$ is

$$
\begin{aligned}
d\tilde{V}_{n,t+1} &= \frac{\partial E}{\partial V_{n-1,t}}\left(V_{n-1,t},V_{n,t},H_{n,t}\right)dV_{n-1,t} + \frac{\partial E}{\partial V_{n,t}}\left(V_{n-1,t},V_{n,t},H_{n,t}\right)dV_{n,t} \\
&\quad + \frac{\partial E}{\partial H_{n,t}}\left(V_{n-1,t},V_{n,t},H_{n,t}\right)dH_{n,t}
\end{aligned} \tag{3.24}
$$

$\tilde{V}_{n,t+1}$ varies with the spacing $H_{n,t}$, the lead vehicle speed $V_{n-1,t}$, and the following vehicle speed $V_{n,t}$. Next, each model input is discussed.

(1) spacing $H_{n,t}$

The variation of $H_{n,t}$ in $V_{n,t+1}$ is regarded as the sensitivity to $H_{n,t}$, and $\psi_{H,n}$ denotes the sensitivity. Thus

$$
\begin{aligned}
\psi_{H,n} &= \frac{\partial E}{\partial H_{n,t}}\left(V_{n-1,t},V_{n,t},H_{n,t}\right) \\
&= \frac{v_{n,d}\gamma\lambda}{L}\left(\frac{\left(V_{n-1,t}\right)^{\alpha}}{\left(V_{n,t}\right)^{\beta}}\left(\frac{H_{n,t}-S_n}{L}\right)^{\gamma-1}\right)\exp\left(-\lambda\frac{\left(V_{n-1,t}\right)^{\alpha}}{\left(V_{n,t}\right)^{\beta}}\left(\frac{H_{n,t}-S_n}{L}\right)^{\gamma}\right). \\
&= \frac{v_{n,d}\gamma}{L}\frac{\lambda\dfrac{\left(V_{n-1,t}\right)^{\alpha}}{\left(V_{n,t}\right)^{\beta}}\left(\dfrac{H_{n,t}-S_n}{L}\right)^{\gamma}}{\left(\dfrac{H_{n,t}-S_n}{L}\right)\exp\left(\lambda\dfrac{\left(V_{n-1,t}\right)^{\alpha}}{\left(V_{n,t}\right)^{\beta}}\left(\dfrac{H_{n,t}-S_n}{L}\right)^{\gamma}\right)}
\end{aligned} \tag{3.25}
$$

Eq. (3.25) indicates that $\psi_{H,n} \geq 0$. Since driver maintains higher velocity $V_{n,t+1}$ with higher spacing, $\psi_{H,n}$ is greater than zero. But a driver has his maximum speed $v_{n,d}$ and $V_{n,t+1} \leq v_{n,d}$, a driver cannot always increase his speed with spacing. Thus, $\psi_{H,n} = 0$ occurs at large spacing. On the other hand, when the spacing approaches infinity, the following vehicle is not influenced by the lead vehicle. Hence, $V_{n,t+1}$ is not sensitive to the changes in $H_{n,t}$, and then $\psi_{H,n} = 0$. When spacing approaches infinity, the sensitivity $\psi_{H,n}$ is

$$\lim_{H_{n,t} \to \infty} \frac{\partial E}{\partial H_{n,t}}\left(V_{n-1,t}, V_{n,t}, H_{n,t}\right) = 0. \tag{3.26}$$

As spacing $H_{n,t}$ approaches infinity, $\psi_{H,n}$ equals zero under any positive parameter values. Eq. (3.26) conforms to assumption (4.a.ii).

Shorter spacing makes drivers pay more attention to the movement of their lead vehicles, and thus the sensitivity $\psi_{H,n}$ varies with spacing. The variation of $H_{n,t}$ in $\psi_{H,n}$ is

$$\begin{aligned}
\frac{\partial \psi_{H,n}}{\partial H_{n,t}} &= \frac{\partial^2 E}{\partial H_{n,t}^{\;2}}\left(V_{n-1,t}, V_{n,t}, H_{n,t}\right) \\
&= \frac{v_{n,d}\lambda\gamma}{L^2}\frac{\left(V_{n-1,t}\right)^\alpha}{\left(V_{n,t}\right)^\beta}\left(\frac{H_{n,t}-S_n}{L}\right)^{\gamma-2}\left(-\lambda\gamma\frac{\left(V_{n-1,t}\right)^\alpha}{\left(V_{n,t}\right)^\beta}\left(\frac{H_{n,t}-S_n}{L}\right)^\gamma + \gamma - 1\right). \\
&\quad \cdot \exp\left(-\lambda\frac{\left(V_{n-1,t}\right)^\alpha}{\left(V_{n,t}\right)^\beta}\left(\frac{H_{n,t}-S_n}{L}\right)^\gamma\right)
\end{aligned}$$

$$\tag{3.27}$$

The term $-\lambda\gamma\dfrac{\left(V_{n-1,t}\right)^\alpha}{\left(V_{n,t}\right)^\beta}\left(\dfrac{H_{n,t}-S_n}{L}\right)^\gamma + \gamma - 1$ decides whether $\dfrac{\partial \psi_{H,n}}{\partial H_{n,t}}$ is positive or negative. If $\gamma \leq 1$, $\dfrac{\partial \psi_{H,n}}{\partial H_{n,t}}$ is always less than or equal to 0. When $\gamma > 1$,

$\dfrac{\partial \psi_{H,n}}{\partial H_{n,t}} > 0$ may occur at short spacing $H_{n,t}$. Figs. 3-2 and 3-3 show examples of the relationship between $V_{n,t+1}$ and $H_{n,t}$ and the relationship between $\psi_{H,n}$ and $H_{n,t}$. Both (a) and (b) diagram of Figs 3-2 and 3-3 indicate that when the spacing is not

very short, a driver is more sensitive to the changes in spacing. Hence, the sensitivity $\psi_{H,n}$ increases with reducing spacing.
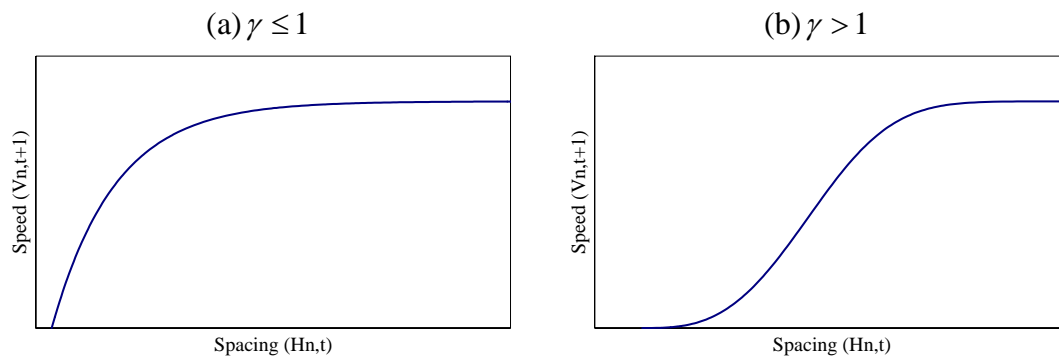

(a) $\gamma \leq 1$ (b) $\gamma > 1$

Figure 3-2 Examples of the relationship between $V_{n,t+1}$ and $H_{n,t}$ under no changes in $V_{n,t}$ and $V_{n-1,t}$
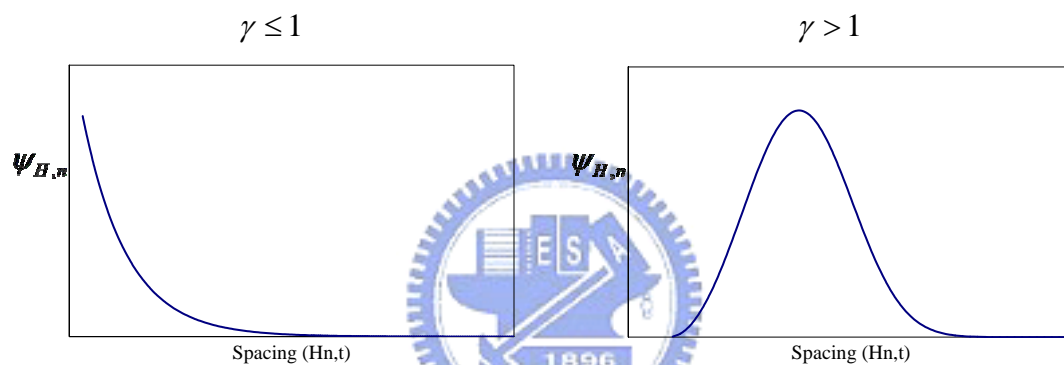

$\gamma \leq 1$ $\gamma > 1$

Figure 3-3 Examples of the relationship between $\psi_{H,n}$ and $H_{n,t}$ under no changes in $V_{n,t}$ and $V_{n-1,t}$

Parameter γ of (a) and (b) diagram in Figs 3-2 and 3-3 are different. They reflect the model assumption (4.a.iii). When spacing is very short, a driver may perceive that the spacing is too short, running at a very low velocity $V_{n,t+1}$ is his unique choice even though the spacing becomes slightly longer. Hence, the sensitivity $\psi_{H,n}$ may be very large or very small at short $H_{n,t}$

At identical following vehicle speed $V_{n,t}$, drivers pay different attention to the lead vehicles with different speeds $V_{n-1,t}$. The sensitivity $\psi_{H,n}$ varies with lead vehicle speed $V_{n-1,t}$:

35

$$\frac{\partial \psi_{H,n}}{\partial V_{n-1,t}} = \frac{\partial^2 E}{\partial V_{n-1,t} \partial H_{n,t}} \left(V_{n-1,t}, V_{n,t}, H_{n,t} \right)$$

$$= \frac{v_{n,d} \lambda \alpha \gamma}{L} \frac{\left(V_{n-1,t}\right)^{\alpha-1}}{\left(V_{n,t}\right)^{\beta}} \left(\frac{H_{n,t} - S_n}{L} \right)^{\gamma-1} \left(1 - \lambda \frac{\left(V_{n-1,t}\right)^{\alpha}}{\left(V_{n,t}\right)^{\beta}} \left(\frac{H_{n,t} - S_n}{L} \right)^{\gamma} \right). \qquad (3.28)$$

$$\cdot \exp\left(-\lambda \frac{\left(V_{n-1,t}\right)^{\alpha}}{\left(V_{n,t}\right)^{\beta}} \left(\frac{H_{n,t} - S_n}{L} \right)^{\gamma} \right)$$

The term $1 - \lambda \frac{\left(V_{n-1,t}\right)^{\alpha}}{\left(V_{n,t}\right)^{\beta}} \left(\frac{H_{n,t} - S_n}{L} \right)^{\gamma}$ decides whether $\frac{\partial \psi_{H,n}}{\partial V_{n-1,t}}$ is positive or negative.

At identical $V_{n,t}$, $\frac{\partial \psi_{H,n}}{\partial V_{n-1,t}} > 0$ occurs at short spacing $H_{n,t}$, while $\frac{\partial \psi_{H,n}}{\partial V_{n-1,t}} < 0$

occurs at long spacing $H_{n,t}$. It implies that the sensitivity $\psi_{H,n}$ increases with lead

vehicle $V_{n-1,t}$ at short spacing, and $\psi_{H,n}$ increases with reducing lead vehicle $V_{n-1,t}$

at long spacing. This conforms to the model assumption (4.a.vi) and (4.a.vii). Drivers

pay closer attention to the lead vehicle with lower speed $V_{n-1,t}$ than to the lead

vehicle with higher speed $V_{n-1,t}$ at long spacing. Thus, lower lead vehicle speed

$V_{n-1,t}$ makes drivers be more sensitive to the movement of the lead vehicle. On the

other hand, if the spacing is very short, running at a very low velocity $V_{n,t+1}$ is the

only choice for the driver whose lead vehicle speed $V_{n-1,t}$ is low. Otherwise, if the

lead vehicle speed is faster, a driver has more flexibility in choosing his vehicle speed

$V_{n,t+1}$. Higher lead vehicle speed $V_{n-1,t}$ makes drivers have more flexibility in

choosing their speed $V_{n,t+1}$ at short spacing, so drivers are more sensitive to the

movement of their lead vehicles. Hence, the sensitivity $\psi_{H,n}$ increases with lead

vehicle speed $V_{n-1,t}$ at short spacing. Examples of the relationship between $V_{n,t+1}$

and $H_{n,t}$ and the relationship between $\psi_{H,n}$ and $H_{n,t}$ with different lead vehicle

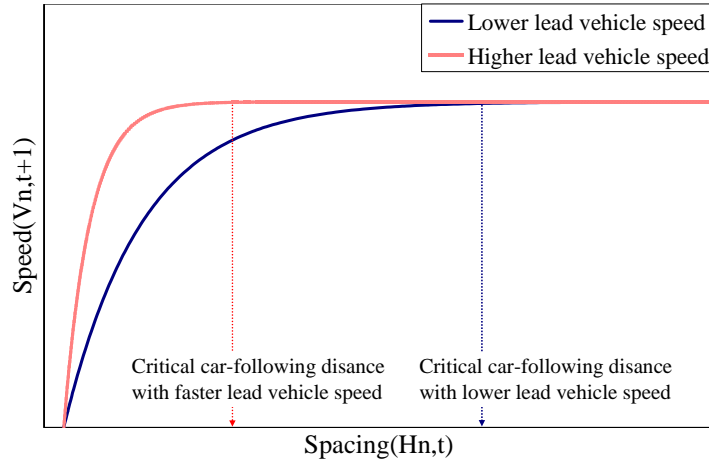speed are shown in Figs. 3-4 and 3-5.

Figure 3-4 Examples of the relationship between $V_{n,t+1}$ and $H_{n,t}$ with different $V_{n-1,t}$
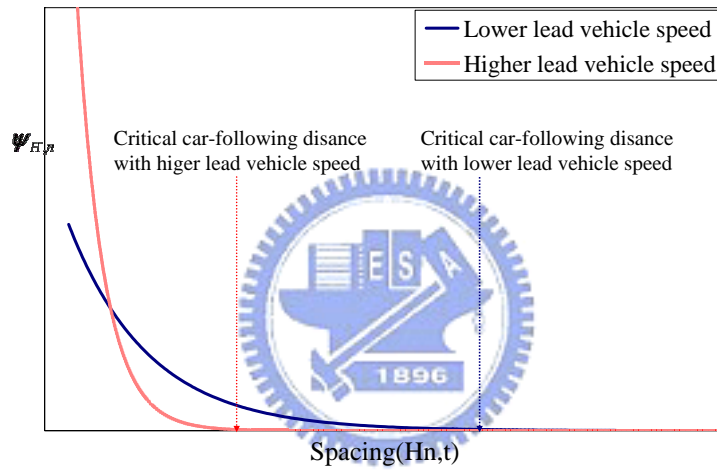

Figure 3-5 Examples of the relationship between $\psi_{H,n}$ and $H_{n,t}$ with different $V_{n-1,t}$

Figs. 3-4 and 3-5 show examples of the relationship between $V_{n,t+1}$ and $H_{n,t}$ and the relationship between $\psi_{H,n}$ and $H_{n,t}$ with different lead vehicle speed. They not only indicate sensitivity $\psi_{H,n}$ varies with lead vehicle speed but also indicate that critical car-following distance varies with lead vehicle speed. As sensitivity $\psi_{H,n}$ decreases with increasing lead vehicle speed $V_{n-1,t}$ at long spacing, the critical car-following distance increases with reducing lead vehicle speed $V_{n-1,t}$, and it conforms to the assumption (4.a.iv).

At identical lead vehicle speed $V_{n-1,t}$, drivers with different speeds $V_{n,t}$ pay different attention to the lead vehicles, and thus the sensitivity $\psi_{H,n}$ varies with vehicle speed $V_{n,t}$:

$$
\begin{aligned}
\frac{\partial \psi_{H,n}}{\partial V_{n,t}} &= \frac{\partial^2 E}{\partial V_{n,t} \partial H_{n,t}}\left(V_{n-1,t}, V_{n,t}, H_{n,t}\right) \\
&= v_{n,d} \frac{\lambda \beta \gamma}{L} \frac{(V_{n-1,t})^\alpha}{(V_{n,t})^{\beta+1}} \left(\frac{H_{n,t} - S_n}{L}\right)^{\gamma-1} \left(\lambda \frac{(V_{n-1,t})^\alpha}{(V_{n,t})^\beta}\left(\frac{H_{n,t} - S_n}{L}\right)^\gamma - 1\right) \cdot \\
&\quad \cdot \exp\left(-\lambda \frac{(V_{n-1,t})^\alpha}{(V_{n,t})^\beta}\left(\frac{H_{n,t} - S_n}{L}\right)^\gamma\right)
\end{aligned}
\tag{3.29}
$$

The term $\lambda \frac{(V_{n-1,t})^\alpha}{(V_{n,t})^\beta}\left(\frac{H_{n,t} - S_n}{L}\right)^\gamma - 1$ decides whether $\frac{\partial \psi_{H,n}}{\partial V_{n,t}}$ is positive or negative.

At identical $V_{n-1,t}$, $\frac{\partial \psi_{H,n}}{\partial V_{n,t}} < 0$ occurs at short spacing $H_{n,t}$, while $\frac{\partial \psi_{H,n}}{\partial V_{n-1,t}} > 0$

occurs at long spacing $H_{n,t}$. It implies that the sensitivity $\psi_{H,n}$ increases with reducing vehicle speed $V_{n,t}$ at short spacing, and $\psi_{H,n}$ increases with vehicle speed $V_{n,t}$ at long spacing. This conforms to the model assumption (4.a.viii) and (4.a.ix). Drivers with higher speed $V_{n,t}$ pay closer attention to the lead vehicle. Thus, higher vehicle speed $V_{n,t}$ makes drivers be more sensitive to the movement of the lead vehicle. On the other hand, if the spacing is too short, running at a very low velocity $V_{n,t+1}$ is the unique choice for the driver whose vehicle speed $V_{n,t}$ is high. Otherwise, a driver with lower speed $V_{n,t}$ has more flexibility in choosing his speed $V_{n,t+1}$, and thus the sensitivity $\psi_{H,n}$ increases with reducing $V_{n,t}$. Examples of the relationship between $V_{n,t+1}$ and $H_{n,t}$ and the relationship between $\psi_{H,n}$ and $H_{n,t}$ with different vehicle speed $V_{n,t}$ are shown in Figs. 3-6 and 3-7.

Figs. 3-6 and 3-7 show examples of the relationship between $V_{n,t+1}$ and $H_{n,t}$ and the relationship between $\psi_{H,n}$ and $H_{n,t}$ with different vehicle speed $V_{n,t}$. They not only indicate sensitivity $\psi_{H,n}$ varies with vehicle speed $V_{n,t}$ but also indicate that critical car-following distance varies with vehicle speed $V_{n,t}$. As sensitivity $\psi_{H,n}$

increases with vehicle speed $V_{n,t}$ at high spacing, the critical car-following distance

increases with vehicle speed $V_{n,t}$, and it conforms to the assumption (4.a.v).
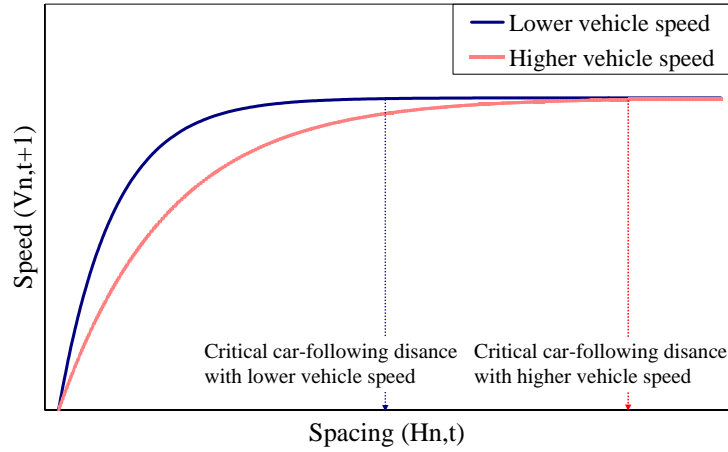

Figure 3-6 Examples of the relationship between $V_{n,t+1}$ and $H_{n,t}$ with different $V_{n,t}$
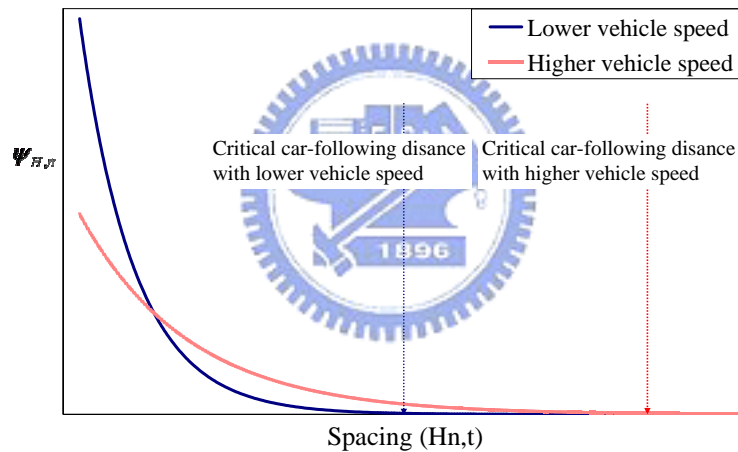

Figure 3-7 Examples of the relationship between $\psi_{H,n}$ and $H_{n,t}$ with different $V_{n,t}$

(2) Lead vehicle speed $V_{n-1,t}$

The variation of $V_{n-1,t}$ in $V_{n,t+1}$ is regarded as the sensitivity to $V_{n-1,t}$, and $\psi_{V,n-1}$ denotes the sensitivity. Thus

$$
\begin{aligned}
\psi_{V,n-1} &= \frac{\partial E}{\partial V_{n-1,t}}\left(V_{n-1,t}, V_{n,t}, H_{n,t}\right) \\
&= v_{n,d}\alpha\lambda\left(\frac{\left(V_{n-1,t}\right)^{\alpha-1}}{\left(V_{n,t}\right)^{\beta}}\left(\frac{H_{n,t}-S_n}{L}\right)^{\gamma}\right)\exp\left(-\lambda\frac{\left(V_{n-1,t}\right)^{\alpha}}{\left(V_{n,t}\right)^{\beta}}\left(\frac{H_{n,t}-S_n}{L}\right)^{\gamma}\right).
\end{aligned} \tag{3.30}
$$

Eq. (3.30) indicates that $\psi_{V,n-1} \geq 0$. Since driver maintains higher velocity $V_{n,t+1}$ with higher lead vehicle speed $V_{n-1,t}$, $\psi_{V,n-1}$ is greater than zero. If the lead vehicle speed could approach infinity, a driver may not perceive the obstacle created by the lead vehicle. Hence, $V_{n,t+1}$ is not sensitive to the changes in $V_{n-1,t}$, and then $\psi_{V,n-1} = 0$. When lead vehicle speed approaches infinity, the sensitivity $\psi_{V,n-1}$ is

$$\lim_{V_{n-1,t} \to \infty} \frac{\partial E}{\partial V_{n-1,t}}\left(V_{n-1,t}, V_{n,t}, H_{n,t}\right) = 0. \tag{3.31}$$

As lead vehicle speed $V_{n-1,t}$ approaches infinity, $\psi_{V,n-1}$ equals zero under any positive parameter values. Eq. (3.31) conforms to assumption (4.b.ii).

Lower lead vehicle speed makes drivers pay more attention to the movement of their lead vehicles, and thus the sensitivity $\psi_{V,n-1}$ varies with lead vehicle speed. The variation of $V_{n-1,t}$ in $\psi_{V,n-1}$ is

$$\frac{\partial \psi_{V,n-1}}{\partial V_{n-1,t}} = v_{n,d}\lambda\alpha\frac{(V_{n-1,t})^{\alpha-2}}{(V_{n,t})^{\beta}}\left(\frac{H_{n,t}-S_n}{L}\right)^{\gamma}\left(-\lambda\alpha\frac{(V_{n-1,t})^{\alpha}}{(V_{n,t})^{\beta}}\left(\frac{H_{n,t}-S_n}{L}\right)^{\gamma} + \alpha - 1\right)$$
$$\cdot \exp\left(-\lambda\frac{(V_{n-1,t})^{\alpha}}{(V_{n,t})^{\beta}}\left(\frac{H_{n,t}-S_n}{L}\right)^{\gamma}\right) \tag{3.32}$$

The term $-\lambda\alpha\frac{(V_{n-1,t})^{\alpha}}{(V_{n,t})^{\beta}}\left(\frac{H_{n,t}-S_n}{L}\right)^{\gamma} + \alpha - 1$ decides whether $\frac{\partial \psi_{V,n-1}}{\partial V_{n-1,t}}$ is positive or negative. If $\alpha \leq 1$, $\frac{\partial \psi_{V,n-1}}{\partial V_{n-1,t}}$ is always less than or equal to 0. When $\alpha > 1$,

$\frac{\partial \psi_{V,n-1}}{\partial V_{n-1,t}} > 0$ may occur at low $V_{n-1,t}$. The relationship between $V_{n,t+1}$ and $V_{n-1,t}$ and the relationship between $\psi_{V,n-1}$ and $V_{n-1,t}$ are similar to Figs. 3-2 and 3-3 (i.e., if $\alpha \leq 1$, they are similar to Figs. 3-2(a) and 3-3(a), and otherwise they are similar to Figs. 3-2(b) and 3-3(b)). When the lead vehicle speed is not very low, a driver is more sensitive to the changes in lead vehicle speed. Hence, the sensitivity $\psi_{V,n-1}$ increases with reducing lead vehicle speed.

Figs. 3-2 and 3-3 reflect the model assumptions (4.b.ii) and (4.b.iii). When lead vehicle speed is very low, a driver may perceive that the lead vehicle is too slow,

running at a very low velocity $V_{n,t+1}$ is his unique choice even though the lead vehicle becomes slightly faster. Hence, the sensitivity $\psi_{V,n-1}$ may be very large or very small at low $V_{n-1,t}$.

At identical following vehicle speed $V_{n,t}$, drivers pay different attention to the lead vehicles with different spacing. The sensitivity $\psi_{V,n-1}$ varies with spacing, that is

$$\frac{\partial \psi_{V,n-1}}{\partial H_{n,t}} = \frac{\partial^2 E}{\partial V_{n-1,t} \partial H_{n,t}} \left(V_{n-1,t}, V_{n,t}, H_{n,t}\right). \tag{3.33}$$

Eq. (3.33) equals Eq. (3.28). The term $1 - \lambda \dfrac{\left(V_{n-1,t}\right)^{\alpha}}{\left(V_{n,t}\right)^{\beta}} \left(\dfrac{H_{n,t} - S_n}{L}\right)^{\gamma}$ decides whether

$\dfrac{\partial \psi_{V,n-1}}{\partial H_{n,t}}$ is positive or negative. At identical $V_{n,t}$, $\dfrac{\partial \psi_{V,n-1}}{\partial H_{n,t}} > 0$ occurs at lower

$V_{n-1,t}$, while $\dfrac{\partial \psi_{V,n-1}}{\partial H_{n,t}} < 0$ occurs at higher $V_{n-1,t}$. It implies that the sensitivity

$\psi_{V,n-1}$ increases with spacing at lower $V_{n-1,t}$, and $\psi_{V,n-1}$ increases with reducing spacing at higher $V_{n-1,t}$. This conforms to the model assumption (4.b.iv) and (4.b.v). If the lead vehicle speed is not very low, drivers pay closer attention to the movement of the lead vehicle at shorter spacing. Otherwise, if the lead vehicle runs very slow, drivers have more flexibility in choosing their vehicle speed $V_{n,t+1}$ at longer spacing.

Hence, the sensitivity $\psi_{V,n-1}$ increases with spacing at low lead vehicle speed $V_{n-1,t}$, and increases with reducing spacing at high lead vehicle speed. Examples of the relationship between $V_{n,t+1}$ and $V_{n-1,t}$, and the relationship between $\psi_{V,n-1}$ and $V_{n-1,t}$ at different spacing are shown in Figs. 3-8 and 3-9.
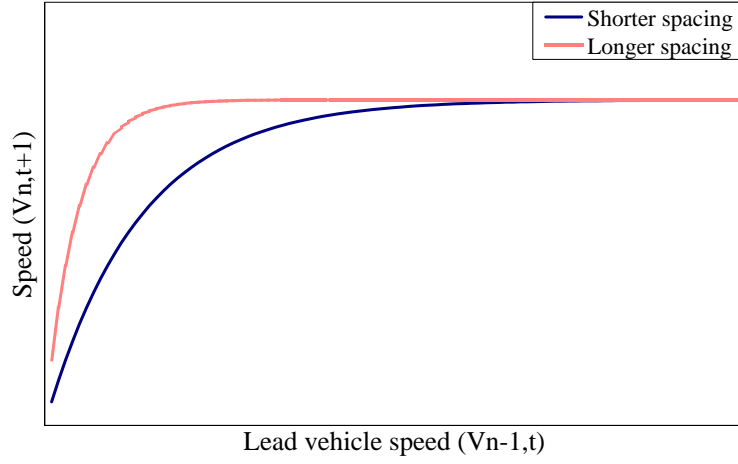
Figure 3-8 Examples of the relationship between $V_{n,t+1}$ and $V_{n-1,t}$ with different spacings
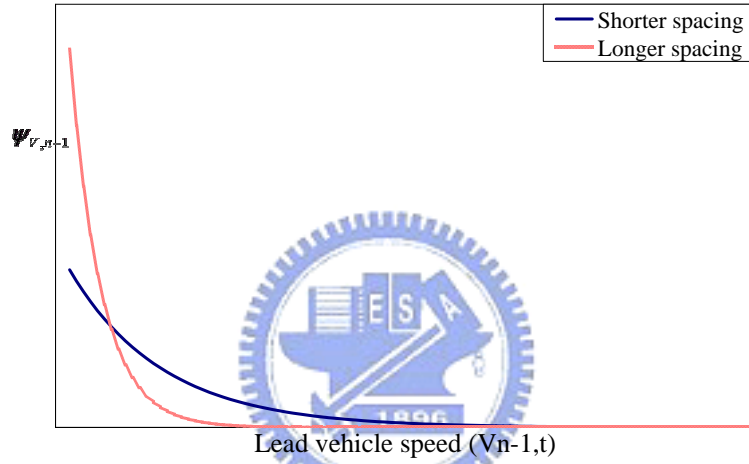

Figure 3-9 Examples of the relationship between $\psi_{V,n-1}$ and $V_{n-1,t}$ with different spacings

At identical spacing, drivers with different speeds $V_{n,t}$ pay different attention to the lead vehicles. The sensitivity $\psi_{V,n-1}$ varies with vehicle speed $V_{n,t}$:

$$
\begin{aligned}
\frac{\partial \psi_{V,n-1}}{\partial V_{n,t}} &= \frac{\partial^2 E}{\partial V_{n-1,t}\partial V_{n,t}}\left(V_{n-1,t},V_{n,t},H_{n,t}\right) \\
&= v_{n,d}\lambda\alpha\beta\frac{\left(V_{n-1,t}\right)^{\alpha-1}}{\left(V_{n,t}\right)^{\beta+1}}\left(\frac{H_{n,t}-S_n}{L}\right)^{\gamma}\left(\lambda\frac{\left(V_{n-1,t}\right)^{\alpha}}{\left(V_{n,t}\right)^{\beta}}\left(\frac{H_{n,t}-S_n}{L}\right)^{\gamma}-1\right). \quad (3.34) \\
&\quad \cdot \exp\left(-\lambda\frac{\left(V_{n-1,t}\right)^{\alpha}}{\left(V_{n,t}\right)^{\beta}}\left(\frac{H_{n,t}-S_n}{L}\right)^{\gamma}\right)
\end{aligned}
$$

The term $\lambda \dfrac{\left(V_{n-1,t}\right)^{\alpha}}{\left(V_{n,t}\right)^{\beta}} \left(\dfrac{H_{n,t} - S_n}{L}\right)^{\gamma} - 1$ decides whether $\dfrac{\partial \psi_{V,n-1}}{\partial V_{n,t}}$ is positive or negative.

At identical spacing, $\dfrac{\partial \psi_{V,n-1}}{\partial V_{n,t}} < 0$ occurs at low lead vehicle speed $V_{n-1,t}$, while

$\dfrac{\partial \psi_{V,n-1}}{\partial V_{n,t}} > 0$ occurs at high lead vehicle speed $V_{n-1,t}$. It implies that the sensitivity

$\psi_{V,n-1}$ increases with reducing vehicle speed $V_{n,t}$ at low $V_{n-1,t}$, and $\psi_{V,n-1}$ increases with vehicle speed $V_{n,t}$ at high lead vehicle speed $V_{n-1,t}$. This conforms to the model assumption (4.b.vi) and (4.b.vii). Drivers with higher speed $V_{n,t}$ pay closer attention to his lead vehicle if his lead vehicle speed is not very low. Thus, higher vehicle speed $V_{n,t}$ makes drivers be more sensitive to the movement of the lead vehicle. On the other hand, if his lead vehicle runs at a very low speed, running at a very low velocity $V_{n,t+1}$ is the only choice for the driver whose vehicle speed $V_{n,t}$ is high. Otherwise, a driver with lower speed $V_{n,t}$ has more flexibility in choosing his speed, and thus the sensitivity $\psi_{V,n-1}$ increases with reducing $V_{n,t}$. Examples of the relationship between $V_{n,t+1}$ and $H_{n,t}$ and the relationship between $\psi_{V,n-1}$ and $H_{n,t}$ with different vehicle speed $V_{n,t}$ are shown in Figs. 3-10 and 3-11.
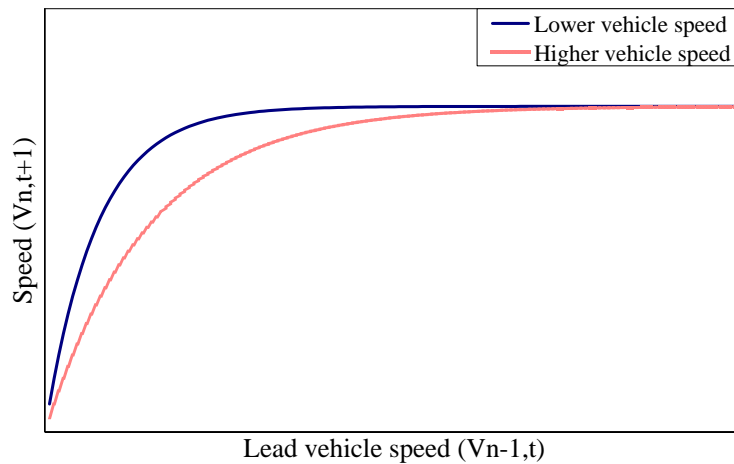

Figure 3-10 Examples of the relationship between $V_{n,t+1}$ and $V_{n-1,t}$ with different $V_{n,t}$
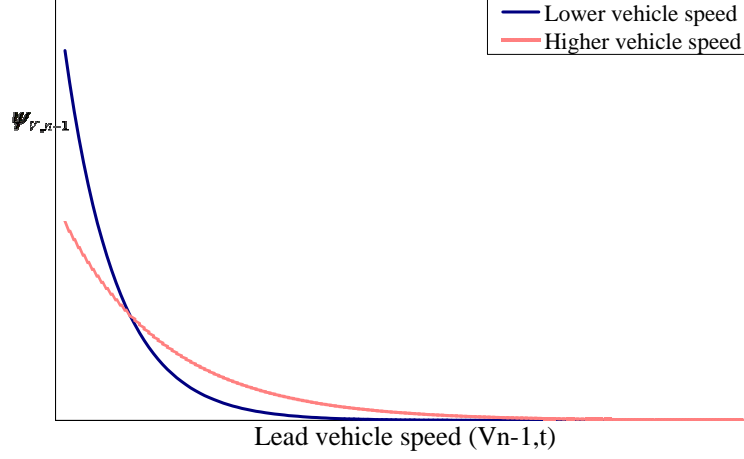
Figure 3-11 Examples of the relationship between $\psi_{V,n-1}$ and $V_{n-1,t}$ with different $V_{n,t}$

(3) Following vehicle speed $V_{n,t}$

The variation of $V_{n,t}$ in $V_{n,t+1}$ is regarded as the sensitivity to $V_{n,t}$, and $\psi_{V,n}$ denotes the sensitivity. Thus

$$
\begin{aligned}
\psi_{V,n} &= \frac{\partial E}{\partial V_{n,t}}\left(V_{n-1,t}, V_{n,t}, H_{n,t}\right) \\
&= -v_{n,d}\beta\lambda\left(\frac{\left(V_{n-1,t}\right)^{\alpha}}{\left(V_{n,t}\right)^{\beta+1}}\left(\frac{H_{n,t}-S_n}{L}\right)^{\gamma}\right)\exp\left(-\lambda\frac{\left(V_{n-1,t}\right)^{\alpha}}{\left(V_{n,t}\right)^{\beta}}\left(\frac{H_{n,t}-S_n}{L}\right)^{\gamma}\right).
\end{aligned}
\tag{3.35}
$$

Eq. (3.35) indicates that $\psi_{V,n} \leq 0$. Since a driver may slow down if his speed $V_{n,t}$ is too high, and may speed up if he runs too slow. If the spacing approaches infinity, the spacing is out of critical car-following spacing, and then $\psi_{V,n} = 0$. Thus, $\psi_{V,n}$ is less than or equal to zero. The sensitivity $\psi_{V,n}$ varies with spacing. The variation of $V_{n,t}$ in $\psi_{H,n}$ is

$$
\begin{aligned}
\frac{\partial \psi_{V,n}}{\partial V_{n,t}} &= \frac{\partial^2 E}{\partial V_{n,t}^2}\left(V_{n-1,t}, V_{n,t}, H_{n,t}\right) \\
&= -v_{n,d}\lambda\beta\frac{\left(V_{n-1,t}\right)^{\alpha}}{\left(V_{n,t}\right)^{\beta+2}}\left(\frac{H_{n,t}-S_n}{L}\right)^{\gamma}\left(\lambda\beta\frac{\left(V_{n-1,t}\right)^{\alpha}}{\left(V_{n,t}\right)^{\beta}}\left(\frac{H_{n,t}-S_n}{L}\right)^{\gamma}-\beta-1\right). \\
&\quad \cdot\exp\left(-\lambda\frac{\left(V_{n-1,t}\right)^{\alpha}}{\left(V_{n,t}\right)^{\beta}}\left(\frac{H_{n,t}-S_n}{L}\right)^{\gamma}\right)
\end{aligned}
\tag{3.36}
$$

The term $\lambda\beta\dfrac{(V_{n-1,t})^{\alpha}}{(V_{n,t})^{\beta}}\left(\dfrac{H_{n,t}-S_n}{L}\right)^{\gamma}-\beta-1=0$ decides whether $\dfrac{\partial\psi_{V,n}}{\partial V_{n,t}}$ is positive or

negative. When $\lambda\beta\dfrac{(V_{n-1,t})^{\alpha}}{(V_{n,t})^{\beta}}\left(\dfrac{H_{n,t}-S_n}{L}\right)^{\gamma}-\beta-1=0$, $\left|\dfrac{\partial\psi_{V,n}}{\partial V_{n,t}}\right|$ has its local maximum.

Suppose the term $\lambda\beta\dfrac{(V_{n-1,t})^{\alpha}}{(V_{n,t})^{\beta}}\left(\dfrac{H_{n,t}-S_n}{L}\right)^{\gamma}-\beta-1=0$ occurs at the point $V_{n,t}^{*}$ (i.e.,

$\lambda\beta\dfrac{(V_{n-1,t})^{\alpha}}{(V_{n,t}^{*})^{\beta}}\left(\dfrac{H_{n,t}-S_n}{L}\right)^{\gamma}-\beta-1=0$). If $V_{n,t}<V_{n,t}^{*}$, the absolute value of sensitivity

$\psi_{V,n}$ decreases as $V_{n,t}$ decreases, and if $V_{n,t}>V_{n,t}^{*}$, the absolute value of sensitivity

$\psi_{V,n}$ decreases as $V_{n,t}$ increases. When $V_{n,t}$ is very large (i.e., $V_{n,t}>>V_{n,t}^{*}$) or very

small (i.e., $V_{n,t}<<V_{n,t}^{*}$), a driver may consider that he runs too fast or too slow, and

thus has less flexibility in choosing his speed $V_{n,t+1}$. Finally, $V_{n,t+1}$ is not very

sensitive to the changes in $V_{n,t}$ while $V_{n,t}$ is very large or very small. On the other

hand, a driver is sensitive to its lead vehicle, if he does not run very fast or very slow.

At identical lead vehicle speed $V_{n-1,t}$, suppose $\lambda\beta\dfrac{(V_{n-1,t})^{\alpha}}{(V_{n,t})^{\beta}}\left(\dfrac{H_{n,t}-S_n}{L}\right)^{\gamma}-\beta-1=0$

occurs at $V_{n,t}^{*}$ and $H_{n,t}^{*}$ (i.e., $\lambda\beta\dfrac{(V_{n-1,t})^{\alpha}}{(V_{n,t}^{*})^{\beta}}\left(\dfrac{H_{n,t}^{*}-S_n}{L}\right)^{\gamma}-\beta-1=0$), $V_{n,t}^{*}$ increases

with $H_{n,t}^{*}$. According to aforementioned analysis, if $V_{n,t}>V_{n,t}^{*}$, the driver may

consider that he runs very fast or too fast. When the spacing is short, a driver may

think that he runs very fast even though his speed is not very high, and thus $V_{n,t}^{*}$

occurs at low value. The relationship between $V_{n,t+1}$ and $V_{n,t}$ and the relationship

between $\psi_{V,n}$ and $V_{n,t}$ with different spacings are shown in Figs. 3-12 and 3-13.
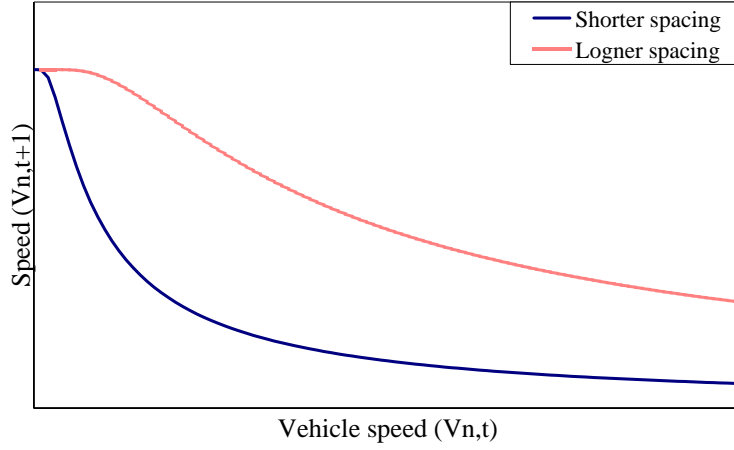
Figure 3-12 the relationship between $V_{n,t+1}$ and $V_{n,t}$ with different spacings
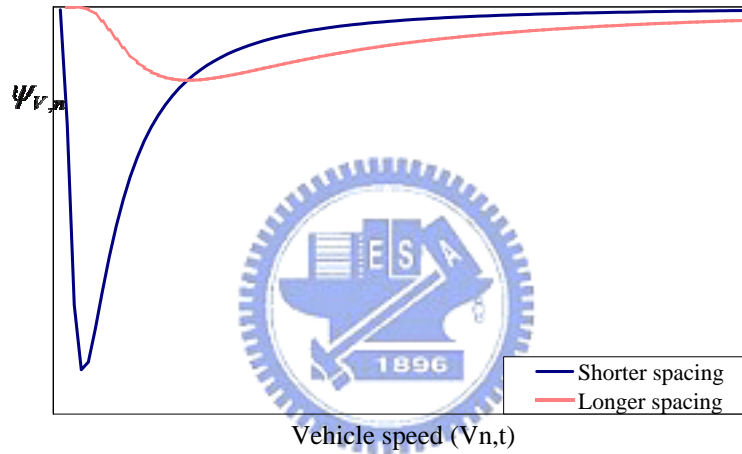

Figure 3-13 the relationship between $\psi_{V,n}$ and $V_{n,t}$ with different spacings

When the lead vehicle and the following vehicle speeds are identical, the proposed model is represented as

$$\tilde{V}_{n,t+1} = E\big(V_{n-1,t}, V_{n,t}, H_{n,t}\big) = v_{n,d}\left(1 - \exp\left(-\lambda\big(V_{n,t}\big)^{\alpha-\beta}\left(\frac{H_{n,t} - S_n}{L}\right)^{\gamma}\right)\right). \qquad (3.37)$$

$\alpha - \beta < 0$ implies driver with higher vehicle speed perceives the repulsion more, and $\alpha - \beta = 0$ implies drivers with different speed result in the same repulsion. The following vehicle and its leader have identical speed often occurs in equilibrium state. Next section, this dissertation will discuss the equilibrium state.

Chapter 4
Equilibrium State and Stability Analysis

In this chapter, the equilibrium state and local stability between two moving cars are discussed. The discussion is on the stability of a following vehicle when its lead vehicle is in equilibrium state and the following vehicle has no acceleration limit. If the lead vehicle is not in equilibrium state, the following vehicle never keeps in equilibrium state.

4.1 Equilibrium State

4.1.1 Microscopic Equilibrium State

A system is either in equilibrium state or disequilibrium state. A vehicle is in equilibrium state if its speed and spacing never change as time passes. Equilibrium state is discussed below. A car-following process can be considered as a dynamical system. The process of a car following a leader that runs at equilibrium velocity is the dynamical system presented as Eqs. (4.1) to (4.3).

$$\mathbf{X}_{n,t+1} = \begin{bmatrix} V_{n,t+1} \\ H_{n,t+1} \end{bmatrix} = F(\mathbf{X}_{n,t}) = F \begin{bmatrix} V_{n,t} \\ H_{n,t} \end{bmatrix} \tag{4.1}$$

$$V_{n,t+1} = f(V_{n,t}, H_{n,t}) = v_{n,d} \left(1 - \exp\left(-\lambda \frac{(V_{n-1,e})^{\alpha}}{(V_{n,t})^{\beta}} \left(\frac{H_{n,t} - S_n}{L} \right)^{\gamma} \right) \right) \tag{4.2}$$

$$H_{n,t+1} = g(V_{n,t}, H_{n,t}) = H_{n,t} + 0.5T(V_{n-1,e} - V_{n,t} + V_{n-1,e} - V_{n,t+1}) \tag{4.3}$$

$V_{n-1,e}$ is the equilibrium velocity of the lead vehicle. According to (4.2) and (4.3), the equilibrium state occurs when $V_{n,t} = V_{n,e} = V_{n-1,e} = V_{n,t+1}$. Hence, Eq. (4.2) becomes

$$V_{n-1,e} = v_{n,d} \left(1 - \exp\left(-\lambda \frac{(V_{n-1,e})^{\alpha}}{(V_{n-1,e})^{\beta}} \left(\frac{H_{n,e} - S_n}{L} \right)^{\gamma} \right) \right)$$

when the following vehicle is in equilibrium state. Thus, the equilibrium spacing between vehicle *n-1* and vehicle *n* is shown as Eq. (4.4).

$$H_{n,e} = L \sqrt[r]{\frac{\ln\left(1 - \frac{V_{n-1,e}}{v_{n,d}} \right)}{-\lambda (V_{n-1,e})^{\alpha-\beta}}} + S_n \tag{4.4}$$

Hence, the equilibrium state of the proposed car-following model is

$$\mathbf{X}_{n,e} = \left(V_{n,e}, H_{n,e}\right)^T = \left(V_{n-1,e}, L\sqrt[r]{\frac{\ln\left(1 - \dfrac{V_{n-1,e}}{v_{n,d}}\right)}{-\lambda\left(V_{n-1,e}\right)^{\alpha-\beta}} + S_n}\right)^T$$, and it is the unique equilibrium

state.

Eq. (4.4) indicates that the equilibrium spacing is only dependent on the individual maximum speed of the following vehicle and the equilibrium speed of the lead vehicle. This conforms to Chakroborty's finding [Chakroborty & Kikuchi, 1999] that equilibrium spacing is only dependent on the final speed. Chakroborty's research did not discuss the difference among drivers, but the proposed model considers it. Thus, different drivers have different equilibrium spacing under identical equilibrium speed, and aggressive drivers have shorter equilibrium spacings.

If the individual maximum speed of the following vehicle is less than the equilibrium speed, Eq. (4.4) becomes meaningless. This is reasonable, because the following vehicle will maintain its speed as its individual maximum speed and depart from car-following process.

A driver may have different critical car-following distances under different external environments. For example, the critical car-following distance of freeway is longer than the one of urban street. This study employs individual maximum speed $v_{n,d}$ to reflect the influence of external environment. Let the individual maximum speeds of urban street and freeway be $v_{n,da}$ and $v_{n,db}$, respectively, and $v_{n,da} < v_{n,db}$. The critical car-following distance of urban street D_a is

$$D_a = \lim_{\varepsilon \to 1} L\left(-\lambda^{-1}\left(\varepsilon v_{n,da}\right)^{\beta-\alpha}\ln\left(1 - \frac{\varepsilon v_{n,da}}{v_{n,da}}\right)\right)^{1/r} + S_n, \tag{4.5}$$

and the critical car-following distance of freeway D_b is

$$D_b = \lim_{\varepsilon \to 1} L\left(-\lambda^{-1}\left(\varepsilon v_{n,db}\right)^{\beta-\alpha}\ln\left(1 - \frac{\varepsilon v_{n,db}}{v_{n,db}}\right)\right)^{1/r} + S_n. \tag{4.6}$$

The ratio of $D_a - S_n$ to $D_b - S_n$ is

$$\frac{D_a - S_n}{D_b - S_n} = \lim_{\varepsilon \to 1} \frac{L\left(-\lambda^{-1}\left(\varepsilon v_{n,da}\right)^{\beta-\alpha} \ln\left(1 - \frac{\varepsilon v_{n,da}}{v_{n,da}}\right)\right)^{1/r}}{L\left(-\lambda^{-1}\left(\varepsilon v_{n,db}\right)^{\beta-\alpha} \ln\left(1 - \frac{\varepsilon v_{n,db}}{v_{n,db}}\right)\right)^{1/r}} = \frac{v_{n,da}^{\frac{\beta-\alpha}{r}}}{v_{n,db}^{\frac{\beta-\alpha}{r}}} \tag{4.7}$$

Different parameter values result in different ratios of critical car-following distance. If $\beta - \alpha = 0$, it implies the critical car-following distances of freeway and urban street are identical. If $\beta - \alpha > 0$, it implies the critical car-following distance of freeway is longer than the one of urban street. Fig. 4-1 is an example of the equilibrium speed-spacing relationships under different maximum speed.
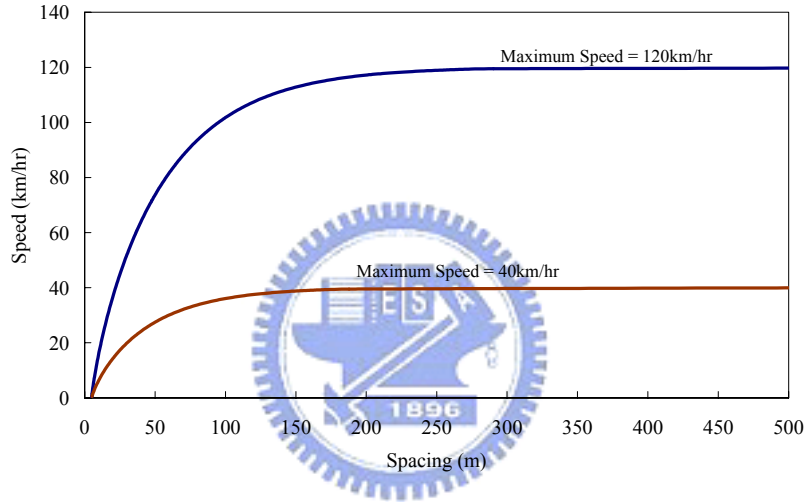

Figure 4-1 Example of equilibrium speed-spacing relationships under different maximum speeds ($\beta - \alpha = 0.2$, $\gamma = 1$)

4.1.2 Fundamental Diagram Based on Microscopic Equilibrium State

A vehicle is in equilibrium state if its speed and spacing never change as time passes. Eq. (4.4) is the microscopic equilibrium state, and it represents that a following vehicle keeps a specific equilibrium spacing if the equilibrium speed is $V_{n-1,e}$. If every driver has identical driver behavior (i.e., identical individual maximum speed), the macroscopic equilibrium state can be derived easily from Eq. (4.4). The reciprocal of spacing is density, thus flow equals speed divides spacing, and the flow rate can be represented as

$$q_e = V_e \left(L \sqrt[r]{-\lambda^{-1}\left(V_e\right)^{\beta-\alpha} \ln\left(1 - \frac{V_e}{v_d}\right)} + S \right)^{-1}, \tag{4.8}$$

where q_e is the equilibrium flow rate, V_e is the equilibrium speed, v_d denotes drivers' maximum speed, and S denotes drivers' standstill distance. When every driver has the same individual maximum speed, the free-flow speed equals the individual maximum speed. Fig. 4-2 is the equilibrium speed-flow relationship as estimated by the proposed model. It is assumed that driver characteristics are homogenous. It shows different free-flow speeds result in different speed-flow curve.
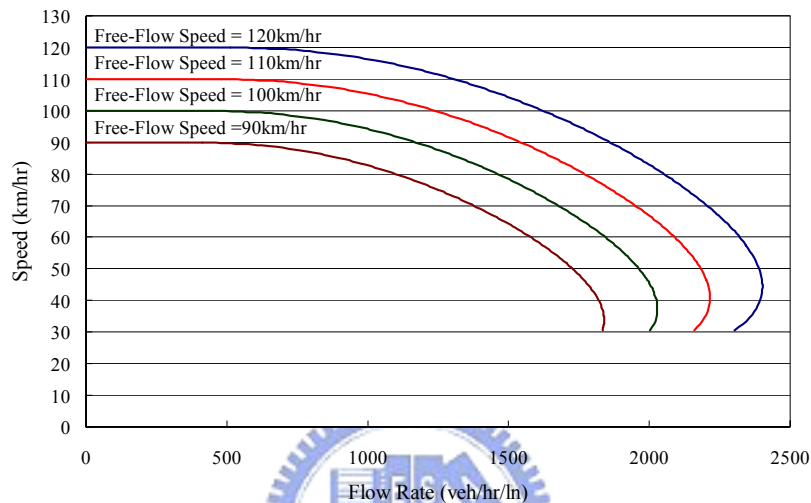

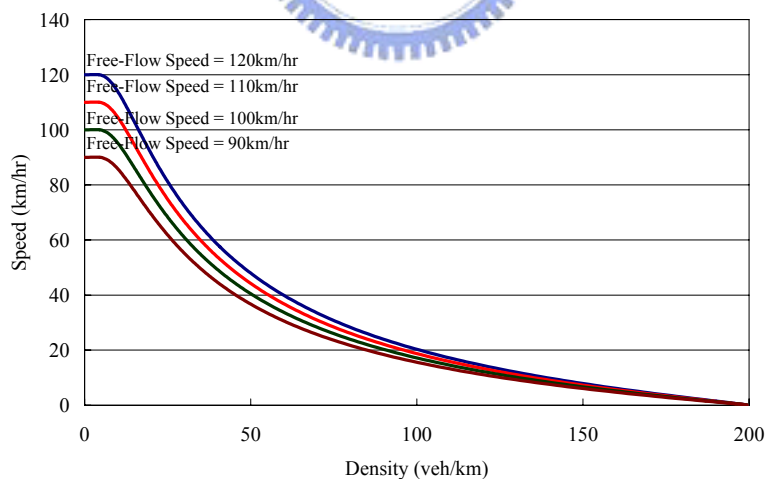Figure 4-2 Estimated speed-flow relationships.

Figure 4-3 Estimated speed-density relationships.

Fig. 2-7 is the speed-flow relationship of the undersaturated traffic flow for basic freeway segments. The undersaturated flow is regarded as stable traffic, i.e., traffic flow reaches the equilibrium state. Fig. 2-7 indicates that the average speed under identical flow rate and the capacity increases with free-flow speed. The speed is

insensitive to flow in the low range. Fig. 4-2 shows that the relationship between free-flow speed and average speed or capacity is similar to that shown in Fig. 2-7. The estimated speed is also insensitive to flow in the low range.

Fig. 4-3 is the speed-density relationship as estimated by the proposed model. It indicates that the difference between different drivers or different environments increases with reducing density, since drivers could behave their desired behavior under low density. On the other hand, when the density becomes jam density, no matter what kind of drivers (i.e., aggressive or conservative drivers) and what kind of environments (e.g., urban streets or freeways), the unique choice for drivers is to stop.

Since different parameters $\beta - \alpha$ and γ result in different q_e under identical equilibrium speed, different parameters result in different fundamental diagram patterns. Fig. 4-4 are different fundamental diagram patterns under different parameters. No matter what the parameter values are, all fundamental diagrams indicate that the difference between different drivers or different environments increases with reducing density.
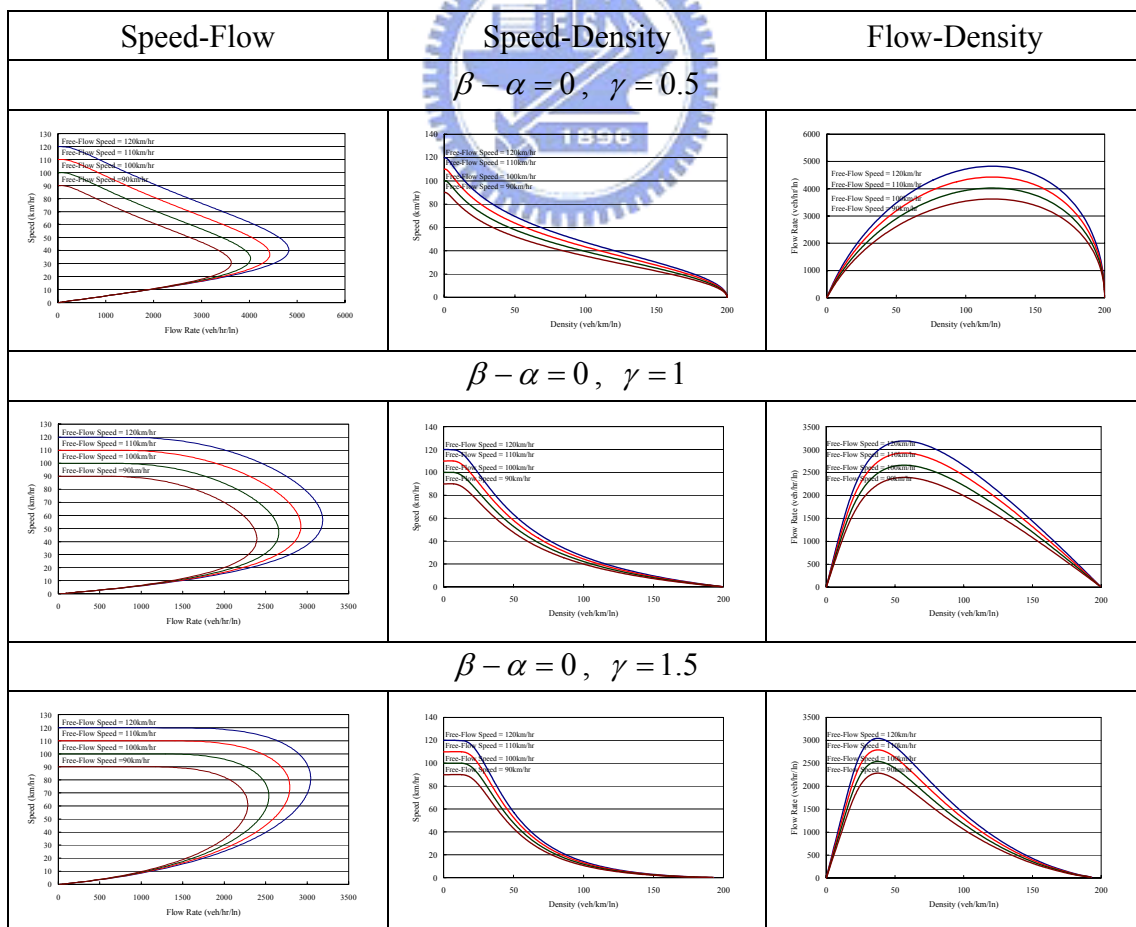

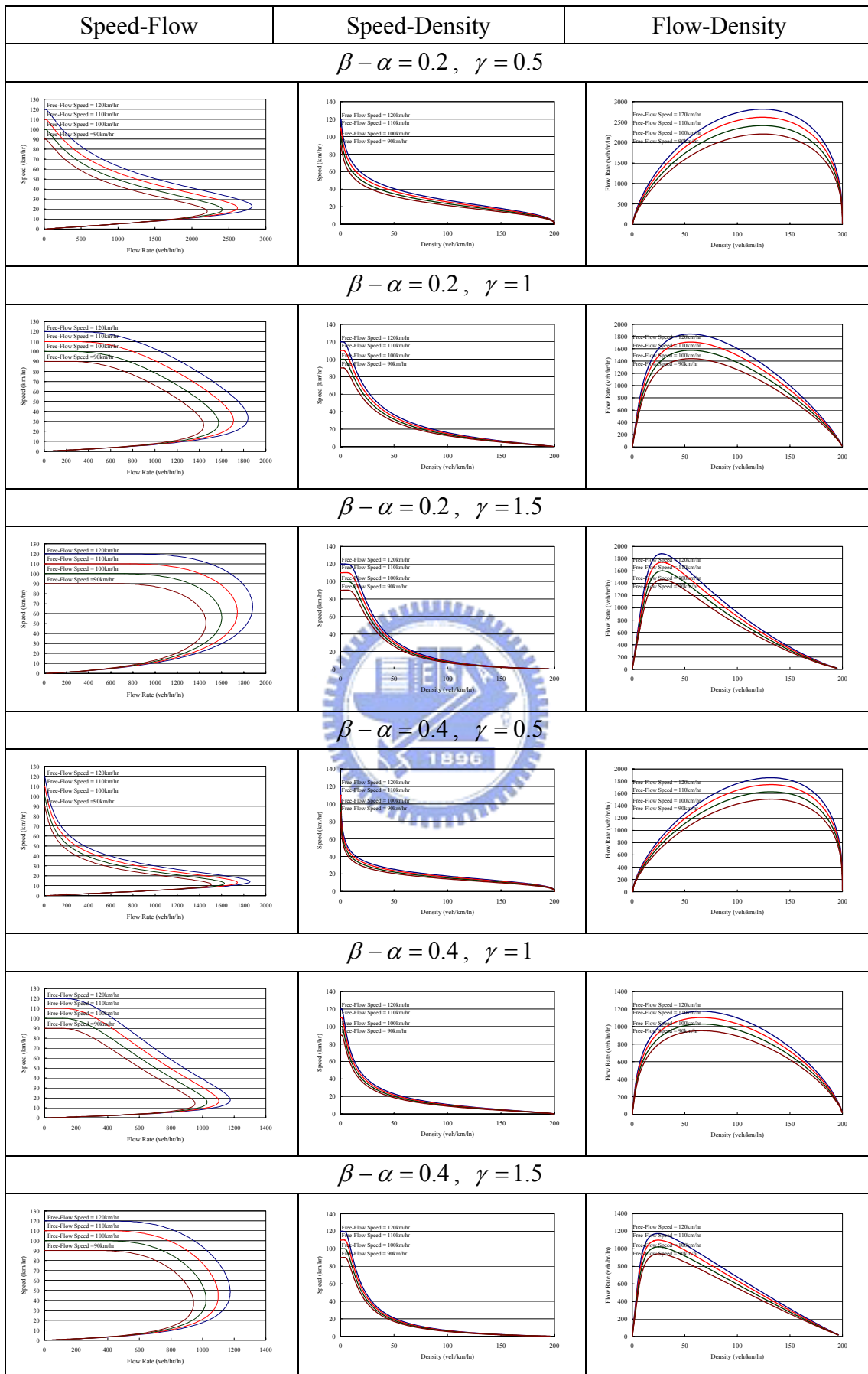Figure 4-4 Estimated fundamental diagrams under different parameters.

Speed-Flow	Speed-Density	Flow-Density
$\beta - \alpha = 0.2$, $\gamma = 0.5$		

$\beta - \alpha = 0.2$, $\gamma = 1$		

$\beta - \alpha = 0.2$, $\gamma = 1.5$		

$\beta - \alpha = 0.4$, $\gamma = 0.5$		

$\beta - \alpha = 0.4$, $\gamma = 1$		

$\beta - \alpha = 0.4$, $\gamma = 1.5$		

Figure 4-4 Estimated fundamental diagrams under different parameters (con.)

4.2 Necessary and Sufficient Conditions for Linearized Stability

In this section, the linearized stability is discussed. If equilibrium state is asymptotically stable, all nearby solutions actually converge to the equilibrium state as time tends to infinity [Wiggins, 1990]. If equilibrium state is asymptotically stable, the car-following process will lead to equilibrium state (local stability and asymptotic stability) and traffic is regarded as stable traffic. Necessary and sufficient conditions for linearized stability are provided.

Theorem

(a) Necessary Condition for linearized stability

If equilibrium state $\mathbf{X}_{n,e} = (V_{n,e}, H_{n,e})^T$ of the dynamical system presented as Eqs. (4.1) to (4.3) is asymptotically stable,

$$(1-D_n)^{\left(1-\frac{1}{D_n}\right)} \leq \exp\left(\frac{1}{\beta}\right) \cap T \leq \left(1 - \left(\beta\left(\frac{1}{D_n}\right)[\ln(1-D_n)](1-D_n)\right)^{-1}\right) \cdot \left(\frac{2\beta(H_{n,e}-S_n)}{\mathcal{W}_{n,e}}\right),$$

where $D_n = \dfrac{V_{n,e}}{V_{n,d}}$.

(b) Sufficient Condition for linearized stability

If

$$(1-D_n)^{\left(1-\frac{1}{D_n}\right)} < \exp\left(\frac{1}{\beta}\right) \cap T < \left(1 - \left(\beta\left(\frac{1}{D_n}\right)[\ln(1-D_n)](1-D_n)\right)^{-1}\right) \cdot \left(\frac{2\beta(H_{n,e}-S_n)}{\mathcal{W}_{n,e}}\right),$$

equilibrium state $\mathbf{X}_{n,e} = (V_{n,e}, H_{n,e})^T$ of the dynamical system presented as Eqs. (4.1) to (4.3) is asymptotically stable.

Proof:

The Jacobian matrix of the proposed dynamical system is shown as Eq. (4.9).

$$DF(\mathbf{X}_{n,t}) = \begin{bmatrix} \dfrac{\partial f(V_{n,t}, H_{n,t})}{\partial V_{n,t}} & \dfrac{\partial f(V_{n,t}, H_{n,t})}{\partial H_{n,t}} \\ \dfrac{\partial g(V_{n,t}, H_{n,t})}{\partial V_{n,t}} & \dfrac{\partial g(V_{n,t}, H_{n,t})}{\partial H_{n,t}} \end{bmatrix} \tag{4.9}$$

If all absolute values of eigenvalues of $DF(\mathbf{X}_{n,e})$ are less than 1, equilibrium state

is asymptotically stable [Alligood et al, 1997]. If equilibrium state is stable, all absolute values of eigenvalues of $D\mathbf{F}\left(\mathbf{X}_{n,e}\right)$ are less than or equal to 1 [Li & Szidarovszky, 1999]

The eigenvalues of $DF\left(\mathbf{X}_{n,e}\right)$ are the roots of the following characteristic equation.

$$\Lambda^2 - \left(\frac{\partial f}{\partial V_{n,t}}\left(V_{n,e},H_{n,e}\right) + \frac{\partial g}{\partial H_{n,t}}\left(V_{n,e},H_{n,e}\right)\right)\Lambda + \frac{\partial f}{\partial V_{n,t}}\left(V_{n,e},H_{n,e}\right)\frac{\partial g}{\partial H_{n,t}}\left(V_{n,e},H_{n,e}\right)$$
$$- \frac{\partial f}{\partial H_{n,t}}\left(V_{n,e},H_{n,e}\right)\frac{\partial g}{\partial V_{n,t}}\left(V_{n,e},H_{n,e}\right) = 0$$

(4.10)

Let

$$b = -\frac{\partial f}{\partial V_{n,t}}\left(V_{n,e},H_{n,e}\right) - \frac{\partial g}{\partial H_{n,t}}\left(V_{n,e},H_{n,e}\right)$$

$$c = \frac{\partial f}{\partial V_{n,t}}\left(V_{n,e},H_{n,e}\right)\frac{\partial g}{\partial H_{n,t}}\left(V_{n,e},H_{n,e}\right) - \frac{\partial f}{\partial H_{n,t}}\left(V_{n,e},H_{n,e}\right)\frac{\partial g}{\partial V_{n,t}}\left(V_{n,e},H_{n,e}\right)$$

where

$$\frac{\partial f}{\partial V_{n,t}}\left(V_{n,e},H_{n,e}\right) = \beta\left(\frac{V_{n-1,e}}{v_{n,d}}\right)\left(1 - \frac{V_{n-1,e}}{v_{n,d}}\right)\ln\left(1 - \frac{V_{n-1,e}}{v_{n,d}}\right)$$

$$\frac{\partial f}{\partial H_{n,t}}\left(V_{n,e},H_{n,e}\right) = -\frac{\gamma V_{n,e}}{\beta\left(H_{n,e} - S_n\right)}\frac{\partial f}{\partial V_{n,t}}\left(V_{n,e},H_{n,e}\right)$$

$$\frac{\partial g}{\partial V_{n,t}}\left(V_{n,e},H_{n,e}\right) = -\frac{1}{2}T\left(1 + \frac{\partial f}{\partial V_{n,t}}\left(V_{n,e},H_{n,e}\right)\right)$$

$$\frac{\partial g}{\partial H_{n,t}}\left(V_{n,e},H_{n,e}\right) = 1 - \frac{1}{2}T\frac{\partial f}{\partial H_{n,t}}\left(V_{n,e},H_{n,e}\right)$$

Hence,

$$\Lambda = \frac{-b \pm \sqrt{b^2 - 4c}}{2}$$

(4.11)

Necessary Condition for $|\Lambda| < 1$

If $b^2 - 4c < 0$, Λ is a complex number and the absolute value of Λ is $\sqrt{c}$. Hence, if $|\Lambda| < 1$, it implies

$$c < 1 \tag{4.12}$$

If $b^2 - 4c \geq 0$, there are two cases: $b \geq 0$ and $b < 0$.

If $b \geq 0$ and all $|\Lambda| < 1$, according to (4.11), it implies

$$-2 < -b - \sqrt{b^2 - 4c} \tag{4.13a}$$

$$\rightarrow b - c < 1 \tag{4.13b}$$

If $b < 0$, and all $|\Lambda| < 1$, according to (4.11), it implies

$$-b + \sqrt{b^2 - 4c} < 2 \tag{4.14a}$$

$$\rightarrow b + c > -1 \tag{4.14b}$$

(4.12), (4.13), and (4.14) are necessary conditions for $|\Lambda| < 1$ under different conditions.

If $b^2 - 4c < 0$

$$\because (1+c)^2 - 4c = (1-c)^2 \geq 0 \tag{4.15}$$

$$\therefore b^2 < (1+c)^2 \tag{4.16}$$

If $b^2 - 4c \geq 0$

$$\because |\Lambda| < 1$$

$$\therefore b^2 < 4 \tag{4.17}$$

Since (4.13), (4.14), and (4.17), $c < 1 \cap |b| < 1 + c$ is the necessary condition for $|\Lambda| < 1$ under $b^2 - 4c \geq 0$.

Hence, $c < 1 \cap |b| < 1 + c$ is the necessary condition for $|\Lambda| < 1$ under all conditions.

Sufficient Condition for $|\Lambda| < 1$

$c < 1 \cap |b| < 1 + c$ is also the sufficient condition for $|\Lambda| < 1$. The proof is provided as follows.

If $b^2 - 4c < 0$,

$\because \ |\Lambda| = \sqrt{c}$, and $\ c < 1$

$\therefore \ |\Lambda| < 1$

$\because \ $ (4.15), (4.16) and above-mentioned proof

$\therefore \ c < 1 \ \cap \ |b| < 1 + c \ $ is the sufficient condition for $\ |\Lambda| < 1 \ $ under

$b^2 - 4c < 0$.

If $\ b^2 - 4c \geq 0 \ $ and $\ b \geq 0$,

$\quad \because \ |b| < 1 + c \ \cap \ c < 1$

$\quad \rightarrow 0 \leq b^2 - 4c < (1+c)^2 - 4c = (1-c)^2$ (4.18)

$\quad \rightarrow -(1-c) < -\sqrt{b^2 - 4c} \leq 0$ (4.19)

$\quad \because \ |b| < 1 + c \ \cap \ c < 1$

$\quad \rightarrow -(1+c) < b < (1+c)$ (4.20)

$\quad \rightarrow -(1+c) < -b \leq 0$ (4.21)

$\quad \because (4.19)$ and (4.21)

$\quad -2 < -b - \sqrt{b^2 - 4c} \leq 0$

$\quad \rightarrow |\Lambda| < 1$
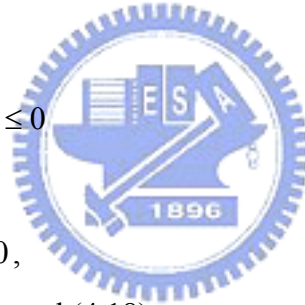
If $\ b^2 - 4c \geq 0 \ $ and $\ b < 0$,

$\quad \because \ |b| < 1 + c$, $\ c < 1$, and (4.18)

$\quad \rightarrow 0 \leq \sqrt{b^2 - 4c} < 1 - c$ (4.22)

$\quad \because \ b^2 < (1+c)^2$, $\ c < 1$, and (4.20)

$\quad \rightarrow 0 < -b < 1 + c$ (4.23)

$\quad \because (4.22)$ and (4.23)

$\quad 0 < -b + \sqrt{b^2 - 4c} < 2$

$\quad \rightarrow |\Lambda| < 1$

Hence, $\ c < 1 \ \cap \ |b| < 1 + c \ $ is the sufficient condition for $\ |\Lambda| < 1 \ $ under all

conditions.

Necessary Condition for the linearized stability of the proposed dynamical system

According to the theorem derived by Li & Szidarovszky [1999] and aforementioned proof, if the proposed dynamical system is stable, it implies

$|b| \le 1 + c$ and $c \le 1$.

$|b| \le 1 + c$

$$\Rightarrow \left(-\frac{\partial f}{\partial V_{n,t}}(V_{n,e}, H_{n,e}) - \frac{\partial g}{\partial H_{n,t}}(V_{n,e}, H_{n,e}) \right)^2 \le$$
$$\left(1 + \frac{\partial f}{\partial V_{n,t}}(V_{n,e}, H_{n,e}) \frac{\partial g}{\partial H_{n,t}}(V_{n,e}, H_{n,e}) - \frac{\partial f}{\partial H_{n,t}}(V_{n,e}, H_{n,e}) \frac{\partial g}{\partial V_{n,t}}(V_{n,e}, H_{n,e}) \right)^2$$
,

$$\Rightarrow \left(-\frac{\partial f}{\partial V_{n,t}}(V_{n,e}, H_{n,e}) \cdot \left(1 + \frac{T\gamma V_{n,e}}{2\beta(H_{n,e} - S_n)} \right) - 1 \right)^2 \le$$
$$\left(1 + \frac{\partial f}{\partial V_{n,t}}(V_{n,e}, H_{n,e}) \cdot \left(1 - \frac{T\gamma V_{n,e}}{2\beta(H_{n,e} - S_n)} \right) \right)^2$$
,

$$\Rightarrow \frac{4T\gamma V_{n,e}}{2\beta(H_{n,e} - S_n)} \left(\frac{\partial f}{\partial V_{n,t}}(V_{n,e}, H_{n,e}) + 1 \right) \ge 0 .$$

$$\because \frac{4T\gamma V_{n,e}}{2\beta(H_{n,e} - S_n)} > 0 ,$$

$$\therefore \frac{\partial f}{\partial V_{n,t}}(V_{n,e}, H_{n,e}) > -1 ,$$

$$\Rightarrow \frac{\partial f}{\partial V_{n,t}}(V_{n,e}, H_{n,e}) \ge -1 . \tag{4.24}$$

If

$$(1 - D_n)^{\left(1 - \frac{1}{D_n} \right)} \le \exp\left(\frac{1}{\beta} \right) , \tag{4.25}$$

it implies $\frac{\partial f}{\partial V_{n,t}}(V_{n,e}, H_{n,e}) \ge -1$.

$c \le 1$

$$\Rightarrow \frac{\partial f}{\partial V_{n,t}}(V_{n,e}, H_{n,e}) \cdot \left(1 - \frac{T\gamma V_{n,e}}{2\beta(H_{n,e} - S_n)} \right) \le 1$$

$$\Rightarrow T \le \left(1 - \left(\beta\left(\frac{1}{D_n}\right)[\ln(1-D_n)](1-D_n)\right)^{-1}\right) \cdot \left(\frac{2\beta(H_{n,e}-S_n)}{\gamma W_{n,e}}\right). \tag{4.26}$$

Sufficient Condition for the linearized stability of the proposed dynamical system

  According to the theorem [Alligood, 1997] and aforementioned proof, if the presented dynamical system is stable, it implies $|b| < 1+c$ and $c < 1$

$$|b| < 1+c$$

$$\Rightarrow \frac{\partial f}{\partial V_{n,t}}(V_{n,e}, H_{n,e}) > -1. \tag{4.27}$$

If

$$(1-D_n)^{\left(1-\frac{1}{D_n}\right)} < \exp\left(\frac{1}{\beta}\right), \tag{4.28}$$

it implies $\dfrac{\partial f}{\partial V_{n,t}}(V_{n,e}, H_{n,e}) > -1$.

$$c < 1$$

$$\Rightarrow T < \left(1 - \left(\beta\left(\frac{1}{D_n}\right)[\ln(1-D_n)](1-D_n)\right)^{-1}\right) \cdot \left(\frac{2\beta(H_{n,e}-S_n)}{\gamma W_{n,e}}\right). \tag{4.29}$$

  Both Eqs. (4.25) and (4.26) are the necessary conditions for linearized stability. Eqs. (4.28) and (4.29) are the sufficient conditions.

                               ■

  From Eqs. (4.25), (4.26), (4.28), and (4.29) some traffic characteristics can be found.

 1. Higher $\dfrac{V_{n,e}}{V_{n,d}}$ makes traffic stable, lower $\dfrac{V_{n,e}}{V_{n,d}}$ makes traffic unstable: When the individual maximum speed of the following vehicle is close to the equilibrium speed of its lead vehicle (i.e. the speed is also its equilibrium speed), traffic will lead to equilibrium state, i.e. stable traffic. Otherwise, when the difference between the individual maximum speed of the following vehicle and the equilibrium speed of its lead vehicle is great, traffic may be unstable. The unstable traffic is often observed

under heavy traffic. From the proposed model, it can be explained that unstable heavy traffic may be due to the large difference between the driver's individual maximum speed and equilibrium speed.

2. Lower T makes traffic stable, higher T makes traffic unstable: When the driver's reaction time is less, traffic will be stable. Otherwise, when the driver's reaction time is high, unstable traffic is likely to occur. The similar result of the influence of driver's reaction time on traffic stability is also found in GM model and other classical models [Herman et al, 1959; May, 1995; Zhang & Jarrett, 1997; Holland, 1998]. Furthermore, under the same equilibrium speed and with a lower $\dfrac{V_{n,e}}{v_{n,d}}$, the reaction time should be less to make stable traffic possible. It implies when the individual maximum speed of the following vehicle isn't close to equilibrium speed, drivers should react more frequently. Otherwise, traffic may be unstable.

4.3 Numerical examples

Examples for stable traffic and unstable traffic are presented in this section. The model parameters for these simulations are: $\lambda = 1$, $\alpha = 1$, $\beta = 1.1$, $\gamma = 1$ $L = 20$ (they have not been calibrated), $S_n = 5\text{m}$, $T = 0.5\text{sec}$, $a_{\max} = 5\text{m/s}^2$, and $a_{\min} = -5\text{m/s}^2$.
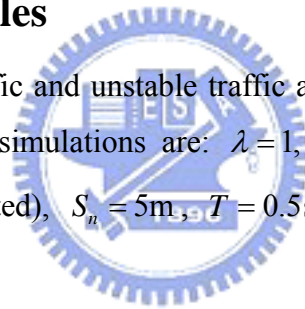
4.3.1 Stable Traffic

The fact that the spacing between the lead vehicle and the following vehicle reaches a particular value after perturbation (to the spacing) caused by the actions of the lead vehicle is referred to as the stability in car-following behavior [May, 1990; Chakroborty & Kikuchi, 1999]. Researchers identified two types of traffic stability: local stability and asymptotic stability. Local stability is concerned with the car-following behavior of just two vehicles: the lead vehicle and one following vehicle. Asymptotic stability is concerned with the car-following behavior of a line of vehicles [May, 1990; Chakroborty & Kikuchi, 1999].

An example of movement process of four vehicles is illustrated below. The individual maximum speeds of the first vehicle, the second one, the third one, and the last one are 50, 60, 70, and 80km/hr, respectively. The initial speeds of these vehicles

are their individual maximum speeds. The initial spacings between these vehicles are 100m.

Figure 4-5 shows car-following trajectories of these four vehicles. As there is no vehicle in front of the first vehicle, the first vehicle runs at its individual maximum speed (i.e. 50km/hr). According to Section 4.2, following vehicles satisfy the necessary and sufficient condition for linearized stability, therefore, they finally run at equilibrium state. They run at their individual maximum speed initially, and decelerate later and finally keep their speed at 50km/hr. The platoon is then stable.
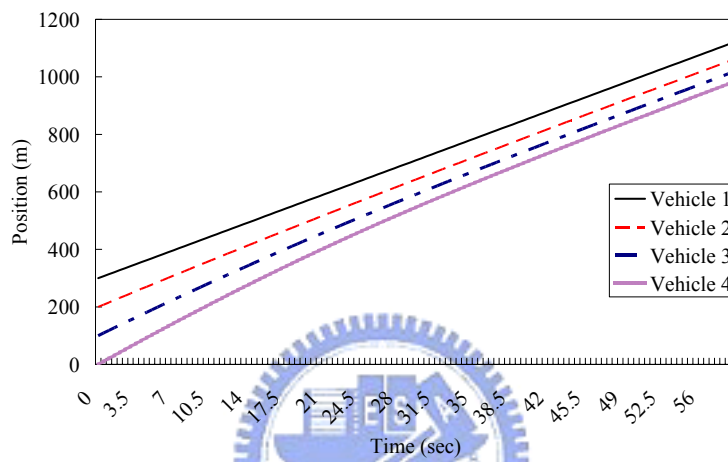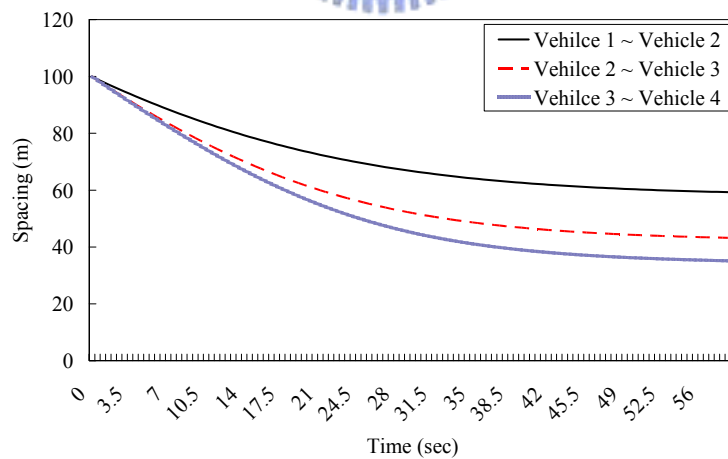

Figure 4-5 Car-following trajectories.

Figure 4-6 Spacings between vehicles.

Figure 4-6 shows the spacing between these vehicles. All spacing reaches a particular value finally (i.e. equilibrium spacing), and this is asymptotic stability. As mentioned in Section 3, Figure 4-6 also reflects the model assumption that the driver

with higher individual maximum speed maintains a higher speed or a shorter spacing under the same condition. It is a common traffic phenomenon that different drivers may keep different spacing under the same condition.

The stable spacing (i.e. equilibrium spacing) is only dependent on the final speed (or stable speed) and not on anything else [Chakroborty & Kikuchi, 1999]. The following example shows that the same lead vehicle and the same following vehicle will result in the same equilibrium spacing under different initial conditions. The individual maximum speeds of the lead vehicle and the follower are 50 and 60km/hr, respectively. The initial conditions include initial spacing and initial speed of the following vehicle. Six initial condition examples are listed below.

A: spacing = 50m, speed = 60km/hr.

B: spacing = 50m, speed = 30km/hr.

C: spacing = 100m, speed = 60km/hr.

D: spacing = 100m, speed = 30km/hr.

E: spacing = 10m, speed = 60km/hr.

F: spacing = 10m, speed = 30km/hr.

Figures 4-7 and 4-8 are the simulation results. Figure 4-7 indicates that the same lead vehicle and the same following vehicle results in the same equilibrium speed of the follower. Figure 4-8 indicates that the spacing reaches the same equilibrium spacing under different initial conditions. Figures 4-7 and 4-8 indicate that equilibrium spacing is only dependent on the final speed and not on initial condition.
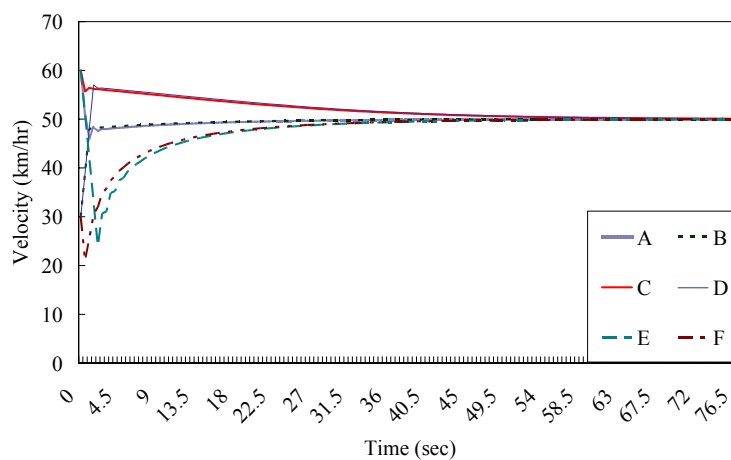

Figure 4-7 Speeds of the following vehicle under different initial conditions.
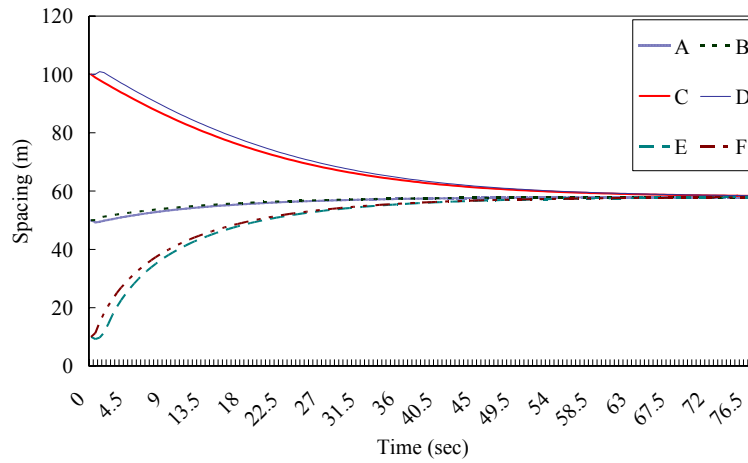
Figure 4-8 Spacings under different initial conditions.

4.3.2 Unstable Traffic

Traffic flow does not always lead to equilibrium state; sometimes unstable traffic occurs. The speed and spacing may change again and again over time. For example, when the traffic condition is heavy, vehicles sometimes fall into the stop-and-go situation. An example is shown to illustrate that the proposed model cannot only describe stable traffic, but also describe unstable traffic. In the following example, the individual maximum speed of the first vehicle is assumed to be 5km/hr so that it will run at 5km/hr to simulate the heavy traffic condition. All the individual maximum speeds of the following vehicles are 90km/hr. All of the initial spacings between a lead vehicle and a following one are 150m. All following vehicles don't satisfy the necessary condition for stability because $\left(1-D_n\right)^{\left(1-\frac{1}{D_n}\right)} > \exp\left(\frac{1}{\beta}\right)$. Thus, traffic is unstable. Figure 4-9 is the velocity profile for the first six following vehicles in the platoon (the second vehicle is the first following vehicle). It shows the stop-and-go traffic condition that vehicles sometimes stop and sometimes move.
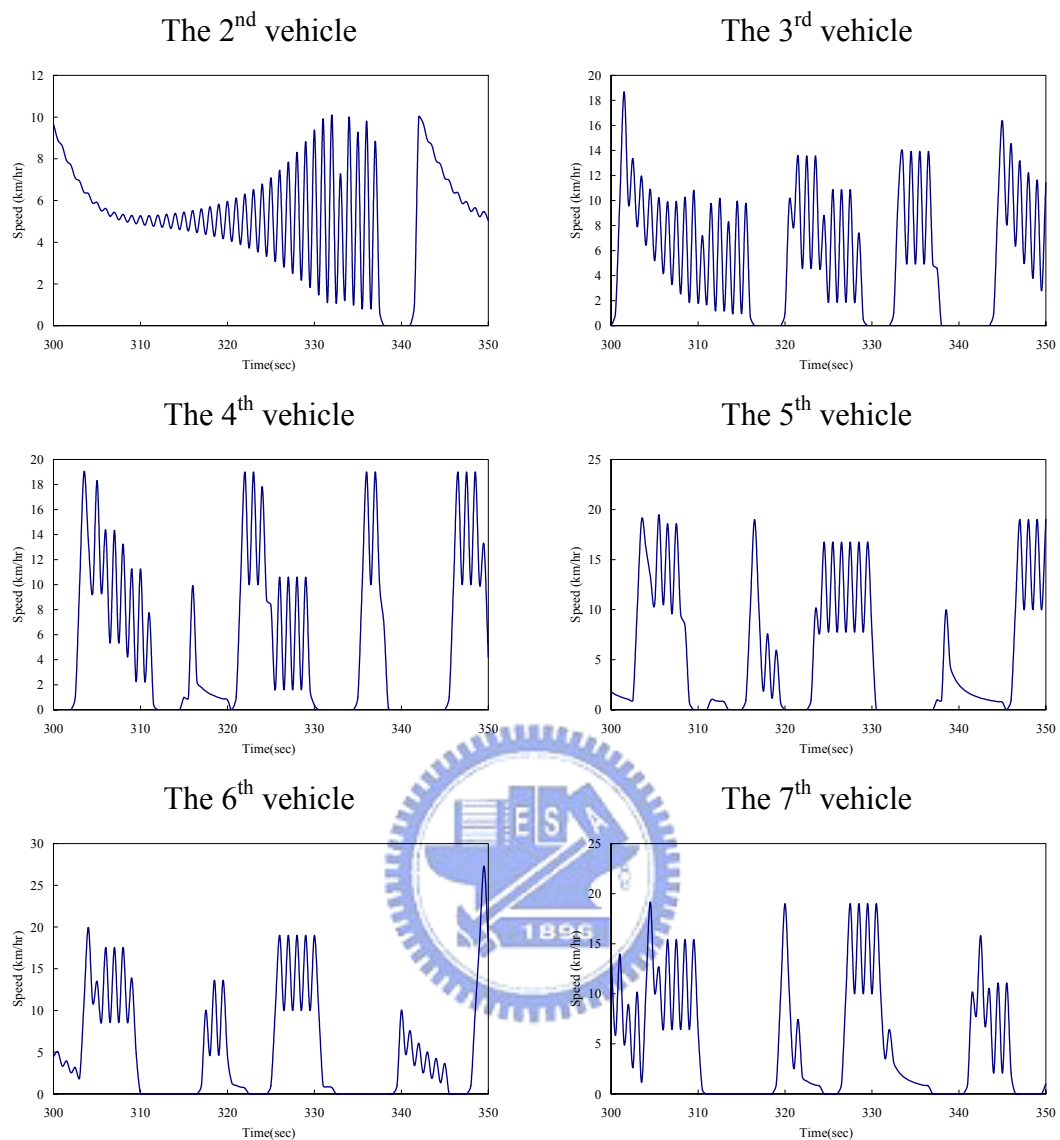
Figure 4-9 Velocity profile under unstable traffic

4.3.3 Relaxation Time

Section 4.2 discusses the stability of equilibrium state, and if all nearby states converge to equilibrium state as time tends to infinity, the equilibrium state is regarded as asymptotically stable. In fact, one cannot observe traffic flow for infinite time. If the traffic converges to the equilibrium state takes much time, the equilibrium state may be hardly observed, and thus it may be regarded as unstable state. For example, if all drivers have identical individual maximum speed 100km/hr, the equilibrium speed-density relationship is shown as Fig. 4-10. The equilibrium state below 17km/hr, i.e. the dashed line in Fig.4-10, is regarded as unstable traffic by the

stability analysis mentioned in Section 4.2. But according to field data, velocity higher than 17 km/hr may be regarded as unstable traffic. For instance, the dotted line may be regarded as unstable traffic since it is hardly observed.
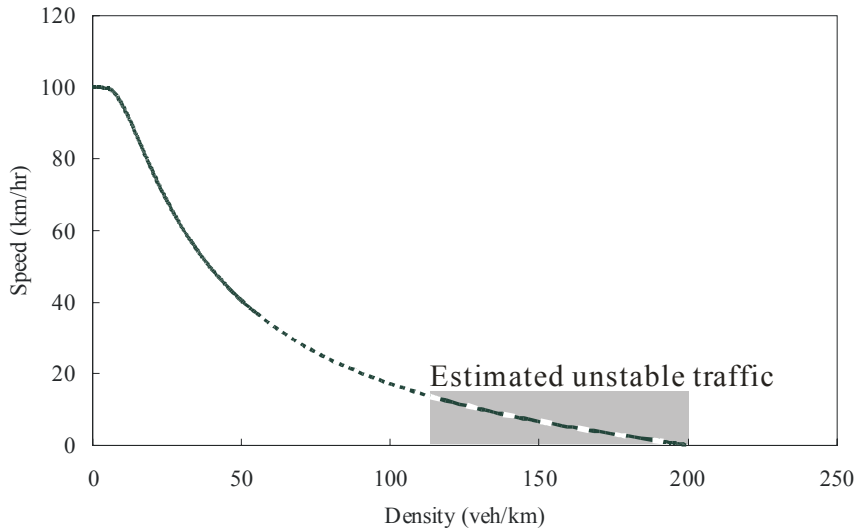

Figure 4-10 Speed-density relationship

This section discusses the relaxation time of different equilibrium states. Figs. 4-11 and 4-12 presents 12 examples, and all initial conditions are equilibrium states. The lead vehicle and the following vehicle run at identical velocity (i.e. equilibrium speed $V_{n,e}$). First, a perturbation occurs at the 3rd time step. In Fig. 4-11, the lead vehicle accelerates its velocity to $V_{n,e} + 5$, decelerates its velocity to $V_{n,e}$ at the 4th time step, and keeps its velocity at $V_{n,e}$ finally. In Fig. 4-12, the lead vehicle decelerates its velocity to $V_{n,e} - 5$, accelerates its velocity to $V_{n,e}$ at the 4th time step, and keeps its velocity at $V_{n,e}$ finally. Since the lead vehicle changes its velocity, the following vehicle cannot keep its velocity as $V_{n,e}$. No matter the perturbation is acceleration or deceleration, the velocity profiles after perturbations indicate that the relaxation time increases with reducing $D_n = \dfrac{V_{n,e}}{V_{n,d}}$.
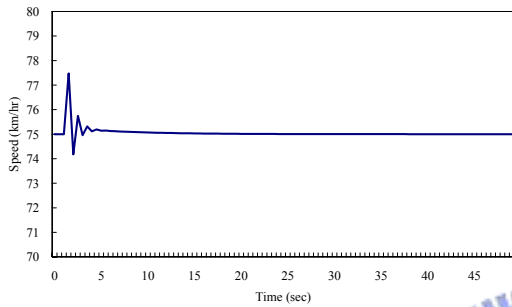
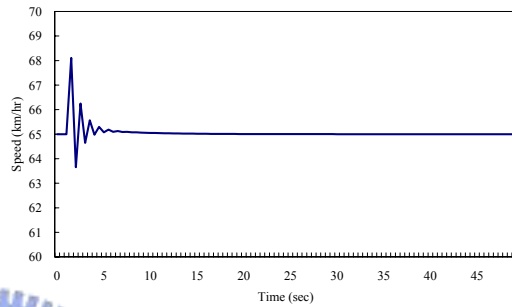Equilibrium speed= 95km/hr, $D_n = 0.95$ Equilibrium speed= 85km/hr, $D_n = 0.85$
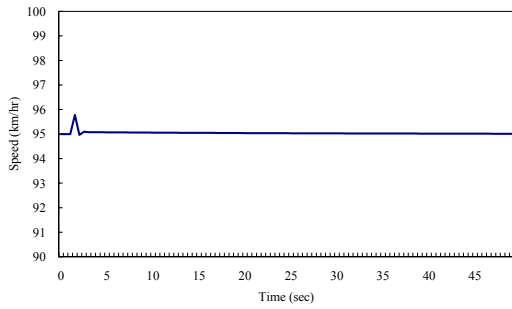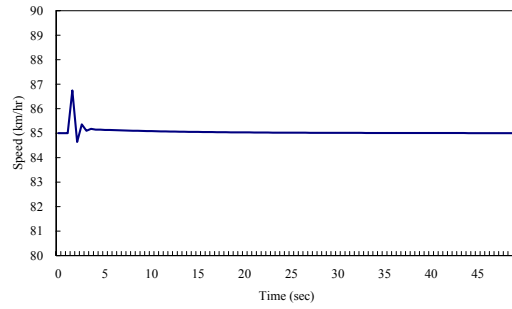
Equilibrium speed= 75km/hr, $D_n = 0.75$ Equilibrium speed= 65km/hr, $D_n = 0.65$

Equilibrium speed= 55km/hr, $D_n = 0.55$ Equilibrium speed= 45km/hr, $D_n = 0.45$

Equilibrium speed= 35km/hr, $D_n = 0.35$ Equilibrium speed= 25km/hr, $D_n = 0.25$

Fig 4-11 Velocity profile of the following vehicle after perturbation (+5km/hr)

Equilibrium speed= 95km/hr, $D_n = 0.95$ Equilibrium speed= 85km/hr, $D_n = 0.85$
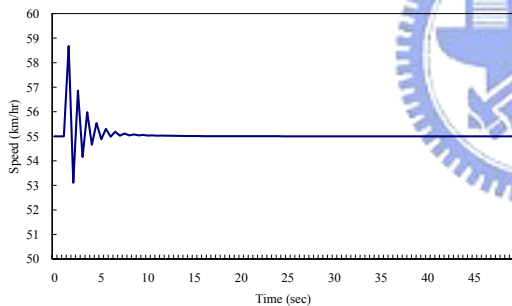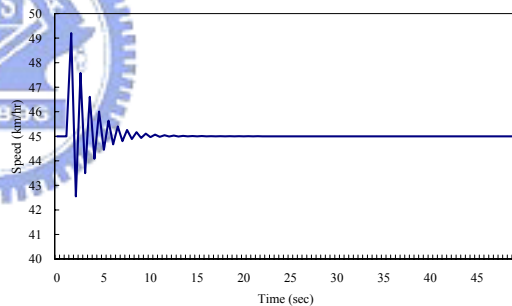
Equilibrium speed= 75km/hr, $D_n = 0.75$ Equilibrium speed= 65km/hr, $D_n = 0.65$
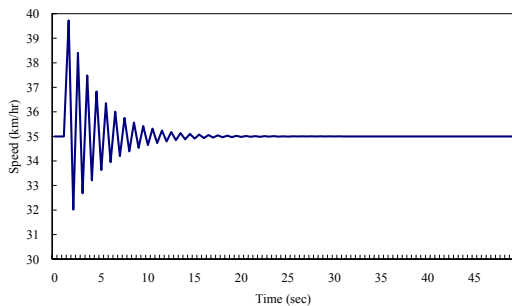
Equilibrium speed= 55km/hr, $D_n = 0.55$ Equilibrium speed= 45km/hr, $D_n = 0.45$

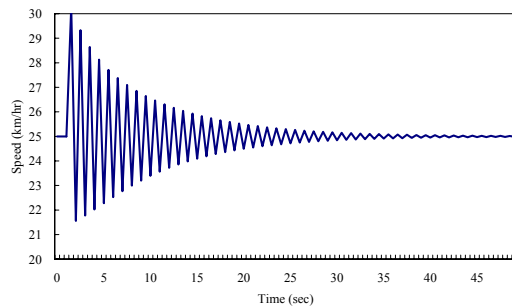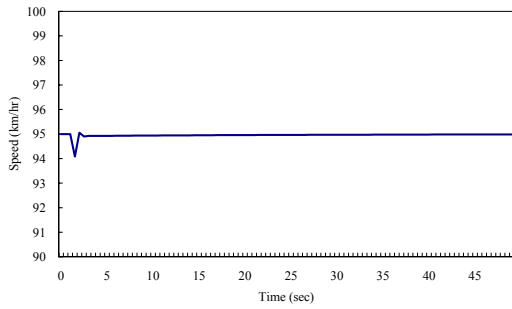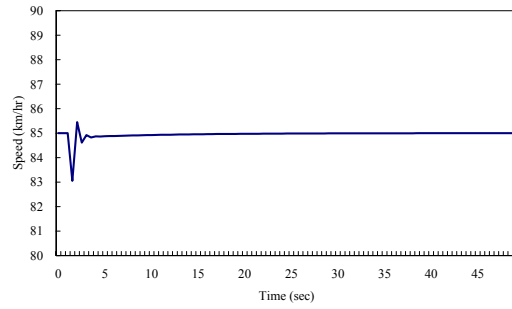Equilibrium speed= 35km/hr, $D_n = 0.35$ Equilibrium speed= 25km/hr, $D_n = 0.25$
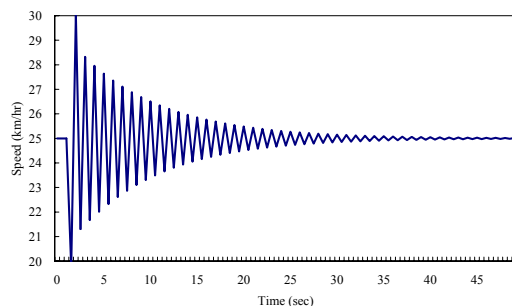
Fig 4-12 Velocity profile of the following vehicle after perturbation (-5km/hr)
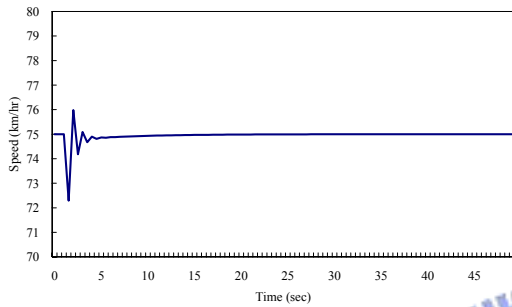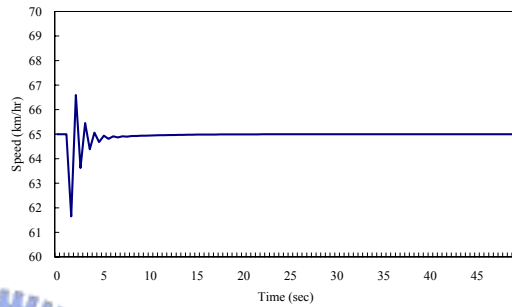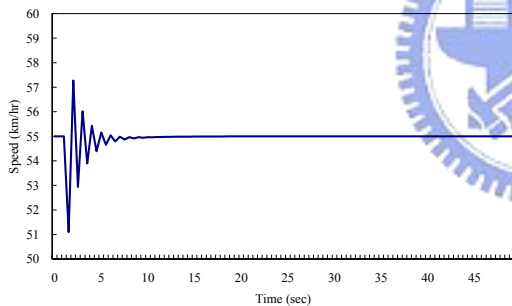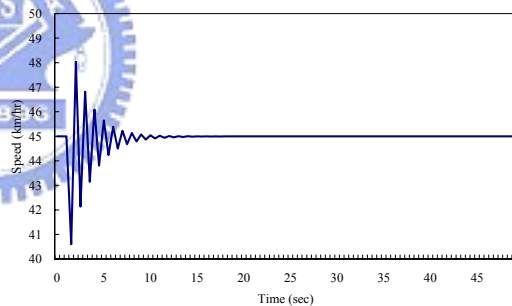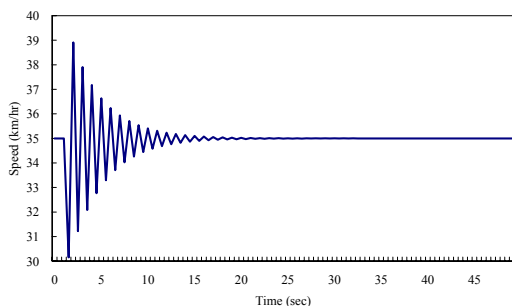
66

Chapter 5
Disequilibrium State

Some traffic phenomena of disequilibrium state will be discussed in this section. This section possesses analytical properties that are logical in representing physical phenomena first. The mathematical analysis guarantees that the disequilibrium phenomena hold under any parameters. Finally, simulation examples are provided. Parameters of these examples are the same as Section 4.3.

5.1 Closing-in and Shying-away

This section discusses closing-in and shying-away. When the following vehicle accelerates even its speed is faster than its leading vehicle's speed, the phenomenon is closing-in. On the contrary, when the follower decelerates even it is slower than its leader, this is shying-away.

Eq. (5.1) is the proposed model,

$$V_{n,t+1} = v_{n,d}\left(1 - \exp\left(-\lambda \frac{(V_{n-1,t})^{\alpha}}{(V_{n,t})^{\beta}}\left(\frac{H_{n,t} - S_n}{L}\right)^{\gamma}\right)\right). \tag{5.1}$$

Let $V_{n-1,t} = \varepsilon V_{n,t}$, and thus

$$V_{n,t+1} = v_{n,d}\left(1 - \exp\left(-\lambda \frac{(\varepsilon V_{n,t})^{\alpha}}{(V_{n,t})^{\beta}}\left(\frac{H_{n,t} - S_n}{L}\right)^{\gamma}\right)\right). \tag{5.2}$$

If the vehicle keeps its speed at the next time step, Eq. (5.2) becomes

$$H_{n,t} = L\left(-\lambda^{-1}(V_{n,t})^{\beta-\alpha}\varepsilon^{-\alpha}\ln\left(1 - \frac{V_{n,t}}{v_{n,d}}\right)\right)^{\frac{1}{r}} + S_n. \tag{5.3}$$

Hence, if

$$H_{n,t} > L\left(-\lambda^{-1}(V_{n,t})^{\beta-\alpha}\varepsilon^{-\alpha}\ln\left(1 - \frac{V_{n,t}}{v_{n,d}}\right)\right)^{\frac{1}{r}} + S_n, \tag{5.4}$$

the following vehicle will accelerate at the next time step. Otherwise, if

$$H_{n,t} < L\left(-\lambda^{-1}(V_{n,t})^{\beta-\alpha}\varepsilon^{-\alpha}\ln\left(1 - \frac{V_{n,t}}{v_{n,d}}\right)\right)^{\frac{1}{r}} + S_n, \tag{5.5}$$

the following vehicle will decelerate at the next time step.

If Eq. (5.4) holds and $\varepsilon < 1$, it implies $V_{n-1,t} < V_{n,t}$, but the following vehicle accelerates at the next time step. This is the so-called closing-in. Otherwise, if Eq. (5.5) holds and $\varepsilon > 1$, it implies $V_{n-1,t} > V_{n,t}$, but the following vehicle decelerates at the next time step. This is the so-called shying-away.

Let $\Phi_{n,t}$ denotes the RHS of Eq. (5.3). Since $\Phi_{n,t}$ is a function of $v_{n,d}$, different drivers have different $\Phi_{n,t}$ under identical traffic condition. $\Phi_{n,t}$ varies with $v_{n,d}$, and

$$
\begin{aligned}
\frac{\partial \Phi_{n,t}}{\partial v_{n,d}} = \frac{1}{r} L &\left(-\lambda^{-1}\left(V_{n,t}\right)^{\beta-\alpha} \varepsilon^{-\alpha} \ln\left(1 - \frac{V_{n,t}}{v_{n,d}}\right) \right)^{\frac{1}{r}-1} \left(-\lambda^{-1}\left(V_{n,t}\right)^{\beta-\alpha} \varepsilon^{-\alpha} \right) \\
&\cdot \left(1 - \frac{V_{n,t}}{v_{n,d}}\right)^{-1} \frac{V_{n,t}}{v_{n,d}^{2}} < 0
\end{aligned} \tag{5.6}
$$

Eq. (5.6) indicates that drivers with higher individual maximum speed have lower $\Phi_{n,t}$. The following vehicle decides to accelerate at the next time step under $H_{n,t} > \Phi_{n,t}$, and decides to decelerate under $H_{n,t} < \Phi_{n,t}$. Thus, drivers with higher individual maximum speed may decide to accelerate and drivers with lower individual maximum speed may decide to decelerate under identical traffic condition. This conforms to the model assumption (1) that aggressive drivers keep higher velocity under identical traffic condition.

Two illustrative examples of closing-in and shying-away are presented. It assumes the lead vehicle keeps its speed at 5 km/hr, the individual maxim speed of the following vehicle is 90 km/hr, and the initial spacing is 50 meters. Fig. 5-1 shows the simulation result from the 5th to the 13th time steps (Relative Speed $= V_{n-1,t} - V_{n,t}$). At T=2.5, the following vehicle speed is 15 km/hr, and it is faster than its lead vehicle. The right-hand side of Eq. (5.3) is 19.34 meters, it implies that the vehicle keeps its speed as 15km/hr at T=3 if the spacing is 19.34 meters at T=2.5. But the spacing is 25.35 meters at T=2.5, it is longer than 19.34 meters. Thus, the following vehicle accelerates at T=3 although it is faster than its leader. The similar situations occur at T=3.5, T=4.5, and T=5.5, and the phenomenon is closing-in.

Fig. 5-2 shows an example of shying-away. The individual maximum speed of the lead and following vehicles are 50 km/hr and 70 km/hr, respectively, and the initial spacing is 20 meters. At T=1, the following vehicle speed is 42 km/hr, and it is slower than its lead vehicle. The right-hand side of Eq. (5.3) is 27.37 meters, it implies that the vehicle keeps its speed as 42 km/hr at T=2 if the spacing is 27.37 meters at T=1. But the spacing is 19.02 meters at T=1, it is shorter than 27.37 meters. Thus, the following vehicle decelerates at T=3 although it is slower than its leader. At T=2, T=3, and T=4 the similar situations occur. This is the so-called shying-away phenomenon.
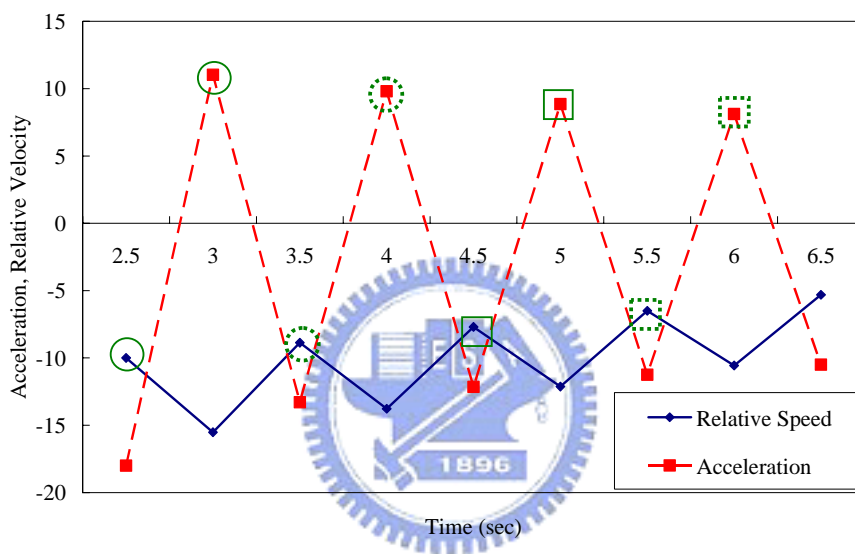
Figure 5-1 Acceleration and relative velocity (closing-in phenomenon)
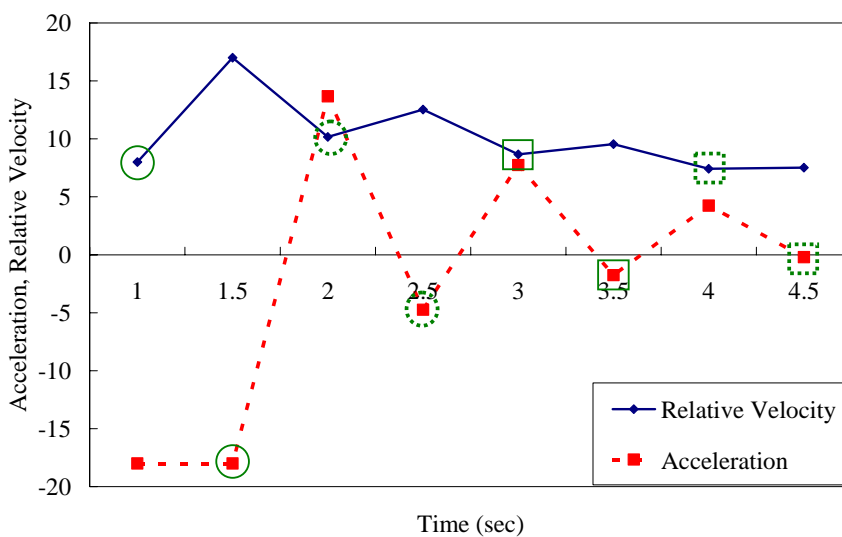
Figure 5-2 Acceleration and relative velocity (shying-away phenomenon)

5.2 Traffic Hysteresis

This section discusses traffic hysteresis pattern based on field data first. Then, the properties of the proposed model and general models are discussed. Microscopic and macroscopic traffic hysteresis examples are provided finally.

5.2.1 Empirical Data of Traffic Hysteresis

Fig. 5-3 is the empirical speed-occupancy data. The data were obtained from detectors using a 5 minute sampling time interval and aggregated across lanes. The solid and dashed lines are guidance lines illustrating the acceleration and deceleration trends. Fig 5-3 illustrates certain traffic characteristics, as follows:

1. The acceleration curve differs from the deceleration curve.

2. Regardless of whether traffic is heavy or light, the acceleration curve may lie above the deceleration curve, and may also lie below deceleration curve.

When the observational object is a road section, a state (k,v) (where k denotes density, and v denotes speed) may accelerate or decelerate at the next time step. The velocity of a road section increases or decreases depends not only on the state of that section, but also on upstream and downstream traffic conditions. When the observation object is a vehicle, a vehicle with any state $(H_{n,t}, V_{n,t})$ may accelerate or decelerate at the next time step. It's because $V_{n,t+1}$ is influenced by the lead vehicle.
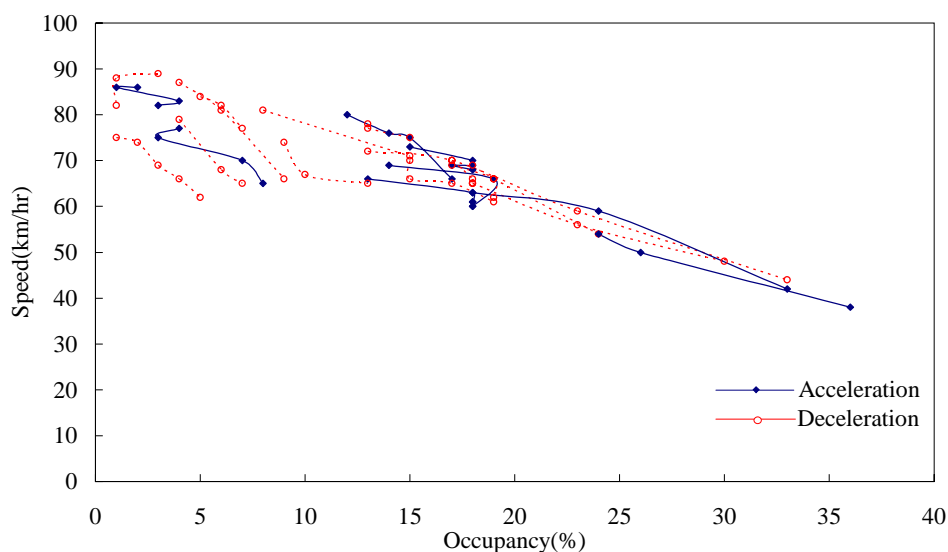
Figure 5-3 Empirical speed-occupancy relationship (1)

Fig. 5-3 indicates that other traffic hysteresis patterns exist aside from the two pattern types obtained by Treiterer and Maes. Kerner [2006] pointed out that traffic flow has three phases (i.e., free flow, synchronized flow, and traffic jam [1997, 1998]), and different phase transitions result in a variety of hysteresis phenomena. This study obtained two hysteresis pattern types differing from Figs. 2-3 and 2-4. Fig. 5-4(a) is contrary to Fig. 2-3, and Fig. 5-4(b) is contrary to Fig. 2-4.
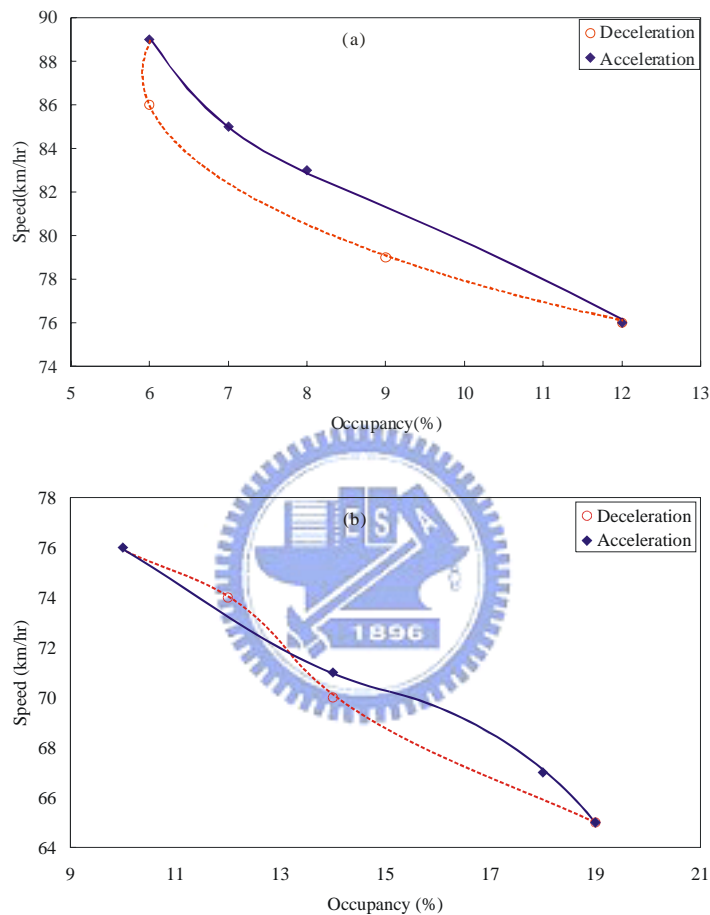
Figure 5-4 Empirical speed-occupancy relationships (2)

5.2.2 Traffic Hysteresis Discussion

In this section, analytical properties of traffic hysteresis are discussed. Firstly, the proposed model is discussed. Secondly, a general model that guarantees the existence of traffic hysteresis is discussed.

(1)The proposed model

Traffic hysteresis implies that the speed-spacing relationships of acceleration and deceleration traffic are not identical. This section discusses the relationships between $V_{n,t+1}$ and $H_{n,t+1}$ under acceleration and deceleration traffic. Since it is focus on

71

acceleration and deceleration traffic, stop conditions are not concerned. Hence, the speed and spacing are shown as Eqs (5.7) and (5.8).

$$V_{n,t+1} = E\left(H_{n,t}, V_{n,t}, V_{n-1,t}\right) = v_{n,d}\left(1 - \exp\left(-\lambda \frac{\left(V_{n-1,t}\right)^{\alpha}}{\left(V_{n,t}\right)^{\beta}}\left(\frac{H_{n,t} - S_n}{L}\right)^{\gamma}\right)\right) \qquad (5.7)$$

$$\begin{aligned}H_{n,t+1} &= J\left(H_{n,t}, V_{n,t}, V_{n,t+1}, V_{n-1,t}, V_{n-1,t+1}\right) \\ &= H_{n,t} + 0.5T\left(V_{n-1,t} + V_{n-1,t+1} - V_{n,t} - V_{n,t+1}\right)\end{aligned} \qquad (5.8)$$

$H_{n,t+1}$ is function of $V_{n,t+1}$, and Eq. (5.8) can be represented as

$$H_{n,t+1} = W\left(Z_{n,t+1}, V_{n,t+1}\right) = Z_{n,t+1} - 0.5TV_{n,t+1}, \qquad (5.9)$$

where $Z_{n,t+1} = H_{n,t} + 0.5T\left(V_{n-1,t} + V_{n-1,t+1} - V_{n,t}\right)$.

Before reaching the equilibrium state, a disequilibrium state $\left(V_{n,t+1}, H_{n,t+1}\right)$ may occur at acceleration or deceleration traffic, i.e. acceleration and deceleration traffic may have identical $V_{n,t+1}$, identical $H_{n,t+1}$, and identical $Z_{n,t+1}$. If the speed-spacing relationships of acceleration and deceleration traffic are identical, the first derivative of W function at the point $\left(Z_{n,t+1}, V_{n,t+1}\right)$ are identical. The first partial derivative of W function at the point $\left(Z_{n,t+1}, V_{n,t+1}\right)$ with respect to $V_{n,t}$ is

$$\frac{\partial W}{\partial V_{n,t}}\left(Z_{n,t+1}, V_{n,t+1}\right) = -0.5T - 0.5T\frac{\partial V_{n,t+1}}{\partial V_{n,t}}. \qquad (5.10)$$

The first partial derivative of W function at the point $\left(Z_{n,t+1}, V_{n,t+1}\right)$ with respect to $H_{n,t}$ is

$$\frac{\partial W}{\partial H_{n,t}}\left(Z_{n,t+1}, V_{n,t+1}\right) = 1 - 0.5T\frac{\partial V_{n,t+1}}{\partial H_{n,t}}. \qquad (5.11)$$

If the speed-spacing relationships of acceleration and deceleration traffic are identical, acceleration and deceleration traffic should have identical $\frac{\partial W}{\partial V_{n,t}}\left(Z_{n,t+1}, V_{n,t+1}\right)$, and identical $\frac{\partial W}{\partial H_{n,t}}\left(Z_{n,t+1}, V_{n,t+1}\right)$, and thus acceleration and deceleration traffic have identical $\frac{\partial V_{n+1,t}}{\partial V_{n,t}}$, and identical $\frac{\partial V_{n+1,t}}{\partial H_{n,t}}$.

Let

$$E\left(H_{n,t,a},V_{n,t,a},V_{n-1,t,a}\right)=V_{n,t+1}=E\left(H_{n,t,d},V_{n,t,d},V_{n-1,t,d}\right). \tag{5.12}$$

where $H_{n,t,a}$ denotes $H_{n,t}$ value for acceleration traffic, $H_{n,t,d}$ denotes $H_{n,t}$ value for deceleration traffic , $V_{n,t,a}$ denotes $V_{n,t}$ value for acceleration traffic, $V_{n,t,d}$ denotes $V_{n,t}$ value for deceleration traffic, $V_{n-1,t,a}$ denotes $V_{n-1,t}$ value for acceleration traffic, $V_{n-1,t,d}$ denotes $V_{n-1,t}$ value for deceleration traffic. If the speed-spacing relationships of acceleration and deceleration traffic are identical,

$$\frac{\partial E}{\partial V_{n,t}}\left(H_{n,t,a},V_{n,t,a},V_{n-1,t,a}\right)=\frac{\partial V_{n,t+1}}{\partial V_{n,t}}=\frac{\partial E}{\partial V_{n,t}}\left(H_{n,t,d},V_{n,t,d},V_{n-1,t,d}\right), \tag{5.13}$$

and

$$\frac{\partial E}{\partial H_{n,t}}\left(H_{n,t,a},V_{n,t,a},V_{n-1,t,a}\right)=\frac{\partial V_{n,t+1}}{\partial H_{n,t}}=\frac{\partial E}{\partial H_{n,t}}\left(H_{n,t,d},V_{n,t,d},V_{n-1,t,d}\right). \tag{5.14}$$

Eq. (5.12) implies that

$$\frac{\left(V_{n-1,t,a}\right)^{\alpha}}{\left(V_{n,t,a}\right)^{\beta}}\left(\frac{H_{n,t,a}-S_n}{L}\right)^{\gamma}=\frac{\left(V_{n-1,t,d}\right)^{\alpha}}{\left(V_{n,t,d}\right)^{\beta}}\left(\frac{H_{n,t,d}-S_n}{L}\right)^{\gamma}. \tag{5.15}$$

The first partial derivative of E function at the acceleration traffic state $\left(H_{n,t,a},V_{n,t,a},V_{n-1,t,a}\right)$ is

$$\begin{aligned}
\frac{\partial V_{n+1,t}}{\partial V_{n,t}} &= \frac{\partial E}{\partial V_{n,t}}\left(H_{n,t,a},V_{n,t,a},V_{n-1,t,a}\right) \\
&= -v_{n,d}\exp\left(-\lambda\frac{\left(V_{n-1,t,a}\right)^{\alpha}}{\left(V_{n,t,a}\right)^{\beta}}\left(\frac{H_{n,t,a}-S_n}{L}\right)^{\gamma}\right)\left(\lambda\beta\frac{\left(V_{n-1,t,a}\right)^{\alpha}}{\left(V_{n,t,a}\right)^{\beta}}\left(\frac{H_{n,t,a}-S_n}{L}\right)^{\gamma}V_{n,t,a}^{-1}\right), \\
&= \Omega V_{n,t,a}^{-1}
\end{aligned}$$

$$\tag{5.16}$$

where $\Omega=-v_{n,d}\exp\left(-\lambda\frac{\left(V_{n-1,t,a}\right)^{\alpha}}{\left(V_{n,t,a}\right)^{\beta}}\left(\frac{H_{n,t,a}-S_n}{L}\right)^{\gamma}\right)\left(\lambda\beta\frac{\left(V_{n-1,t,a}\right)^{\alpha}}{\left(V_{n,t,a}\right)^{\beta}}\left(\frac{H_{n,t,a}-S_n}{L}\right)^{\gamma}\right)$. As

Eq. (5.12),

$$\Omega = -v_{n,d} \exp\left(-\lambda \frac{(V_{n-1,t,a})^\alpha}{(V_{n,t,a})^\beta} \left(\frac{H_{n,t,a} - S_n}{L} \right)^\gamma \right) \left(\lambda\beta \frac{(V_{n-1,t,a})^\alpha}{(V_{n,t,a})^\beta} \left(\frac{H_{n,t,a} - S_n}{L} \right)^\gamma \right)$$
$$= -v_{n,d} \exp\left(-\lambda \frac{(V_{n-1,t,d})^\alpha}{(V_{n,t,d})^\beta} \left(\frac{H_{n,t,d} - S_n}{L} \right)^\gamma \right) \left(\lambda\beta \frac{(V_{n-1,t,d})^\alpha}{(V_{n,t,d})^\beta} \left(\frac{H_{n,t,d} - S_n}{L} \right)^\gamma \right) \quad (5.17)$$

The first partial derivative of E function at the deceleration traffic state $\left(H_{n,t,d}, V_{n,t,d}, V_{n-1,t,d} \right)$ is

$$\frac{\partial V_{n+1,t}}{\partial V_{n,t}} = \frac{\partial E}{\partial V_{n,t}} \left(H_{n,t,d}, V_{n,t,d}, V_{n-1,t,d} \right)$$
$$= -v_{n,d} \exp\left(-\lambda \frac{(V_{n-1,t,d})^\alpha}{(V_{n,t,d})^\beta} \left(\frac{H_{n,t,d} - S_n}{L} \right)^\gamma \right) \left(\lambda\beta \frac{(V_{n-1,t,d})^\alpha}{(V_{n,t,d})^\beta} \left(\frac{H_{n,t,d} - S_n}{L} \right)^\gamma V_{n,t,d}^{-1} \right). \quad (5.18)$$
$$= \Omega V_{n,t,d}^{-1}$$

$V_{n,t,a}$ and $V_{n,t,d}$ denote $V_{n,t}$ for the acceleration and deceleration traffic respectively, and they accelerate or decelerate to the same velocity (i.e. Eq. (5.12)). Hence,

$$\Omega V_{n,t,a}^{-1} \neq \Omega V_{n,t,d}^{-1}, \quad (5.19)$$

and Eq. (5.13) cannot hold. Consequently, the speed-spacing relationships of acceleration and deceleration traffic are different, and traffic hysteresis occurs. Thus, the proposed model always can represent traffic hysteresis under any arbitrary parameters values and any disequilibrium traffic conditions.

(2) General models discussion

This section discusses the speed-spacing relationship of a general model. Assumptions of the general model are listed below.

1. The speed of a following vehicle $V_{n,t+1}$ is influenced by the lead vehicle speed $V_{n-1,t}$, the follower speed $V_{n,t}$, and the spacing $H_{n,t}$.

2. If there are no changes in $V_{n-1,t}$ and $V_{n,t}$, the vehicle speed $V_{n,t+1}$ increases with spacing $H_{n,t}$.

3. $V_{n-1,t}$ and $V_{n,t}$ influence $V_{n,t+1}$. Under different total effects of $V_{n-1,t}$ and $V_{n,t}$, identical spacing still result in different $V_{n,t+1}$ while $H_{n,t} > S_n$.

4. If $H_{n,t} = S_n$, the vehicle will decide to stop under any arbitrary $V_{n-1,t}$ and $V_{n,t}$.

5. Let $V_{n,t+1}$ is a function of $H_{n,t}$, $V_{n,t}$, $V_{n-1,t}$, that is

$$V_{n,t+1} = Y\left(H_{n,t}, V_{n,t}, V_{n-1,t}\right) \tag{5.20}$$

where $H_{n,t} \geq S_n$, $V_{n,t} \geq 0$, $V_{n-1,t} \geq 0$. $Y\left(H_{n,t}, V_{n,t}, V_{n-1,t}\right)$ is differentiable on its entire domain.

6. Vehicles have no acceleration limit.

Thus, the general traffic flow model is represented as following.

1. $\dfrac{\partial Y}{\partial H_{n,t}}\left(H_{n,t}, V_{n,t}, V_{n-1,t}\right) > 0, \qquad \forall H_{n,t} \geq S_n \tag{5.21}$

2. Let $V_{n,t,1}$, $V_{n,t,2}$ denote any arbitrary value of $V_{n,t}$, $V_{n-1,t,1}$, $V_{n-1,t,2}$ represent any arbitrary value of $V_{n-1,t}$, $H_{n,t,1}$ denotes any arbitrary value of $H_{n,t}$ but $H_{n,t,1} > S_n$, and $Y\left(H_{n,t,1}, V_{n,t,1}, V_{n-1,t,1}\right) \neq Y\left(H_{n,t,1}, V_{n,t,2}, V_{n-1,t,2}\right)$. Then,

$Y\left(H_{n,t}, V_{n,t,1}, V_{n-1,t,1}\right) = Y\left(H_{n,t}, V_{n,t,2}, V_{n-1,t,2}\right)$ if and only if $H_{n,t} = S_n$.

Let $H_{n,t,2}$ denotes any arbitrary value of $H_{n,t}$, and $H_{n,t,1} \neq H_{n,t,2}$. If

$$Y\left(H_{n,t,1}, V_{n,t,1}, V_{n-1,t,1}\right) = Y\left(H_{n,t,2}, V_{n,t,2}, V_{n-1,t,2}\right), \tag{5.22}$$

it implies Eq. (5.12) hold. If Eq. (5.14) holds, that is

$$\frac{\partial Y}{\partial H_{n,t}}\left(H_{n,t,1}, V_{n,t,1}, V_{n-1,t,1}\right) = \frac{\partial Y}{\partial H_{n,t}}\left(H_{n,t,2}, V_{n,t,2}, V_{n-1,t,2}\right). \tag{5.23}$$

If Eq. (5.23) cannot always hold, traffic hysteresis occurs under some conditions. Next, this research proves that Eq. (5.23) cannot always hold. Suppose

$$\lim_{\varepsilon \to 0^+} Y\left(\varepsilon + S_n, V_{n,t,1}, V_{n-1,t,1}\right) = \lim_{\varepsilon \to 0^+} Y\left(\varepsilon + S_n + \delta, V_{n,t,2}, V_{n-1,t,2}\right) \tag{5.24}$$

where $\delta > 0$. If Eq. (5.23) always holds, that implies

$$\begin{aligned}
&\lim_{\varepsilon \to 0^+} Y\left(\varepsilon + S_n, V_{n,t,1}, V_{n-1,t,1}\right) - Y\left(S_n, V_{n,t,1}, V_{n-1,t,1}\right) \\
&= \lim_{\varepsilon \to 0^+} Y\left(\varepsilon + \delta + S_n, V_{n,t,2}, V_{n-1,t,2}\right) - Y\left(\varepsilon + S_n + \delta - \varepsilon, V_{n,t,2}, V_{n-1,t,2}\right),
\end{aligned} \tag{5.25}$$

and the following equation holds

$$Y\left(S_n, V_{n,t,1}, V_{n-1,t,1}\right) = Y\left(S_n + \delta, V_{n,t,2}, V_{n-1,t,2}\right). \tag{5.26}$$

As $Y\left(S_n, V_{n,t,1}, V_{n-1,t,1}\right) = Y\left(S_n, V_{n,t,2}, V_{n-1,t,2}\right)$ and Eq. (5.26) holds, the following equation holds

$$Y\left(S_n, V_{n,t,2}, V_{n-1,t,2}\right) = Y\left(S_n + \delta, V_{n,t,2}, V_{n-1,t,2}\right). \tag{5.27}$$

Since $\delta > 0$ and Eq. (5.21), Eq. (5.27) cannot hold. Thus, Eq.(5.26) cannot hold, and then Eq. (5.25) cannot hold. It implies Eq. (5.23) cannot always hold, and thus traffic hysteresis exists.

5.2.3 Microscopic Traffic Hysteresis Example

An example of movement process of two vehicles is illustrated below. The individual maximum speeds of these vehicles are 60km/hr. The initial speeds of these vehicles are their individual maximum speeds, and the initial spacing is 150m. Fig. 5-5 is the speed-spacing trajectory, the solid and dashed lines represent acceleration and deceleration traffic, respectively. Fig. 5-5 indicates that acceleration and deceleration curves forms two loop. The acceleration curve lies above the deceleration curve at long spacing, and it lies below deceleration curve at short spacing.
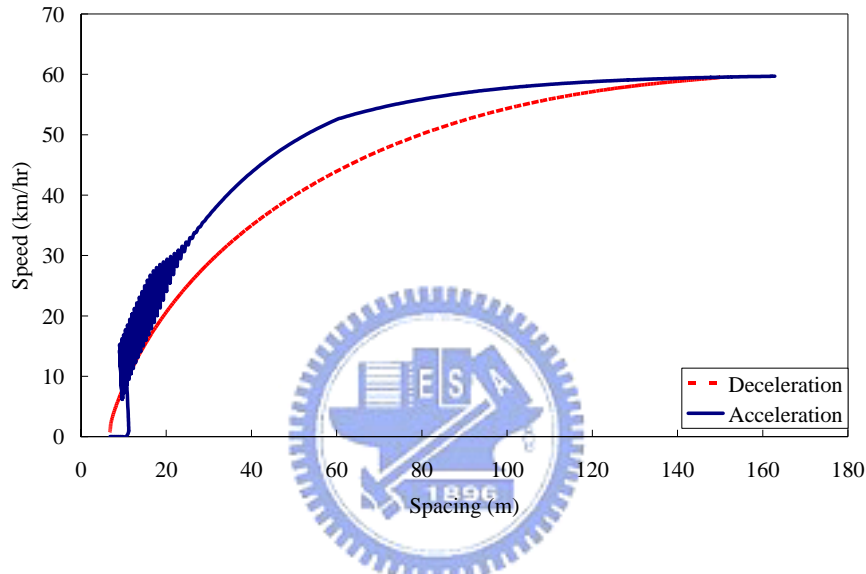
Figure 5-5 Speed-spacing trajectory

5.2.4 Macroscopic Traffic Hysteresis Examples

This section presents microscopic traffic flow simulation examples and aggregates individual data to reproduce traffic hysteresis. Leutzbach [1988] developed a generalized method to measure macroscopic traffic flow data from microscopic traffic flow data. The flow is measured as

$$q = \frac{\sum x_i}{\tau \cdot X}, \tag{5.28}$$

where τ denotes the time length of observation, X represents road length of observation, and x_i is the travel distance of vehicle i . The density is measured as

$$k = \frac{\sum t_i}{\tau \cdot X}, \tag{5.29}$$

where t_i denotes the travel time of vehicle i. Since $q = k \cdot u$, the space-mean speed is

$$u = \frac{\sum x_i}{\sum t_i} \,.$$ (5.30)

All simulation examples describe traffic flow on a single lane with length of 2000 meters. All drivers have identical driving behavior (i.e., identical individual maximum speed). The initial conditions are an equilibrium state, and the density is identical to the boundary condition at the start of the simulation. Road section traffic flow is influenced by upstream and downstream traffic, and thus the boundary conditions include both upstream and downstream boundary conditions. When the upstream boundary condition is k_{up} veh/km, a new vehicle arrives with a spacing $1000/k_{up}$ meters between it and the lasted vehicle. Meanwhile, when the downstream boundary condition is k_{down} veh/km, the lead vehicle of the simulation road keeps its speed as the equilibrium speed of density k_{down}. Furthermore, if the downstream boundary condition is 0 veh/km, the lead vehicle runs at its individual maximum speed. The relationship between equilibrium speed and equilibrium spacing is shown as Eq. (4.4).

The boundary condition of example A is illustrated as Fig. 5-6(a). The downstream boundary is vehicle free. The road density changes with changes in the upstream boundary condition. Hence, road sections cannot keep their states as equilibrium states, and instead decelerate followed by accelerating. The trajectory for the speed-density of the section between 500m and 1500m (the position of upstream boundary is 0m, and that of downstream boundary is 2000m) is as shown in Fig.5-6(b). The solid and dashed lines of Fig. 5-6(b) are guidance lines illustrating the acceleration and deceleration trends. The solid and dashed lines form a hysteresis loop, and the deceleration line lies above acceleration line. It is similar to the observation result obtained by Maes (as shown in Fig. 2-3).
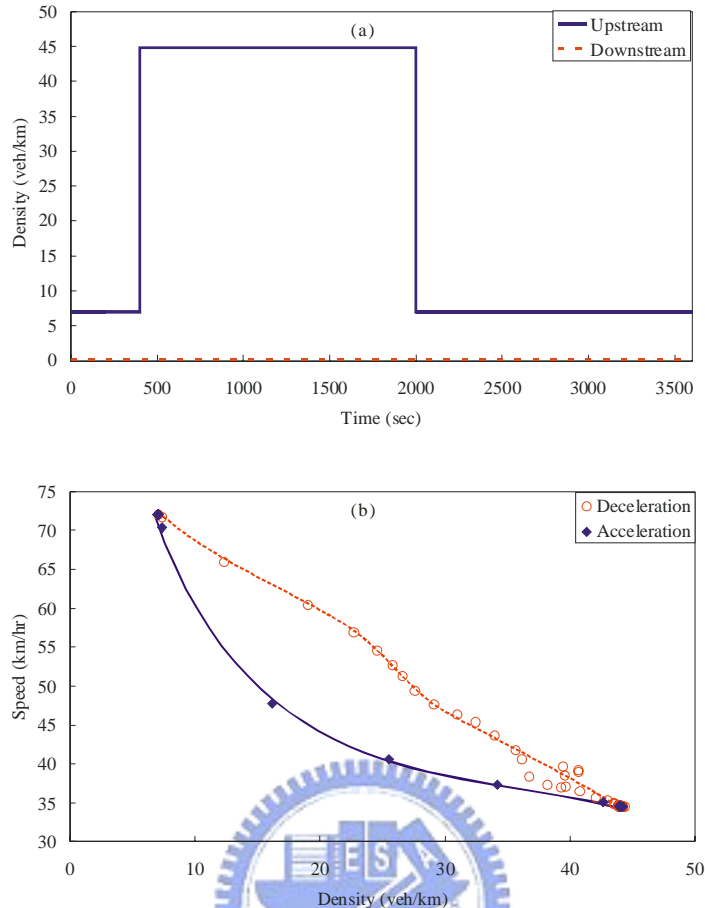
Figure 5-6 Boundary condition and speed-density relationship of example A: (a) Boundary condition (b) Speed-density relationship (t=0~3600sec)

Fig. 5-7 illustrates the boundary condition and speed-density trajectory of example B. The hysteresis pattern resembles the observation results obtained by Treiterer and Meyers (as shown in Fig. 2-4).

As aforementioned, there are at leas two types of hysteresis patterns differing from Treiterer and Maes' observations. The proposed car-following model can also represent the two hysteresis pattern types illustrated in Fig. 5-4. In example C, there is no vehicle at the downstream boundary, and the upstream boundary has very low density, with vehicles entering the system at a speed approaching their maximum. An incident occurs at 1250m between 1000 and 2500 seconds which prevents vehicles passing. The trajectory for the speed-density of the section between 750m and 1250m is as shown in Fig. 5-8, and the hysteresis pattern is similar to Fig. 5-4(a) while differing from Fig. 2-3
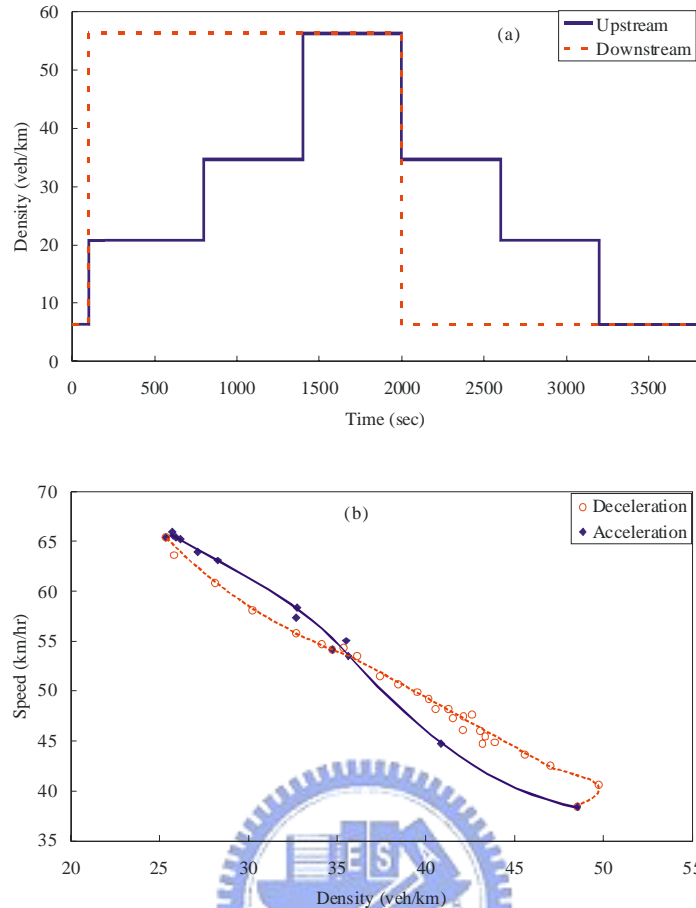
Figure 5-7 Boundary condition and speed-density relationship of example B: (a)
Boundary condition (b) Speed-density relationship (t=0~3600sec)

Fig. 5-9 shows example D, which has a hysteresis pattern similar to Fig. 5-4(b) and contrary to Fig. 2-4.

Zhang and Kim [2005] developed a car-following model which employed different rules for acceleration and deceleration traffic, and thus his car-following model can represent traffic hysteresis. The proposed model employ only one behavior rule for both acceleration and deceleration traffic when the lead and following vehicles are moving. Although all vehicles of Example A, B, D are moving vehicles which employ Eq. (5.1) regardless acceleration and deceleration, the proposed model still represent various traffic hysteresis pattern types.
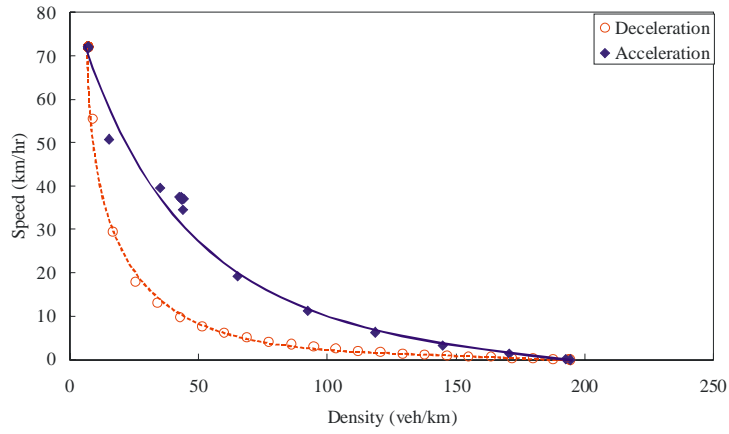
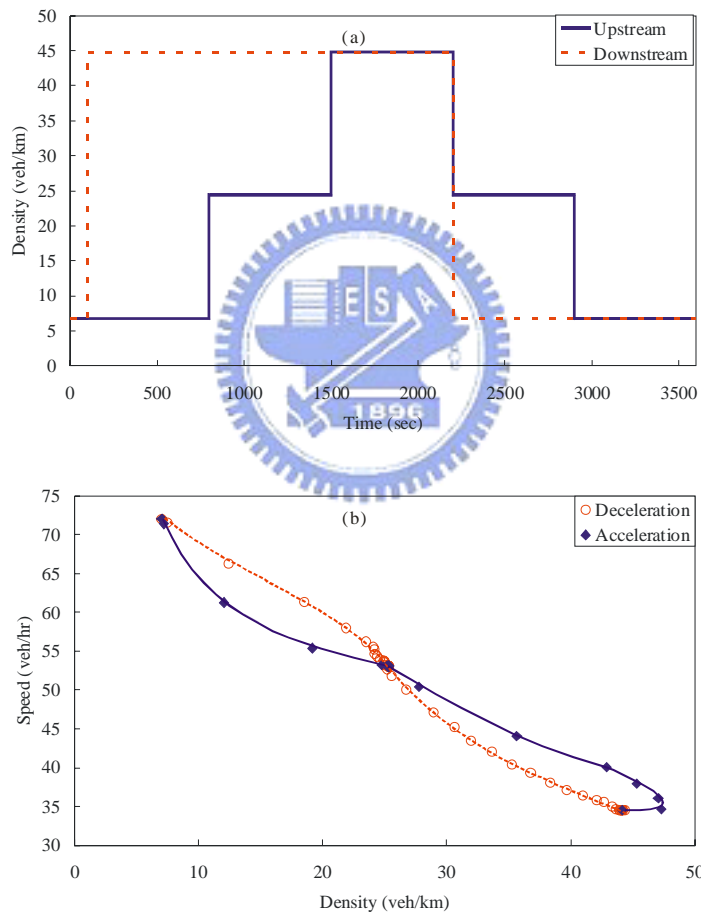Figure 5-8 Speed-density relationship of example C. (t=0~3600sec)

Figure 5-9 Boundary condition and speed-density relationship of example D

Chapter 6
Conclusions and Perspectives

This chapter includes the conclusions of this dissertation and discusses some future research topics.

6.1 Conclusions

This dissertation develops a simple car-following model. Sensitivity analysis, stability analysis, equilibrium state, disequilibrium state, and relaxation time are discussed. Results of this research are summarized as follows.

(1) Car-following model

The proposed model considers that a driver has different behaviors under different external environments, and different drivers have different behaviors. The individual maximum speed which is an exogenous variable is employed to describe different drivers and different external environment.

(2) Sensitivity analysis

Vehicle speed $V_{n,t+1}$ varies with the spacing $H_{n,t}$, the lead vehicle speed $V_{n-1,t}$, and the following vehicle speed $V_{n,t}$. The sensitivity to each variable is discussed. Sensitivity analysis results indicate that sensitivity varies with all variables, and different parameter values represents different driver behaviors.

(3) Stability analysis

When the individual maximum speed of the following vehicle is close to the equilibrium speed of its lead vehicle, traffic will lead to equilibrium state. Otherwise, when the difference between the individual maximum speed of the following vehicle and the equilibrium speed of its lead vehicle is great, traffic may be unstable. Unstable heavy traffic may be due to the large difference between the driver's individual maximum speed and the equilibrium speed.

The stability is also dependent on driver's reaction time. When the driver's reaction time is less, traffic will be stable. Otherwise, when the driver's reaction time is high, unstable traffic is likely to occur. When the individual maximum speed of the following vehicle is not close to the equilibrium speed, drivers should react more frequently. Otherwise, traffic may be unstable.

(4) Equilibrium state

Equilibrium spacing is dependent on the equilibrium speed and the individual maximum speed of the following vehicle. Thus, different drivers have different equilibrium spacing under identical equilibrium speed, and aggressive drivers have shorter equilibrium spacing.

Fundamental diagram based on the microscopic equilibrium state is also discussed. The numerical examples indicate that different parameter values result in different fundamental diagram patterns, and the capacity increases with free-flow speed.

(5) Disequilibrium state

Some traffic phenomena of disequilibrium state are discussed, such as closing-in, shying-away, stop-and-go, and traffic hysteresis. This dissertation identified at least two types of hysteresis patterns differing from Treiterer and Maes' observations based on filed data. Simulation results demonstrate that the proposed model can describe the four hysteresis pattern types.

The mathematical analysis of closing-in, shying-away, and traffic hysteresis are provided, and they guarantee that the disequilibrium phenomena still hold under any parameter values. A general traffic flow model that guarantees the existence of traffic hysteresis is also provided.

(6) Relaxation time

When a perturbation occurs at an equilibrium system, the system will depart from equilibrium state. This study discusses how much time the system needs to return to the equilibrium state. No matter the perturbation is acceleration or deceleration, the velocity profiles after perturbations indicate that the relaxation time increases with reducing $D_n = \dfrac{V_{n,e}}{v_{n,d}}$.

6.2 Perspectives

This research develops a simple car-following model. The original research motivation is to develop a microscopic traffic flow model that can extend to macroscopic traffic flow model and can be a tool to analyze traffic properties. Thus, it can provide real time information for ATIS, and provide better traffic control strategies for ATMS. This dissertation is a fundamental research for a long-term research. The long-term research objectives include:

(1) Traffic information prediction: The long-term objective is to develop a simulator that can provide real time prediction of large-scale traffic network, and the simulator is based on a proposed traffic flow model. In order to achieve the objective, the research procedure is: (a) to develop a microscopic traffic flow model, (b) to develop a mesoscopic traffic flow model, (c) to develop a macroscopic traffic flow model, (d) to develop a simulator. To take advantages of microscopic and macroscopic traffic flow models, the simulator can be based on a combined model.

(2) Traffic control strategies: As the proposed model provide some traffic flow analysis, new concepts could be introduced to design traffic control strategies.

The long-term research objectives and future studying topics are shown in Fig. 6-1. Next, each studying topic is discussed.
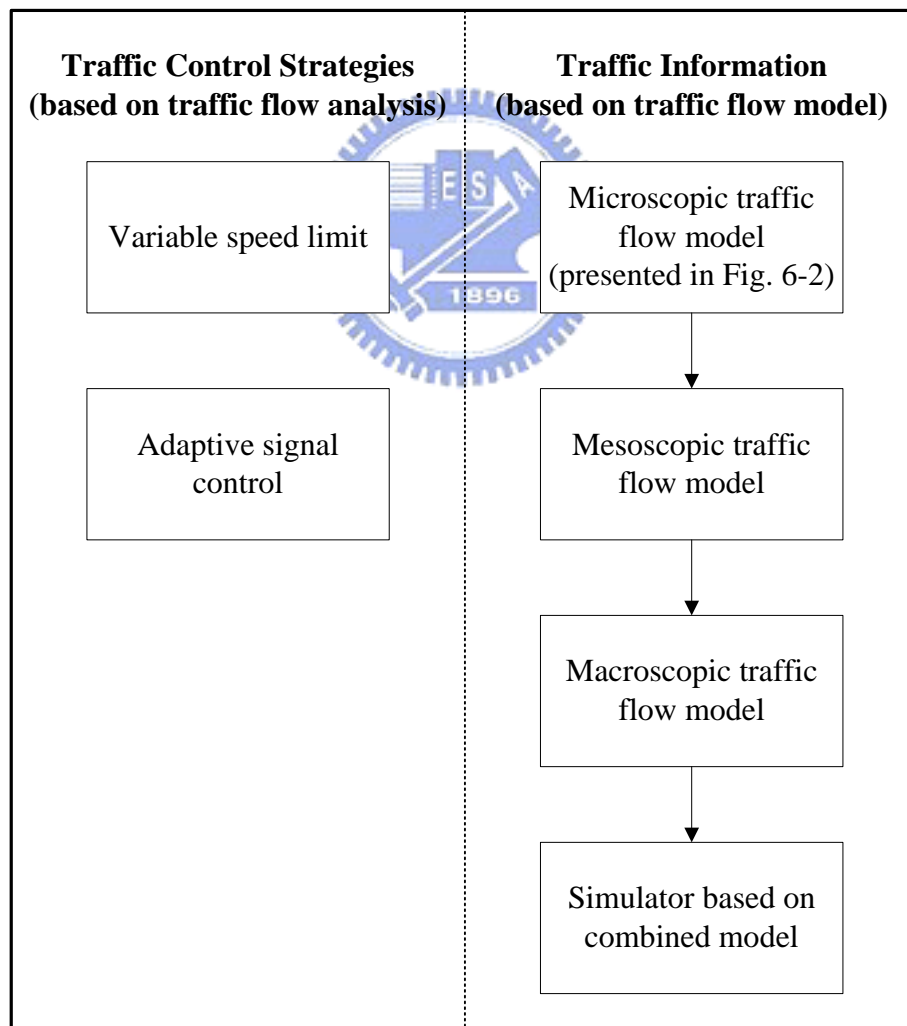

Figure 6-1 Long-term research objectives and future studying topics

(1) <u>Traffic flow model extension</u>

In order to develop a simulator that can provide real time information of large-scale traffic network, traffic flow model should be extended.

(a) Lane-changing model

Microscopic traffic flow includes car-following and lane-changing. This dissertation only develops a simple car-following model, and thus lane-changing model should be developed.

(b) Longitudinal movement model for nonmotorized vehicle

In Taiwan, the traffic flow in most urban streets is mixed traffic flow. Mixed traffic flow contains standard vehicle types such as passenger cars, buses, and trucks, as well as nonstandard vehicles such as motorcycles and bicycles. The behaviors of standard vehicle type and nonstandard vehicle type are different. In the motorcycle lane, the way motorcycles move is not the same as cars, which follow one after another. Thus, longitudinal movement of nonmotorized vehicles differs from car-following of motorized vehicles.

(c) Lateral movement model for nonmotorized vehicle

Nonmotorized vehicles can overtake on the same lane. Therefore, lateral movement of nonmotorized vehicles differs from lane-changing of motorized vehicles.

(d) Mixed traffic flow model

Microscopic traffic flow models for motorized vehicles and nonmotorized vehicles could be integrated as a microscopic mixed traffic flow model.

(e) Calibration and validation

All the aforementioned models should be calibrated and validated. Then, a microscopic traffic flow simulator can be developed. Studying topics of microscopic traffic simulator is shown in Fig. 6-2.
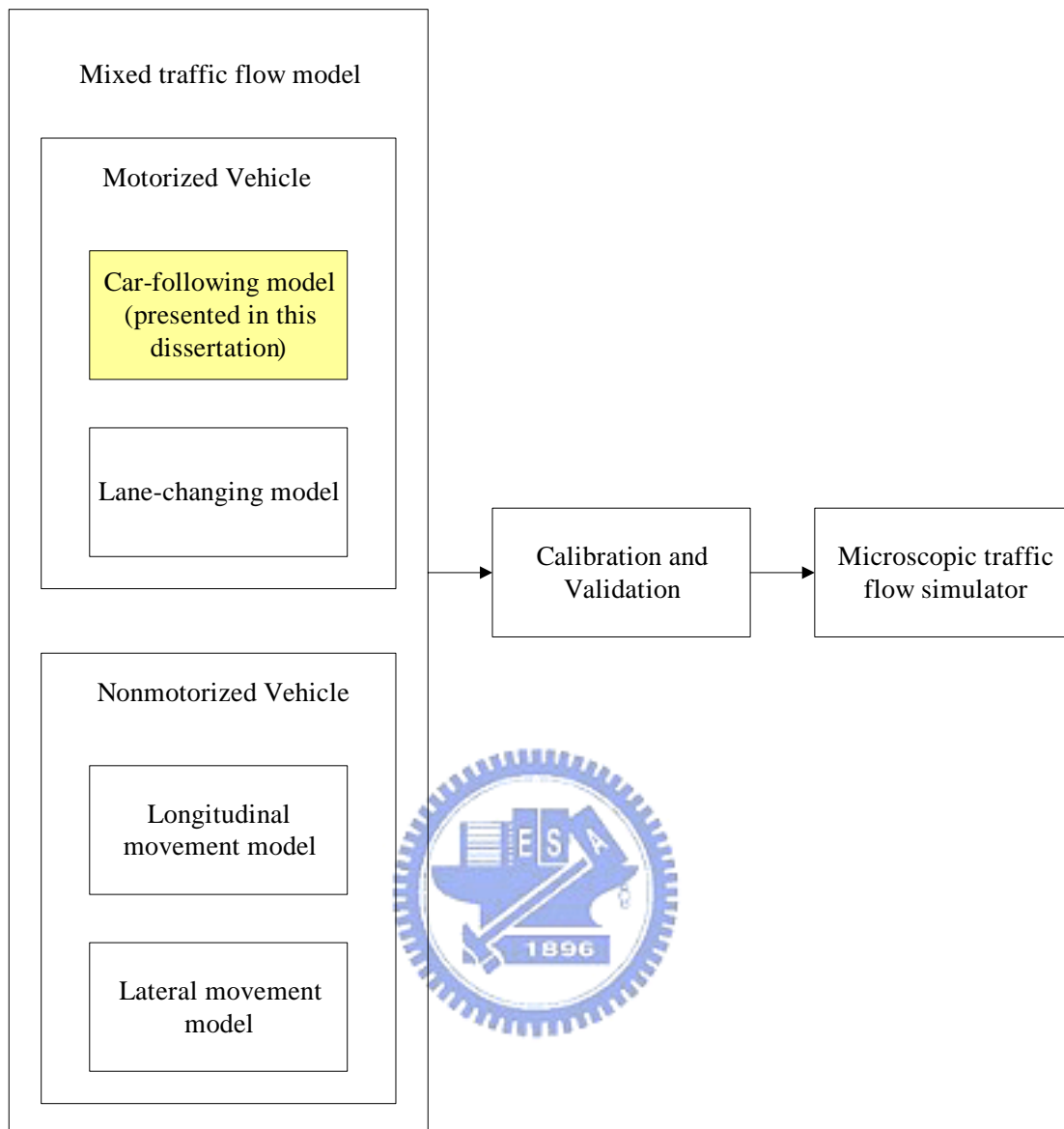
Figure 6-2 Studying topics of microscopic traffic simulator

(f) Mesoscopic traffic flow model

This dissertation discusses the microscopic equilibrium state, and the macroscopic equilibrium state based on the microscopic equilibrium state for homogeneous drivers. In fact, there are various drivers on the road, and thus equilibrium and disequilibrium states for heterogeneous drivers could be a research topic.

As aforementioned, different drivers have different equilibrium spacing under identical equilibrium speed. Thus, the equilibrium spacing for heterogeneous drivers under some specific equilibrium speed is a distribution.

The speed of the lead vehicle of a platoon is the equilibrium speed of the platoon under uninterrupted traffic. If there are many vehicles on a road, they will form several platoons. Thus, different individual maximum speed distributions result in different lead vehicle speed distributions, and then result in different equilibrium speed distributions for uninterrupted traffic. Hence, the equilibrium state for heterogeneous drivers is not a specific value, it is a distribution.

Furthermore, before reaching equilibrium state, Boltzmann transport equation could be developed to describe disequilibrium traffic.

(g) Macroscopic traffic flow model

A dynamic macroscopic traffic flow model can be developed based on the aforementioned mesoscopic traffic flow model. Density, flow, and speed can be derived from the vehicle speed distribution function of Boltzmann transport equation.

(h) Traffic flow simulator based on combined models

As microscopic and macroscopic traffic flow models have their own strengths, traffic flow simulator could be developed based on combined models. For example, microscopic traffic flow model can describe vehicle interaction in detail, and macroscopic traffic flow model has less execution time. Microscopic traffic flow model could be employed to simulate urban intersections, freeway weaving sections, and ramp junctions. Macroscopic traffic flow model could be employed to simulate basic freeway sections.

(2) Traffic control strategy

(a) Variable speed limit

As mentioned in stability analysis, the difference between individual maximum speed and equilibrium speed influence traffic stability. If the difference is large, unstable traffic is likely to occur.

Different equilibrium density results in different equilibrium speed, and then results in different difference between individual maximum speed and equilibrium speed. Speed limit may affect individual maximum speed. Thus, if the speed limit can vary with traffic condition, traffic may be stable under high density.

(b) Adaptive signal control

As mentioned in Chapter 5, the speed-density relationships for acceleration and deceleration traffic are different. Thus, the flow-density relationship of acceleration traffic differs from the one of deceleration traffic. As shockwave speed is dependent on the flow-density relationship and some adaptive signal control strategies consider shockwave speed, traffic hysteresis concept could be introduced to design adaptive signal control strategies.

References

Alligood, K. T., Sauer, T. D., Yorke, J. A., 1997. *Chaos An Introduction to Dynamical Systems*. Springer-Verlag New York.

Aycin, M.F., Benekohal, R.E., 1999. Comparison of car-following models for simulation. *Transportation Research Record* 1678: 116-127.

Bando, H., Hasebe, K., Nakayama, A., Shibata, A., Sugiyama, Y., 1995. Dynamic model of traffic congestion and numerical simulation. *Physical Review E* 51: 1035-1042.

Benekohal, R.F., Treiterrer, J., 1988. CARSIM: car-following model for simulation of traffic in normal and stop-and-go conditions. *Transportation Research Record* 1194: 99-111.

Chakroborty, P., Kikuchi, S., 1999. Evaluation of the General Motors based car-following models and a proposed fuzzy inference model. *Transportation Research Part C* 7: 209-235.

Chandler, R.E., Herman , R., Montroll, E. W., 1958. Traffic dynamics: studies in car following. *Operations Research* 6: 165-184.

Daganzo, C. F., 1994. The cell transmission model: a dynamic representation of highway traffic consistent with the hydrodynamic theory. *Transportation Research Part B* 28: 269-287.

Danganzo, C.F., 2002. A behavioral theory of multi-lane traffic flow. Part I: Long homogeneous freeway sections. *Transportation Research Part B* 36: 131-158.

Drew, D. 1968. *Traffic Flow Theory and Control*, McGraw-Hill.

Edie, L.C., 1961. Car-following and steady-state theory for noncongested traffic. *Operations Research* 9: 66-76.

Fellendorf, M., 1997. Parametrization of microscopic Traffic Flow Models through Image Processing. 8th IFAC Symposium on Transport,Chania, Crete, Greece, June 1997.

Gazis, D. C., Herman, R., Potts, R. B., 1959. Car-following theory of steady-state traffic flow. *Operations Research* 7: 499-505.

Gazis, D. C., R. Herman, and R. W. Rothery, "Nonlinear Follow-the-Leader Models of Traffic Flow," *Operations Research*, Vol. 9, pp.545-567, 1961.

Greenberg, H., 1959. An Analysis of Traffic Flow. *Operations Research* 7: 79-85.

Greenshield, B. D., 1934. A Study of Traffic Capacity. *Highway Research Board Proceedings* 14: 468-477.

Heidemann, D., 2001. A queueing theory model of nonstationary traffic flow, *Transportation Science* 35: 405-412.

Herman, R., E., Montroll, W., Potts, R. B., Rothery, R. W., 1959. Traffic dynamics: analysis of stability in car following. *Operations Research* 7: 86-106.

Holland, E.N., 1998. A generalised stability criterion for motoryway traffic. *Transportation Research Part B* 32: 141-154.

Hoogendoorn, S.P., Bovey, P.H.L., 2001. State-of-the-art of vehicular traffic flow modelling.

http://www.trail.tudelft.nl/T&E/papers_course_IV_9/state-of-the-art.PDF.

Igarashi, Y., Itoh, K., Nakanishi, K., Ogura, K., Yokokawa, K., 2001. Bifurcation phenomena in the optimal velocity model for traffic flow. *Physical Review E* 64: 047102.

Jiang, R., Wu, Q. S., 2003. Study on propagation speed of small disturbance from a car-following approach. *Transportation Research Part B* 37: 85-99.

Kerner, B.S., Rehborn, H., 1997. Experimental properties of phase transitions in traffic flow. *Physical Review Letters* 79: 4030-4033.

Kerner, B.S., Rehborn, H., 1998. Experimental features of self-organization in traffic flow. *Physical Review Letters* 81: 3797-3800.

Kerner, B.S., Klenov, S.L., Hiller, A., Rehborn, H., 2006. Microscopic features of moving traffic jams. *Physical Review E* 73: 046107.

Kikuchi, S., Chakroborty, P., 1992. Car-following model based on fuzzy inference system. *Transportation Research Record* 1365: 82-91.

Leutzbach, W., Rainer, W., 1986. Development and applications of traffic simulation models at the karlsruhe institut fuer verkehrswesen. *Traffic Engineering & Control* 27: 270-278.

Leutzbach, W., 1988. *Introduction to the Theory of Traffic Flow*. Spring-Verlag, Berlin Heidelberg.

Li, W., Szidarovszky, F., 1999. An elementary result in the stability theory of time-invariant nonlinear discrete dynamical systems. *Applied Mathematics and Computation* 102: 35-49.

May, A.D., 1990. *Traffic Flow Fundamentals*. Prentice Hall, Englewood Cliffs, New Jersey.

May, R. M., 1974. *Stability and complexity in model ecosystems*. Princeton University Press, Princeton, NJ.

McDonald, M., Wu, J., Brackstone, M., 1997. Development of a fuzzy logic based microscopic motorway simulation model. *Proceedings of IEEE Conference on Intelligent Transportation Systems*, ITSC 97, Boston, MA, 82-87.

Mcshane, W. R., Roess, R. P., 1990. *Traffic Engineering.* Prentice Hall, Englewood Cliffs, New Jersey.

Munjal, P. K., Pipes, L. A., 1971. Propagation of On-Ramp Density Waves on Nonuniform Unidirectional Two-Lane Freeways. *Transportation Research* 5:. 241-255.

Nagatani, T., 2000. Traffic behavior in a mixture of different vehicles. *Physica A* 284: 405-420

Newell, G. F., 1961. Nonlinear Effects in the Dynamics of Car Following. *Operations Research* 9: 209-229.

Newell, G.F., 2002. A simplified car-following theory: a lower order model. *Transportation Research Part B* 36: 195-205.

Pipes, L.A., 1953. An operational analysis of traffic dynamics. *Journal of Applied Physics* 24: 274-287.

Pipes, L.A., 1967. Car following models and he fundamental diagram of road traffic. *Transportation Research* 1: 21-29.

Reuschel, A., 1950. Vehicles Moves in a Platoon.   *Oesterreichisches Ingenieur-Archir* 4:193-215.

Transportation Research Board, 2000. *Highway Capacity Manual 2000*, National Research Council, Washington, D. C.

Treiber, M., Hennecke, A., Helbing, D., 2000. Congested traffic states in empirical observations and microscopic simulations. *Physical Review E* 62: 1805-1824.

Underwood, R. T., 1961. Speed, Volume, and Density Relationships, Quality and Theory of Traffic Flow. *Yale Bureau of Highway Traffic*, New Haven, Conn: 141-188.

Wicks, D.A., Andrews, B.J., 1980. *Development and Testing of INTRAS, a Microscopic Freeway Simulation Model, Vol. 1: Program Design, Parameter Calibration and Freeway Dynamics Component Development*. Report FHWA-RD-80-106. FHWA, U.S. Department of Transportation.

Widemann, R., 1974. *Simulation des Verkehrsflusses*. University of Karlsruhe, Karlsruhe.

Wiggins, S., 1990. *Introduction to Applied Nonlinear Dynamical Systems and Chaos*. Springer-Verlag, New York.

Wong, G.C.K., Wong, S.C., 2002. A multi-class traffic flow model – an extension of LWR model with heterogeneous drivers. *Transportation Research Part A* 36: 827-841.

Yi, J., Lin, H., Alvarez, L., Horowitz, R., 2003. Stability of macroscopic traffic flow modeling through wavefront expansion. *Transportation Research Part B* 37: 661-679.

Zhang, H.M., 1999a. A mathematical theory of traffic hysteresis. *Transportation Research Part B* 33: 1-23.

Zhang, H.M., 1999b. Analyses of the stability and wave properties of a new continuum traffic theory. *Transp. Res. Pt. B-Methodol.* 33: 399-415

Zhang, H.M., 2001. A note on highway capacity. *Transportation Research Part B* 35: 929-937.

Zhang, H.M., Kim, T., 2005. A car-following theory for multiphase vehicular traffic flow. *Transportation Research Part B* 39: 385-399.

Zhang, Y., Owen, L. E., 1998. An Advanced Traffic Simulation Approach for Modelling ITS Application. *1998 IEEE International Conference on Systems, Man, and Cybernetics* 4: 3228-3233.

Zhang, X., Jarrett, D.F., 1997. Stability analysis of the classical car-following model. *Transportation Research Part B* 31: 441-462.

Zhao, X., Gao, Z., 2005. A new car-following model: full velocity and acceleration difference model. *The European Physical Journal B* 47: 145-150.